Application of a multipoint statistics method to assess potential recharge areas in San Luis Obispo County, California, U.S.A.

Authors: Seogi Kang and Rosemary Knight, Stanford University
This work was done in collaboration with Jef Caers, Stanford University

3 March 2021

INTRODUCTION

This report describes our work applying a multi-point statistics (MPS) method to assess potential recharge locations, in San Luis Obispo County, California, U.S.A. This report is accompanied by presentation material in pdf format; this pdf file is downloadable through this link. In this report, we refer to the content in the presentation using the page number of the presentation.

The study area is located in San Luis Obispo County, California as shown in the location map (Page 2). Airborne electromagnetic (AEM) data were acquired in November 2019 with the SkyTEM 312 system. These AEM data were processed by Aarhus University to remove noisy data. The locations of resulting high-quality AEM data are shown as black lines in the location map (Page 2). Shown are areas where AEM data were omitted; these areas are close to transmission lines and vineyards. IGIS digitized 731drillers' logs from wells within the study area; these are shown as red circles on Page 2. The AEM surveys were designed to fly as close as possible to accurately located wells with drillers' logs so as to construct an accurate resistivity-to-sediment-type transform. The result was a total of 88 wells with drillers' logs within 100 m of AEM data locations; the locations of these wells, treated as co-located with the AEM soundings, are presented on Page 2 as white open circles. Streams in the study area (e.g., the Estrella River) are shown as blue lines in the location map. During the week of the AEM survey, groundwater level measurements were made in 30 wells; their locations are shown on Page 2 as blue solid circles.

An important question that we focused on in this study is: "What is the extent of the clay layer at the Estrella River?" Given that this clay layer can act as a hydraulic barrier to vertical groundwater flow, delineating the clay layer can provide information to guide decisions for recharge operations. To delineate the extent of the clay layer, we applied the MPS method, utilizing the AEM and well data. Our final goal was to obtain the distribution of sediment type, defined as coarse-grained-dominated and fine-grained-dominated, and referred to as coarse-dominated and fine-dominated, at the scale of a 3D grid with a uniform cell size of 200 m × 200 m × 5 m. The horizontal dimensions of 200 m × 200 m was selected to match that used in in the local groundwater model (Sorensen et al., 2005). The vertical dimension of 5 m was a trade-off between vertical resolution of the well data, which ranged from 15 cm to 143 m (on average, 6 m), and that of the AEM data, about 2 m at the surface, increasing to ~40 m at 300 m depth. Uncertainty in the distribution of sediment type was displayed as the probability of coarse-dominated.

As shown on Page 5, there were three key inputs to the specific form of the MPS methodology that we developed. These inputs were derived as profiles or models of sediment type from the AEM and well data and include: (1) a sediment-type starting probability model defined at the grid, derived from the AEM data; (2) sediment-type well profiles upscaled and classified from drillers' logs; (3) a training image capturing the expected geologic patterns in the area. With these three inputs, MPS simulations were carried out to obtain multiple realizations of sediment-type models composed of two units: coarse-dominated and fine-dominated. The obtained sediment-type models allowed us to address the hydrogeologic question as well as capturing the associated uncertainty.

APPLICATION OF THE MPS METHOD

In this section, we describe our workflow to derive inputs for the MPS simulations from the AEM and well data. Our workflow is composed of six steps:

- Step 1: define the grid
- Step 2: prepare the well data
  - A: classify the well data as coarse/fine
  - B: prepare profiles of sediment-type from well data at the scale of grid (upscale to the grid)
- Step 3: derive 3D coarse-fraction (CF) models from AEM data at the scale of the grid
- Step 4: construct a sediment-type starting probability model from the AEM-derived CF-models
- Step 5: detect outliers in the sediment-type well profiles
- Step 6: create a training image

The flow chart of the workflow is shown on Pages 6-8. The unknown random variable that we seek is defined below in Equation 1 as

$$Z = \begin{cases} 1, & CF \geq 0.5 \\ 0, & CF < 0.5 \end{cases}, \quad (1)$$

where Z=1 and 0 represent the two sediment types: coarse-dominated and fine-dominated, respectively; CF values less than 0.5 are determined to fine-dominated and those greater or equal than 0.5 are determined to be coarse-dominated. With MPS simulations, our aim is to obtain multiple realizations of MPS sediment-type (coarse-dominated or fine-dominated) models at the scale of the grid: $\{z_1^{3D}, z_2^{3D}, \dots, z_L^{3D}\}$; here L is the number of MPS sediment-type models.

In Step 1, we defined the grid, shown on Page 4. Given that this was the grid of our MPS sediment-type model, the AEM and well data must be transformed into sediment type at the scale of the grid to provide input to an MPS simulation algorithm.

In Step 2A, we prepared the well data to provide intervals of coarse/fine. For the classification of coarse/fine from the highly variable lithologic descriptions, we used a machine learning technique developed by Stanford researchers; a classifier was constructed using well data from regions in the Central Valley. This process was applied to all 731 drillers' log, as illustrated on Page 10. The classification in terms of coarse/fine are at the well scale, and this will be used later in Step 3. In Step 2B, we prepared the sediment-type from the well data at the scale of the grid. We first calculated a CF value defined in a grid cell from coarse/fine intervals of a well; this can be seen as a vertical upscaling procedure from the well scale to the grid scale as illustrated on Page 11. In addition, if there are multiple wells in a grid cell, we arithmetically averaged corresponding values of CF. This procedure resulted in a total of 539 CF well profiles (which can be provided to the agency) containing values of CF at the scale of the grid as shown on Page 12. Page 13 shows a 3D view of these CF well profiles. Using equation (1) the 539 CF well profiles were converted to sediment-type well profiles as shown on Page 14. From the geostatistical analysis of the z_{wells} we found that the percentage of coarse-dominated in the entire sediment-type well profiles is 36%; vertical and horizontal correlation lengths are 10-20 m and about 500 m, respectively. These sediment-type well profiles will be used in Step 5.

In Step 3, we derived 3D CF models from the AEM data at the scale of the grid. This required three sub-steps: Step 3A – AEM inversions, Step3B – Rock physics transform, and Step3C – Interpolation to the 3D grid. By applying AEM inversions to the AEM data, in Step 3A, we obtained a total of 2002 resistivity models imaging the subsurface structures as well as capturing the uncertainty. The mean of the resistivity models was selected as our primary resistivity model. For these AEM inversions, we used both the

commercial geophysics software, *Aarhus workbench* and the open-source geophysics software, *SimPEG* (Viezzoli et al., 2008; Cockett et al., 2015; Kang et al., 2019).

In Step 3B, we transformed the obtained resistivity models into CF. For this transformation, we constructed a relationship between resistivity and CF using the methodology developed by Goebel and Knight (2020). This method has a two-step procedure. First by using 88 pairs of the co-located well data and AEM resistivity profiles from the primary resistivity model, we constructed resistivity distributions for the coarse and fine using the method from Knight et al. (2018). Given the impact of water content on resistivity, when building these resistivity distributions for the coarse and fine, we distinguished regions above the water table from those below the water table. The water table (or top of the saturated zone more accurately) was estimated from the AEM data and water levels using the methodology developed by Dewar and Knight (2020). From these resistivity distributions, we randomly sampled resistivity values for a suite of values of CF and obtained a relationship between resistivity and CF.

Using the developed resistivity-CF relationship, we transformed 2002 resistivity models to 2002 CF models. The mean of the CF models displaying the spatial variation of coarse- and fine-grained materials is shown in Page 17. Standard deviation of the CF models which displays the uncertainty is shown on Page 18; a darker color indicates a low level of uncertainty. For our rock physics transform we neglected the impact of salinity, given our understanding that there is little variability in TDS values in the study area.

The mean of CF models was defined at the scale of the AEM, and therefore needed to be interpolated over to the 3D grid used in MPS simulations. When interpolating the mean of CF models composed of vertical profiles of CF to the 3D grid, we took into account increasing lateral sampling volume of a vertical profile of CF from AEM as illustrated on Page 17. In addition, we used the standard deviation shown on Page 18 as interpolation weights to put higher emphasis on cells of the primary CF model having a low level of uncertainty (i.e., low standard deviation). With this interpolation process, we obtained a total of 1001 3D CF models as illustrated on left-hand side of Page 19; the mean of the obtained 3D CF model was calculated and shown on the right-hand side of Page 19.

In Step 4, we constructed a sediment-type starting probability model using the obtained 3D CF models in the previous step. For each of 1001 3D CF models, we classified their CF values into either coarse-dominated or fine-dominated using equation (1) as shown on right-hand side of Page 20. This procedure results in 1001 sediment-type models from AEM, from which we calculated the probability model of coarse-dominated as shown on Page 21, which displays the uncertainty of subsurface sediment-type; blue and red colors indicate a low level of uncertainty whereas a yellow color indicates a high level of uncertainty. The probability model of coarse-dominated is referred to as the starting probability model of coarse-dominated. The probability model of fine-dominated was obtained by subtracting the probability model of coarse-dominated from one.

In Step 5, we randomized the selection process of sediment-type well profiles to be used as hard data. This was to take into account the quality of drillers' logs which varied for many reasons (e.g., drilling method, care taken in preparing drillers' log); the quality of the drillers' logs had not been classified. First, we selected a portion of sediment-type well profiles which did not have any neighboring well profiles within 500 m separation distance; a total of 99 well profiles were selected. A 500 m separation distance was used based on the horizontal correlation length of the sediment-type wells. Second, from the other 440 well profiles, we sampled well profiles using an iterative, random-sampling technique and removed redundant well profiles. By repeating this procedure 100 times, we obtained 100 sets of sediment-type well profiles. About 280 well profiles were selected from 440 well profiles for each set. This resulted in the use of roughly 370 well profiles being included in each set of sediment-type well profiles used as hard well data in MPS simulations. We used all 539 sediment-type well profiles throughout 100 MPS simulations, but for each MPS simulation a different set of randomly sampled sediment-type well profiles was used.

The development of a training image, Step 6, required an understanding of the large-scale patterns in sediment type in the study area. We approached this by investigating the mean 3D CF model from the AEM data, which was obtained in Step 3. On Page 25, we show the mean 3D CF model and the interpreted surface (yellow) of the base of Paso Robles Formation (Madsen et al., 2020). For visualizing the mean 3D CF model, we omitted grid cells laterally separated by greater than 500 m from the vertical profiles of CF shown on Page 17 . Given that our interest was in the Alluvium and Paso Robles Formation, we only used cells above the base of the Paso Robles Formation. Using the mean 3D CF model, we calculated the vertical integral for each lateral cell on a 2D plane, and generated 2D maps visualizing the vertical CF from AEM, as shown on Pages 26-29. When computing the vertical integral of CF values, we used four different intervals: top to 20 m, 20 m to 50 m, 50 m to the base of the Paso Robles Formation, top to the base of the Paso Robles Formation. On Page 26, we show a 2D CF map at an interval from the top to 20 m. This map delineates the distribution of coarse- and fine-grained materials for the Alluvium and the top part of the Paso Robles Formation. The study area is dominated by coarse-grained materials at this shallow interval. In the northeastern region, we see lens-like features in south-southeast (SSE) direction (see black arrows on Page 26). On Page 27, we show the 2D map at the interval from 20 m to 50 m. What we see here is mostly coarse-grained and fine-grained materials of the Paso Robles Formation. Compared to the top-to-20-m interval, this interval contains a higher percentage of fine-grained materials. In addition, we also identify lens-like features oriented in an eastward direction (see blue arrows on Page 27) in the western region and in a north-northwest (NNW) direction in the south eastern region (see red arrows on Page 27). At a deeper interval, 50 m to the base of the Paso Robles Formation shown on Page 28, we see an apparent smoothing in the level of spatial heterogeneity in the CF map, compared to the upper intervals (e.g., Page 27); this is related to the decreasing resolution of the AEM data with depth. On Page 29, we show a CF map from the interval extending from the top to the base of the Paso Robles Formation which integrates all depth intervals of interest. In general, below the Estrella River, we see more fine-grained materials in the western part of the study area than in the eastern part. We also see regions containing coarse-grained materials in the northeast and the southeast.

The large-scale trends observed in the 2D CF maps, were consistent with the geologic history of paleo-drainages forming the Paso Robles Formation. Our understanding of this history is based on conversations with Paul Sorensen, hydrogeologist with GSI Water Solutions. Cenozoic uplift generated sediments deposition in the basin, forming the Paso Robles Formation occurring in the early Pliocene. The uplift of the Santa Lucia Range, located northwest of the study area, resulted in the eastward deposition of marine sediments (see blue arrows in Page 27), while the uplift of the La Panza Range, located on the southeast side of the study area, resulted in the deposition of sediments derived from sandstone and granitic materials in the NNW direction (see red arrows in Page 27). We see more fine-grained materials in the west than in the east in the 2D CF map for the interval from the top to the base of the Paso Robles Formation (shown on Page 29). Near the end of the Pliocene, uplift resulted in the formation of Temblor Range, and the subsequent sediment deposition occurred in the SSE direction (see black arrows in Page 26). We interpreted the coarse-grained materials in the northeast as related to this depositional event. When the Paso Robles Formation was created, it was likely deposited as channel deposits, but due to significant subsequent deformation the channel shapes were not preserved. Therefore, our conceptual geologic model is the presence of sand lenses embedded in a clay background.

Using the above understanding of the depositional environment, we created a training image. To simulate the shape of the lenses, we used a half-ellipsoid as shown on Page 33. A table on Page 33 summarizes parameters used to define our training image. The proportion of coarse-dominated was set to 0.36 based upon the proportion of coarse-dominated in sediment-type well profiles. The range for the thickness of the ellipsoid, representing a lens, was determined by variogram analysis of the sediment-type well profiles. The ranges for the width, length, and direction of the ellipsoid were determined based upon observations of (a) the 2D CF maps, (b) Google Earth images showing channels along the Salinas River, and (c) our geologic knowledge about the deposition history. We used a utility code, *tiGenerator,* included in an open-source

geostatistical software package, *SGeMS* (Remy et al., 2009), to construct the training image shown on Page 34. Given the history of paleo-drainage originating from the three different ranges: Santa Lucia, La Panza, and Temblor, we delineated three different regions, aligning the major axis of the coarse-grained lenses within each region with the direction of deposition. As shown on the right-hand side of Page 34, we distinguished three different regions: west, southeast, and northeast. We correspondingly assigned east, NNW, and SSW directions for the orientation of the major axes. Corresponding azimuthal angles are 90, -20, and 20 degrees; the azimuthal angle is defined as 0 in the northward direction, increasing in the clockwise direction.

All three inputs for the MPS simulations were developed as illustrated on Page 35, and were used to generate 200 MPS sediment-type models. For our MPS simulations we used a *SNEISM* algorithm, which is included in *SGeMS* (Remy et al., 2009). For each MPS simulation, we used the same sediment-type starting probability model and training image, but a different set of sediment-type well profiles as illustrated in Step 5. The target percentage of the coarse-dominated was set to 36% based up on the percentage of coarse-dominated in the sediment-type well profiles, which is an input parameter of the MPS simulation; other parameters of the algorithm were set to default values. Each MPS simulation was performed in the entire 3D grid; we then extracted the cells below the base of the Paso Robles Formation.

Shown on the left-hand side of Page 36, is a 3D view of an output MPS sediment-type model. On the right-hand side of Page 36, is a 3D view of the three different regions to which we assigned different orientation directions for the sand lenses. We see the directional trends input into the MPS simulation. The starting probability model of coarse-dominated, on the right hand side of Page 37, shows that the large-scale trend in this model is captured in the MPS sediment-type model. On Page 38, we show two output MPS sediment-type models. Although we have shown only two MPS sediment-type models, we captured the uncertainty by obtaining 198 more models. This ensemble of MPS sediment-type models was used in the later section to assess potential recharge areas.

COMPARISON WITH GEOLOGIC SECTIONS

From the application of the MPS method, we obtained the starting probability model as well as 100 realizations of the MPS sediment-type model. In this section, we compare the starting probability model of coarse-dominated and MPS sediment-type models with geologic cross-sections from the study area: A-A', B-B', and E-E', marked as black lines on Page 40. Pages 41-57 show our comparison, with red and blue shaded colors indicating the coarse-dominated and fine-dominated and vertical cylinders representing the sediment-type well profiles. 3D grid cells below the base of the Paso Robles Formation are shaded with a block pattern.

ASSESSING POTENTIAL RECHARGE AREAS

By using all 200 MPS sediment-type models obtained from the MPS simulations, we examined the extent of the clay layer at the Estrella River. Local agencies are interest in the potential for recharge along the Estrella River. The presence of the clay layer could impede water infiltrating from the surface to aquifers in the Paso Robles Formation, so there is a desire to identify locations where the clay layer is thin or absent.

Shown on the left-hand side of Page 59 is an E-W vertical section of the starting probability model of coarse-dominated. The plan view map showing the location of the vertical section is shown on the right-hand side of Page 59 as a red line; the black and blue lines in this figure indicate the location of AEM soundings and the Estrella River, respectively. We see thin coarse-dominated materials in the top 10-20 m, and fine-dominated materials below (~50 m-thick), which correspond to the clay layer. Below the clay layer, there is a thick coarse-dominated layer interpreted as an aquifer unit in the Paso Robles Formation. The

clay layer, identified at the Estrella River, is extensive within the study area. The red surface shown on Page 60 indicates the base of the clay layer which we interpreted using the starting probability model of coarse-dominated. Given the extensive nature of the clay layer, we extended our region of interest to the entire study area.

Our objective was to obtain many 2D maps of the percentage of coarse-dominated displaying regions where the clay layer is absent or thinning. A 2D map of percent coarse-dominated is generated by computing the vertical percentage of coarse-dominated from the base of the clay layer to the surface using an MPS sediment-type model. This process was repeated for all 200 MPS sediment-type models resulting in 200 2D maps of percent coarse-dominated. The obtained 2D maps of percent coarse-dominated provide useful information for locating potential recharge activities in the study area. Three example maps of percent coarse-dominated are shown on Pages 62 to 64; here, the grey shaded area indicates that the underlying units of the Paso Robles Formation are exposed at the surface. The mean of the percent coarse-dominated maps is shown on left-hand side of Page 65 displaying our best estimate of percent coarse-dominated, vertically integrated from the base of the clay layer to the surface. The standard deviation of the 2D maps of percent coarse-dominated displays the uncertainty; the darker color indicates a low level of uncertainty. On average, the standard deviation is about 18%, which we interpret as a relatively low level of uncertainty.

On the left-hand side of Page 66, we show the 40% contour from the mean of the percent coarse-dominated maps as black lines; we also show other streams in the study area as blue dashed lines. Along the Estrella River, we see relatively low values of percent coarse-dominated (<40%) except for small zones on the eastern side of the river. We interpret there being low recharge potential along the river in the western half of the figure on the left and higher potential in the eastern half. In the northeast side of the river, and basin in general, we see low values of percent coarse-dominated (~10%) except for a few small zones as shown on Page 67. In contrast, as shown on Page 68, along the Huer Huero Creek and Shedo Canyon, we see relatively high values of percent coarse-dominated (>40%). We interpret there being high recharge potential along the Huer Huero Creek and Shedo Canyon. Finally, the 2D map of percent coarse-dominated that we provided is not likely to be capturing spatial variation in the soil in top 30 cm, so we recommend integrating other soil maps with the percent coarse-dominated map when assessing potential recharge locations in the study area.

INTERACTIVE VISUALIZATION OF RESULTS

To facilitate interaction between Stanford researchers and those involved with groundwater management in San Luis Obispo County, we have provided the results of our study with a project file that can be viewed with a leapfrog viewer. This viewer is freely available at the leapfrog viewer website: https://my.seequent.com/releases/leapfrog-viewer/latest; setting up an ID is required to download the viewer. The project file is available through this link.

The project file includes:

1. Starting probability of coarse-dominated (3D grid)
2. An example of an output MPS-sediment type model (3D grid)
3. Sediment-type wells (vertical profiles)
4. Topographic surface (surface)
5. Base of the clay layer (surface)
6. Geologic sections (vertical sections) including: A-A', B-B', E-E'
7. The 2D CF map from top to the base of the Paso Robles Formation
8. Mean of percent coarse-dominated maps (vertical percentage of coarse-dominated from the base of the clay layer to the surface)
9. TDS data compiled from Geotracker (colored points; 155 (blue) -1000 (red))

REFERENCES

Cockett, R., S. Kang, L. J. Heagy, A. Pidlisecky, and D. W. Oldenburg, 2015, SimPEG: An open source framework for simulation and gradient based parameter estimation in geophysical applications: Computers & Geosciences, **85**, **Part A**, 142–154.

Dewar, N., and R. Knight, 2020, Estimation of the top of the saturation zone from airborne electromagnetic data: Geophysics, **85**, EN63–EN76.

Goebel, M., and R. Knight, 2020, Recharge Site Assessment Though the Integration of Surface Geophysics and Cone Penetrometer Testing: Geophyics.

Kang, S., D. Fournier, D. Werthmüller, J. L. Heagy, and W. D. Oldenburg, 2019, simpegEM1D: gradient-based 1D inversion for large-scale airborne electromagnetic data: AGU Annual Meeting 2018.

Knight, R., R. Smith, T. Asch, J. Abraham, J. Cannia, A. Viezzoli, and G. Fogg, 2018, Mapping Aquifer Systems with Airborne Electromagnetics in the Central Valley of California.: Ground Water.

Madsen, T., T. Parker, and M. Halkjær, 2020, HYDROGEOLOGIC CONCEPTUAL MODEL IN PASO ROBLES TRADITIONAL HCM:

Remy, N., A. Boucher, and J. Wu, 2009, Applied Geostatistics with SGeMS: A User's Guide: Cambridge University Press.

Sorensen, P. A., M. M. Javaherian, and M. Maley, 2005, PASO ROBLES GROUNDWATER BASIN STUDY PHASE II: NUMERICAL MODEL DEVELOPMENT, CALIBRATION, and APPLICATION:

Viezzoli, A., A. V. Christiansen, E. Auken, and K. Sørensen, 2008, Quasi-3D modeling of airborne TEM data by spatially constrained inversion: Geophysics, **73**.

Application of a multipoint statistics method to assess potential recharge areas in San Luis Obispo County, California

Seogi Kang, Rosemary Knight, Jef Caers

NOTE – this presentation contains the figures referred to in the accompanying report. This is not intended to be a stand-alone document. All details, definitions of terms, etc. are in the report.

Location map

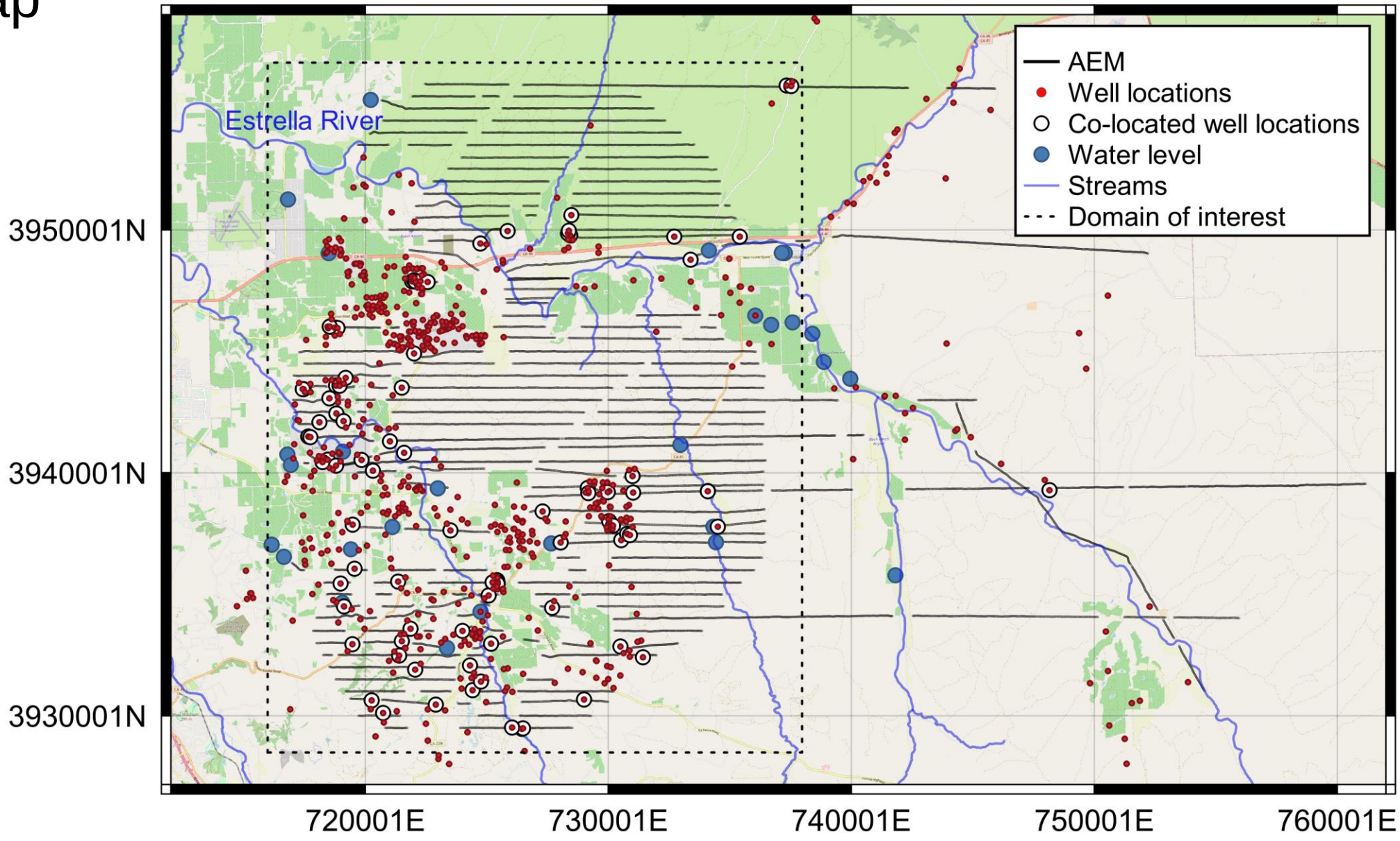

Question

What is the lateral extent of the clay layer at the Estrella River?

"The nature of the near-surface sediments along the Estrella River and if/how they transition to coarser materials away from the river to the northeast. This issue has two potentially significant benefits: 1) better understanding of how surface water in the Estrella River recharges the underlying Paso Robles Formation for evaluation of potential recharge-related areas, and 2) potentially focusing on active surface infiltration projects (recharge projects) on the northeast flank of the river and basin, rather than focusing on the river itself, which appears to me to be a poor location for recharge projects." (from Paul)

Our final model is sediment type

Distribution of coarse-grained (sand)-dominated and fine-grained (clay)-dominated.

Will be referred to as coarse-dominated and fine-dominated

Uncertainty is displayed as probability of coarse-dominated

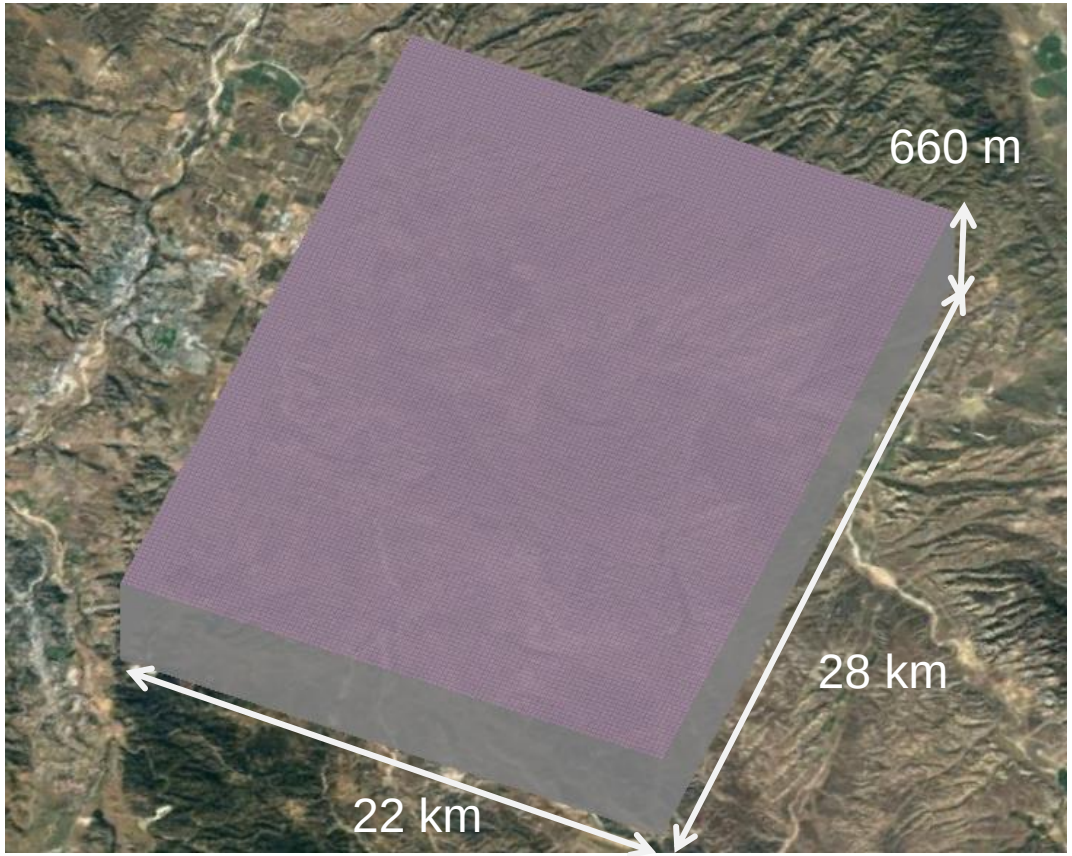

We define sediment type on this grid:

3D grid information
- 200 m x 200 m x 5 m cell
- # of cells = 110 x 142 x 132 = ~ 2M

Why 200 m x 200 m x 5 m cell?
- horizontal: size of the basin groundwater model grid
- vertical: trade-off resolution between AEM and well

Sediment type (Z= 0 or 1)

Z=1 means coarse-dominated

Z=0 means fine-dominated

Multi-point statistics (MPS) method

Sediment-type starting probability model from AEM

Hard well data

Training image (geologic patterns)

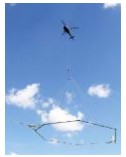

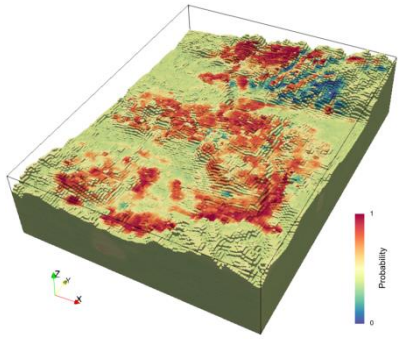

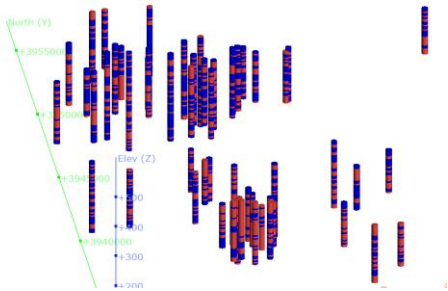

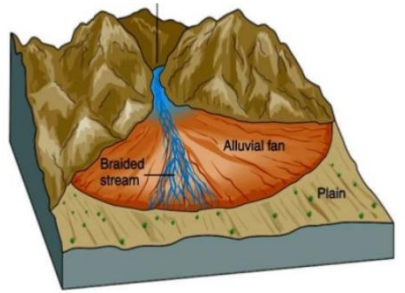

Find multiple sediment type models (coarse-dominated /fine-dominated) satisfying all three inputs

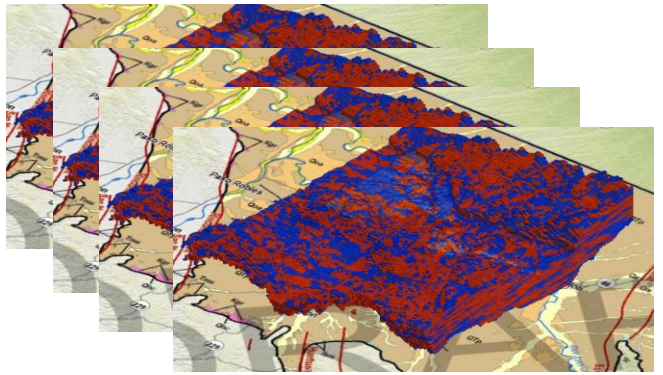

Workflow

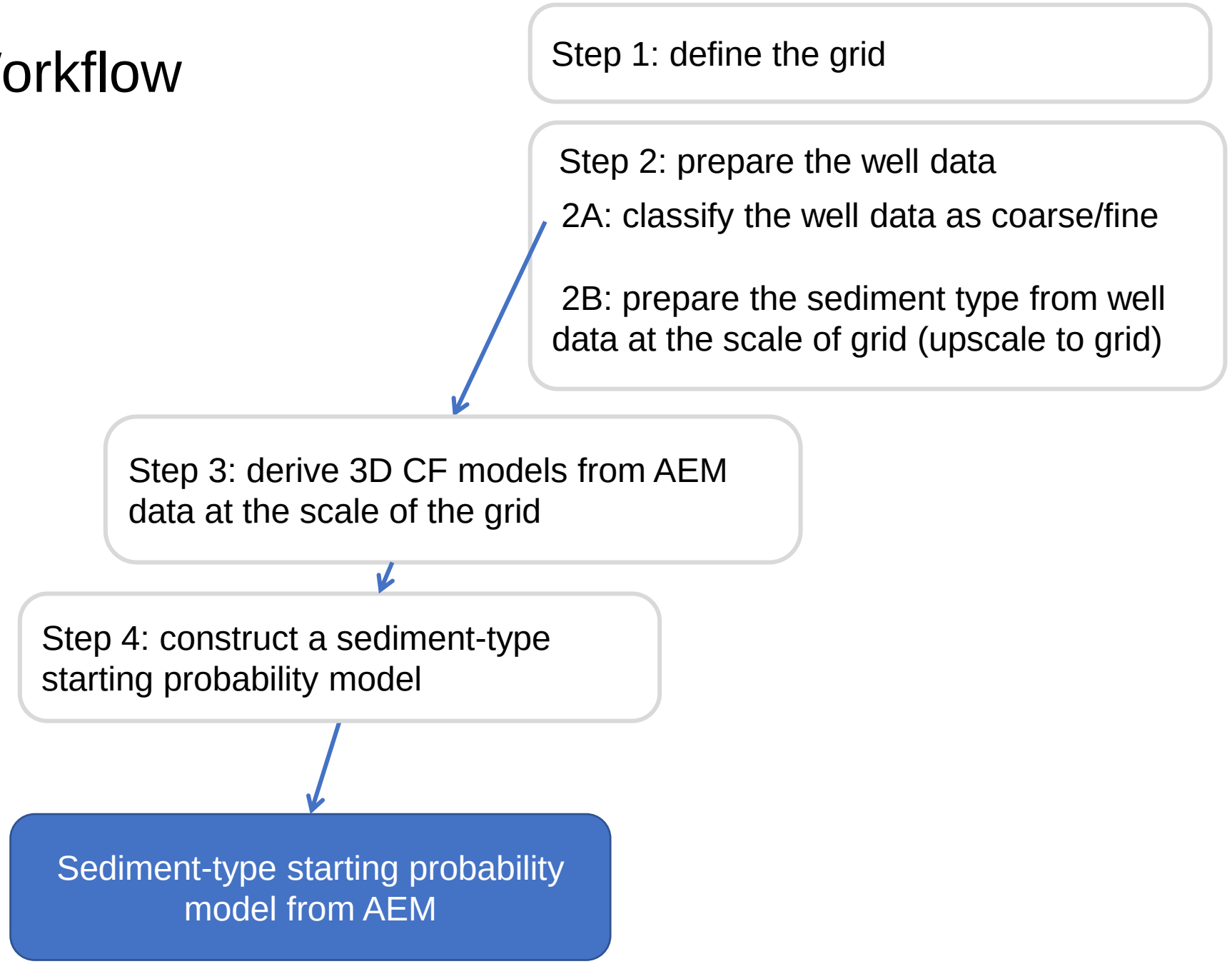

CF: coarse fraction
MPS: multi-point statistics

Workflow

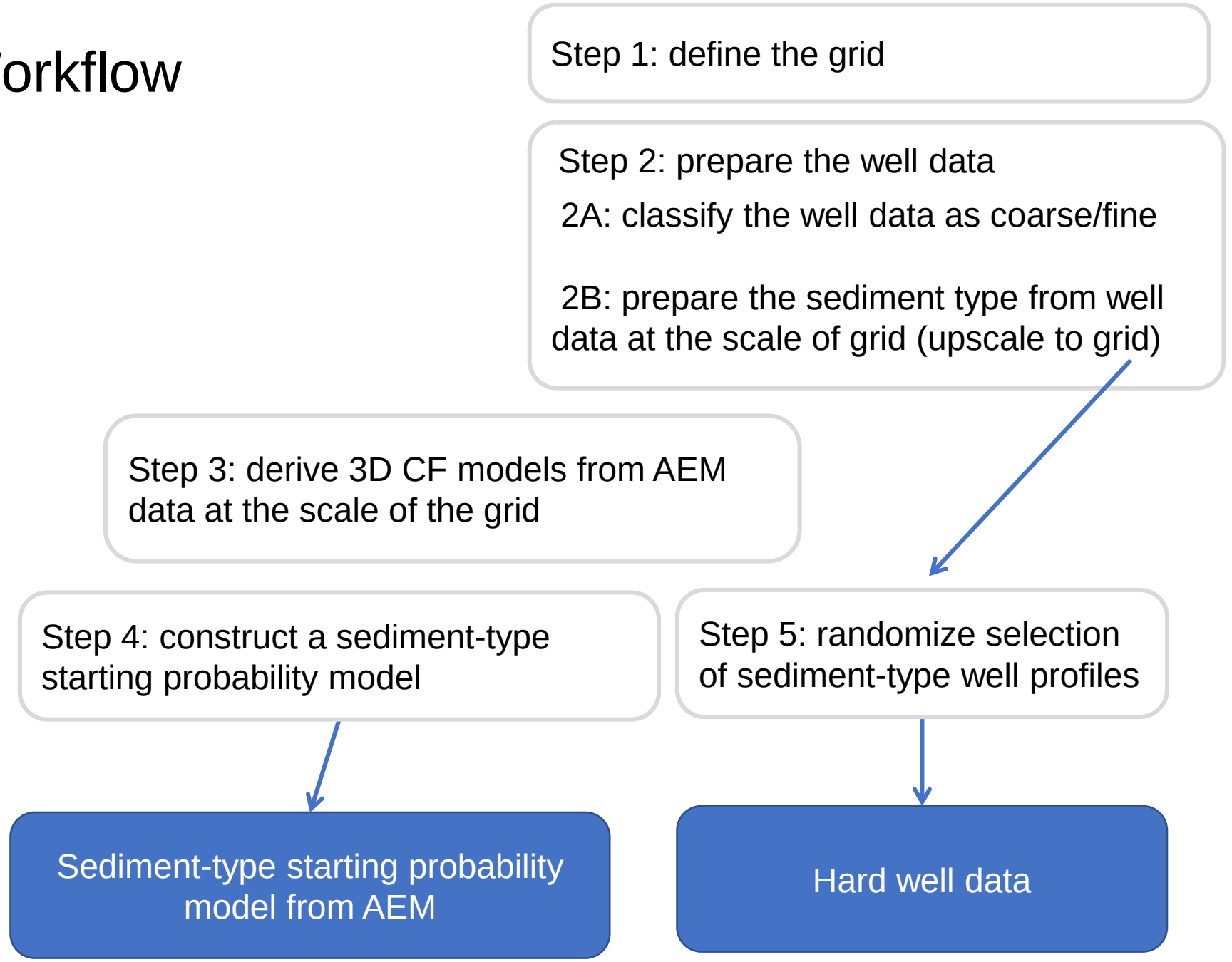

CF: coarse fraction
MPS: multi-point statistics

Workflow

Step 1: define the grid

Step 2: prepare the well data

2A: classify the well data as coarse/fine

2B: prepare the sediment type from well data at the scale of grid (upscale to grid)

CF: coarse fraction
MPS: multi-point statistics

Step 3: derive 3D CF models from AEM data at the scale of the grid

Step 4: construct a sediment-type starting probability model

Step 5: randomize selection of sediment-type well profiles

Step 6: create a training image

Sediment-type starting probability model from AEM

Hard well data

Training image

Step2: Prepare the well data

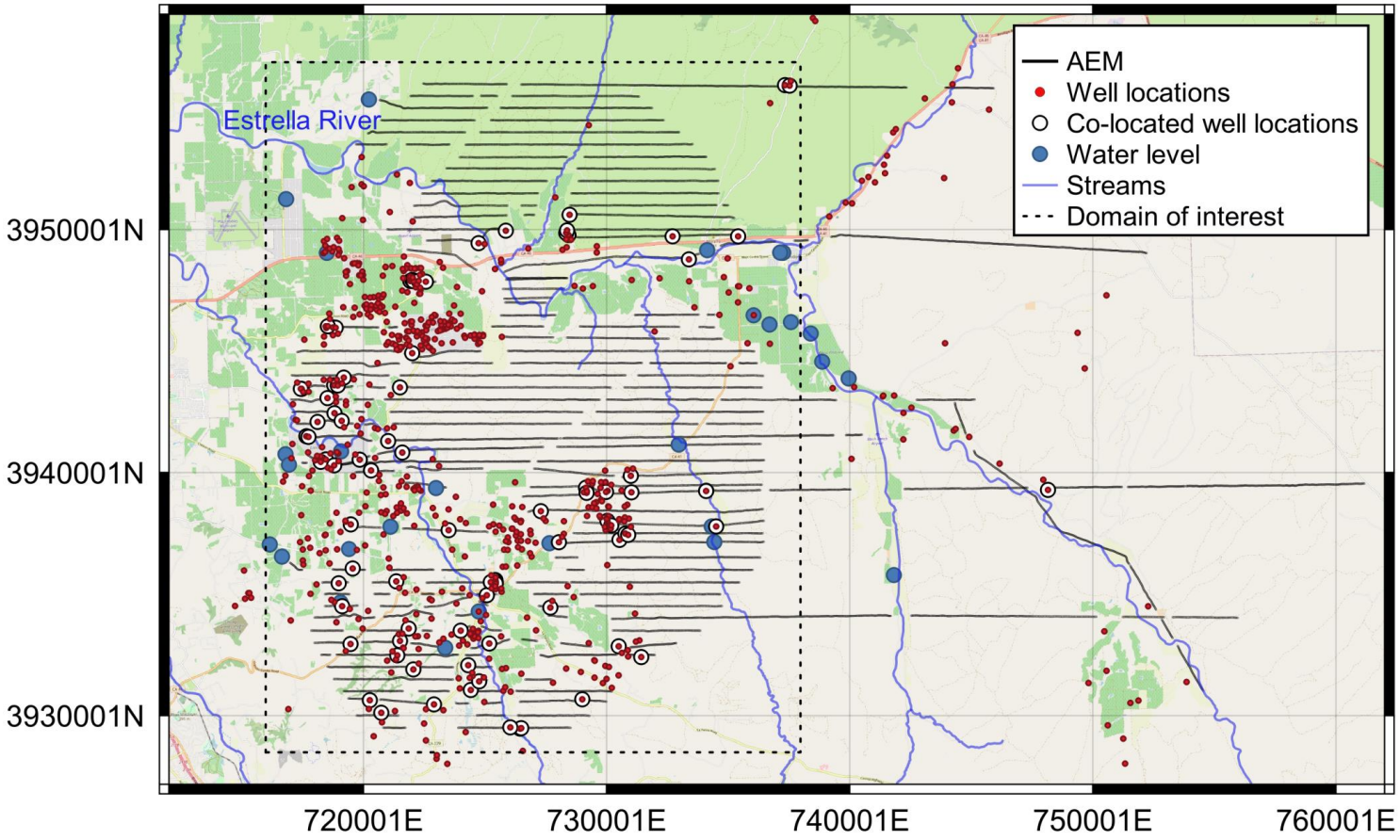

Start with 731 drillers' log from IGIS

- Quality ranking with locational uncertainty
- Quality 1: < 50 m
- Quality 2: 50-100 m
- Quality 3: 100-150 m

Use all of the wells.

Step2A: classify the well data as coarse/fine

Starting information – the descriptions from a driller's log

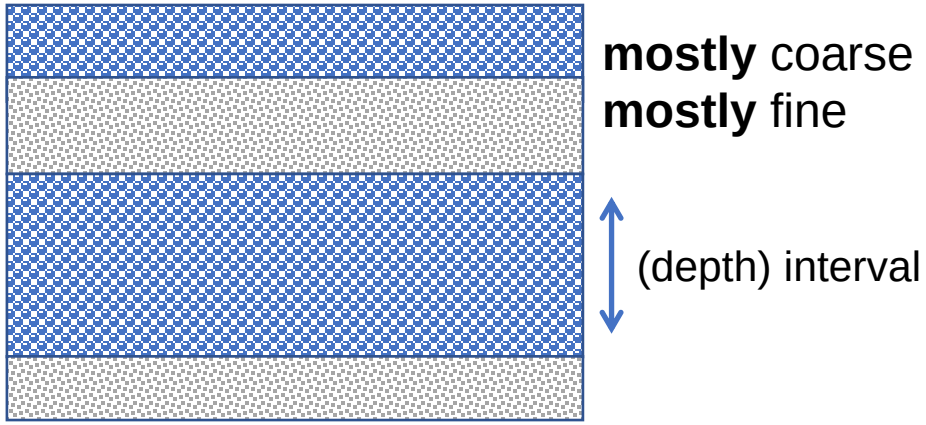

CLASSIFY*

A classified driller's log

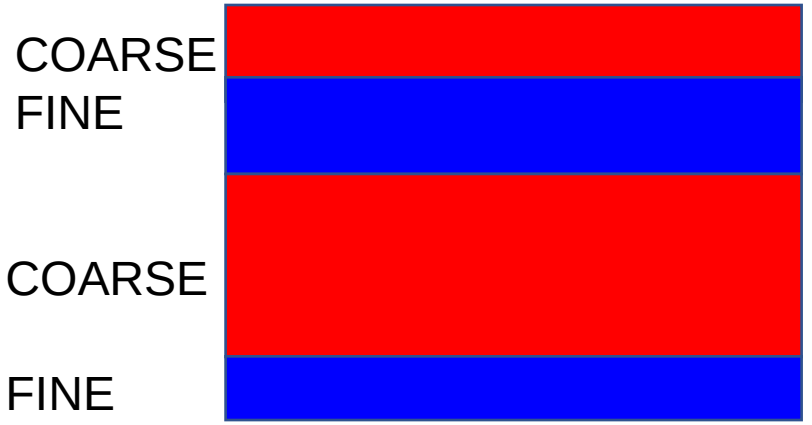

Well SCALE

Well SCALE

* All intervals that are mostly coarse are classified as coarse; all intervals that are mostly fine are classified as fine.

Step2B: prepare the sediment-type from well data at scale of grid

First, vertical upscaling to coarse fraction (CF)

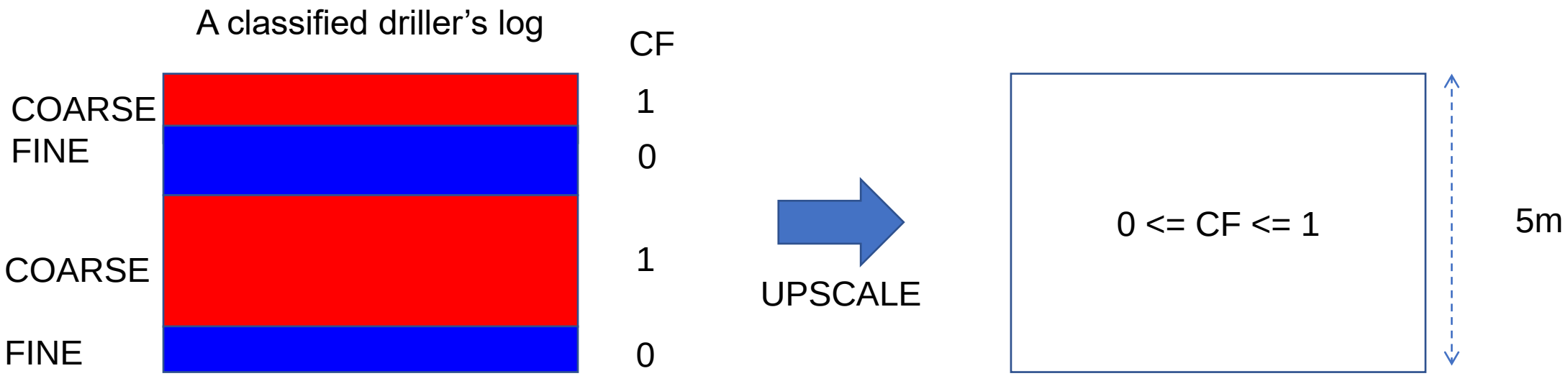

Well SCALE

VERTICAL GRID SCALE
of final model

Step2B: prepare the sediment-type from well data at scale of grid

Upscaling coarse fraction to the lateral dimension of the model cells

Average CF if multiple wells are in a cell (left with 539 CF well profiles)

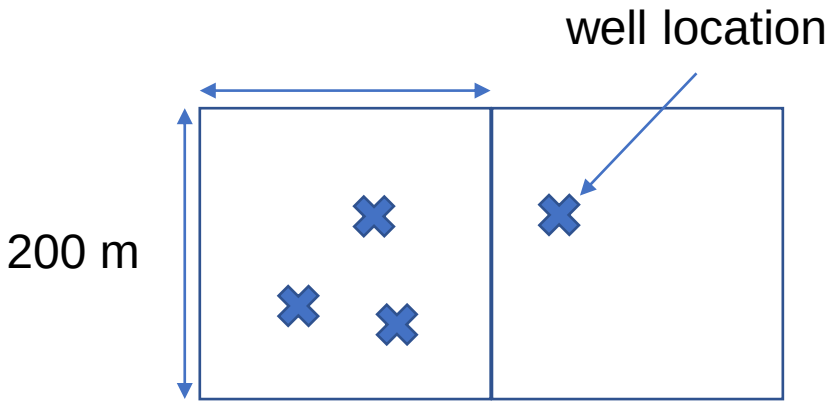

Wells outside of the grid are omitted for modeling.

Total 539 CF well profiles at the scale of the grid

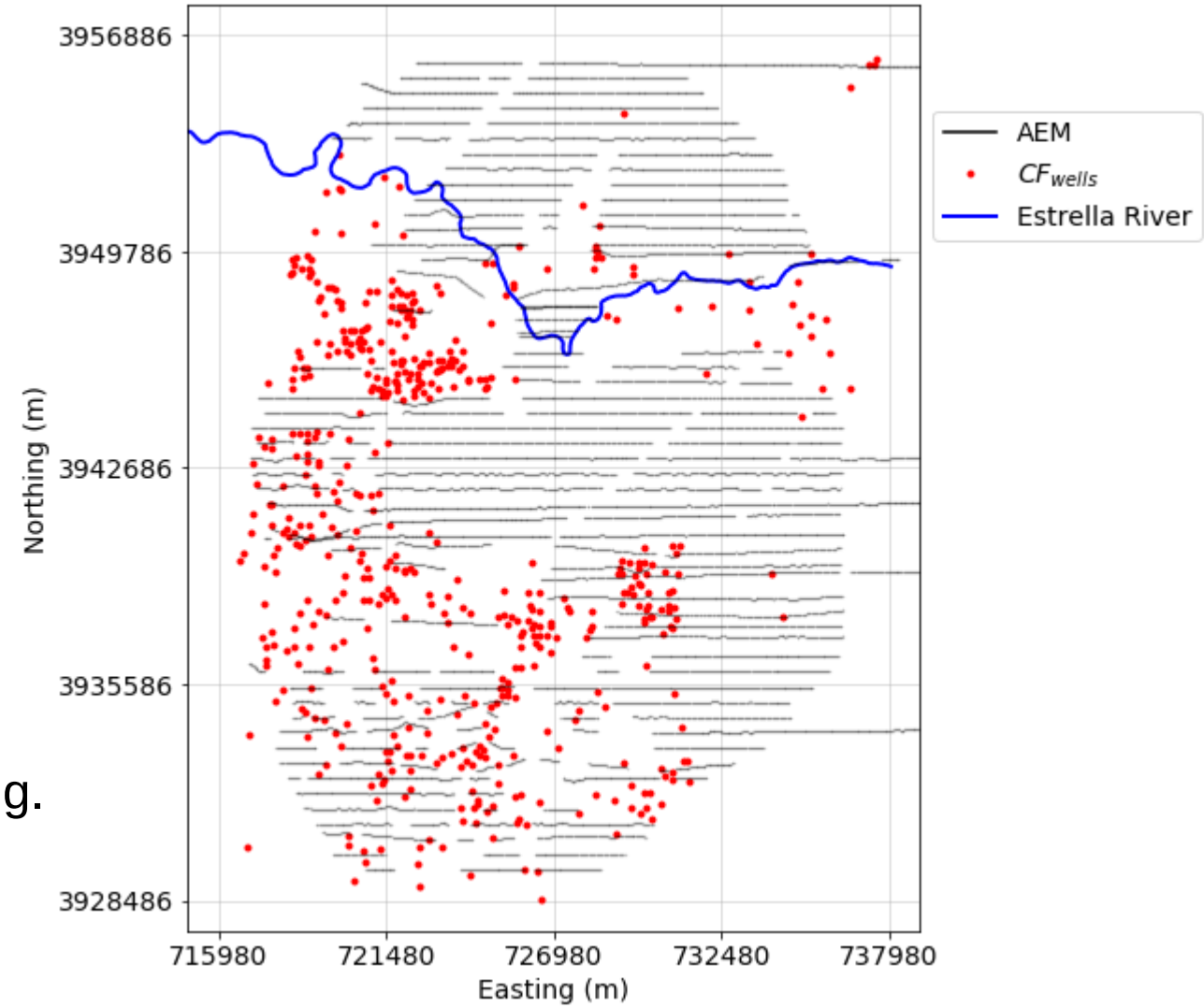

Step2B: prepare the sediment-type from well data at scale of grid

Coarse-fraction well profiles

CF >= 0.5 is coarse-dominated
CF < 0.5 is fine-dominated

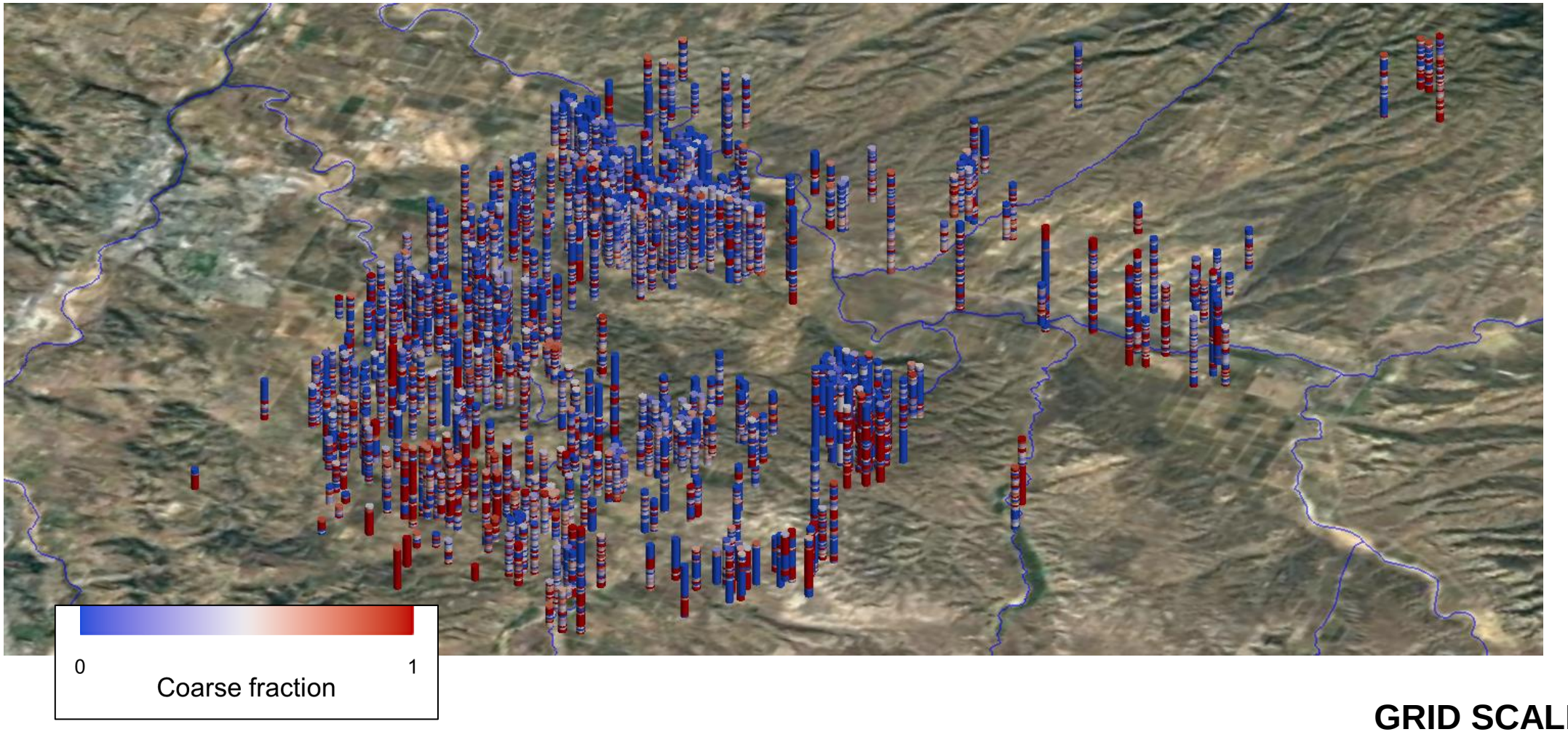

GRID SCALE

Step2B: prepare the sediment-type from well data at scale of grid

Sediment-type well profiles

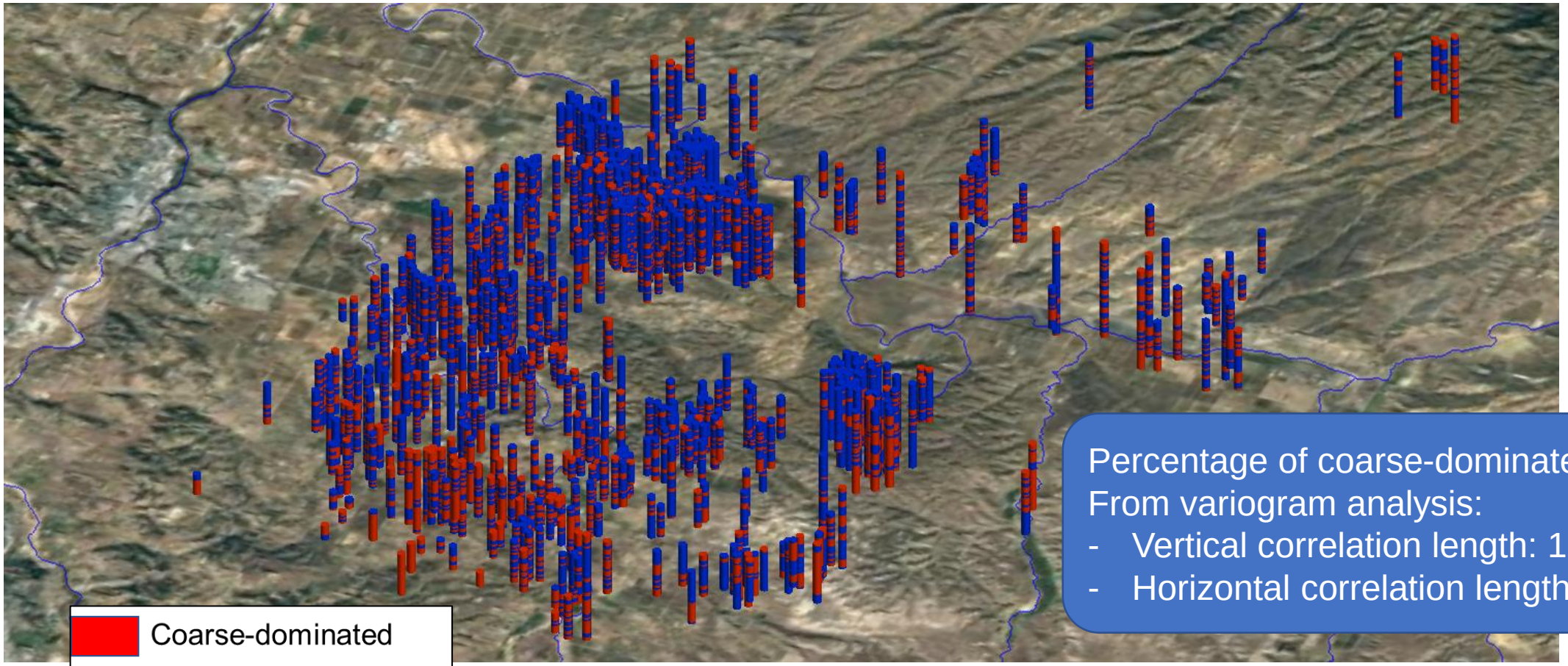

Percentage of coarse-dominated: 36%
From variogram analysis:
- Vertical correlation length: 10-20 m
- Horizontal correlation length: ~500 m

GRID SCALE

Workflow

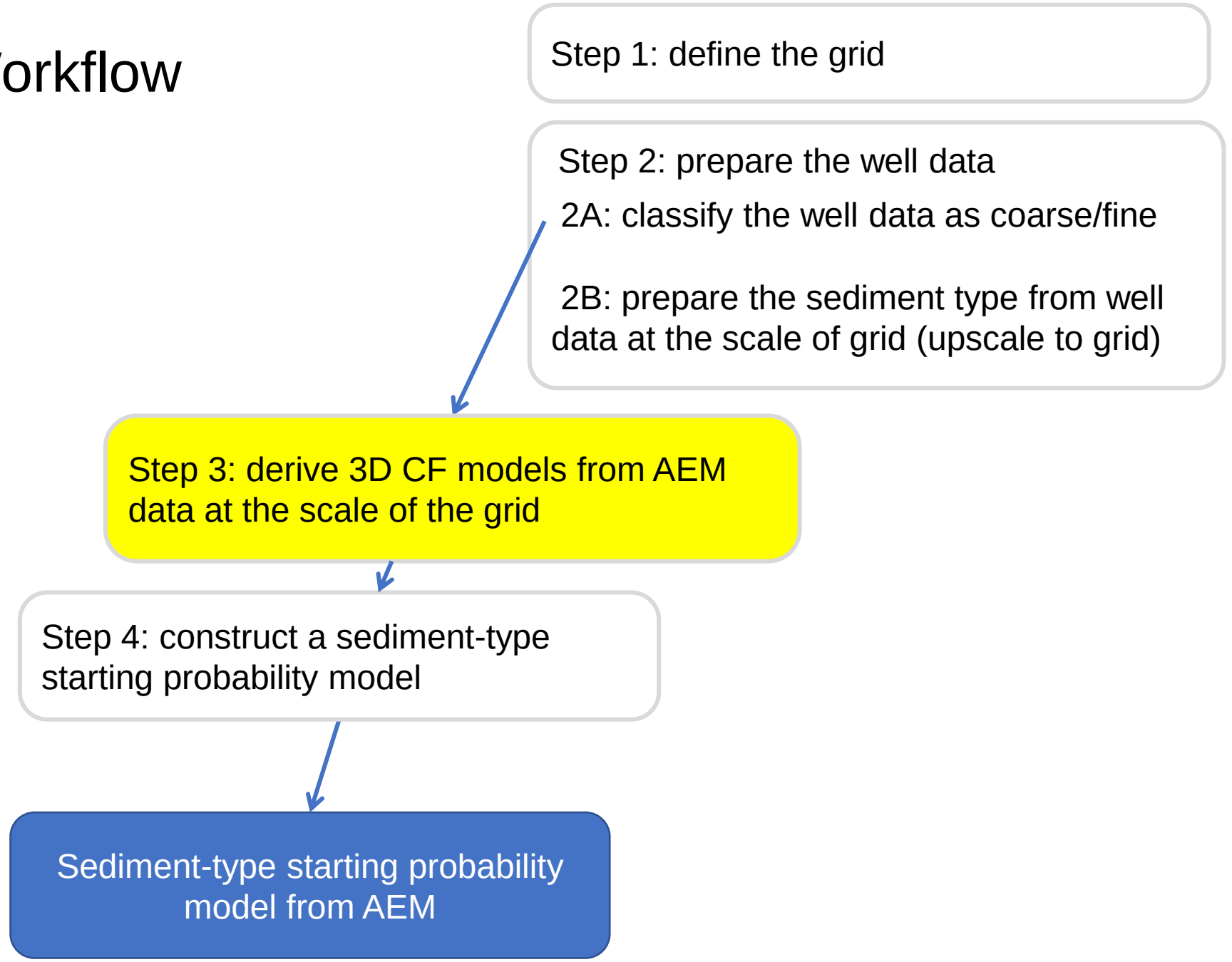

CF: coarse fraction
MPS: multi-point statistics

Step3: derive 3D CF models from AEM data at the scale of grid

- Step3A: AEM inversions
  - Invert AEM data, and obtain many resistivity models
  - Select mean resistivity model as our primary resistivity model

AEM SCALE

- Step3B: Rock physics transform
  - Use the co-located resistivity profiles (from the primary resistivity model and well data to construct relationship between resistivity and CF)
  - Transform all resistivity models to CF models

AEM SCALE

- Step3C: Interpolation to the 3D grid

GRID SCALE

Displaying the mean values (in each cell) of 2002 CF models

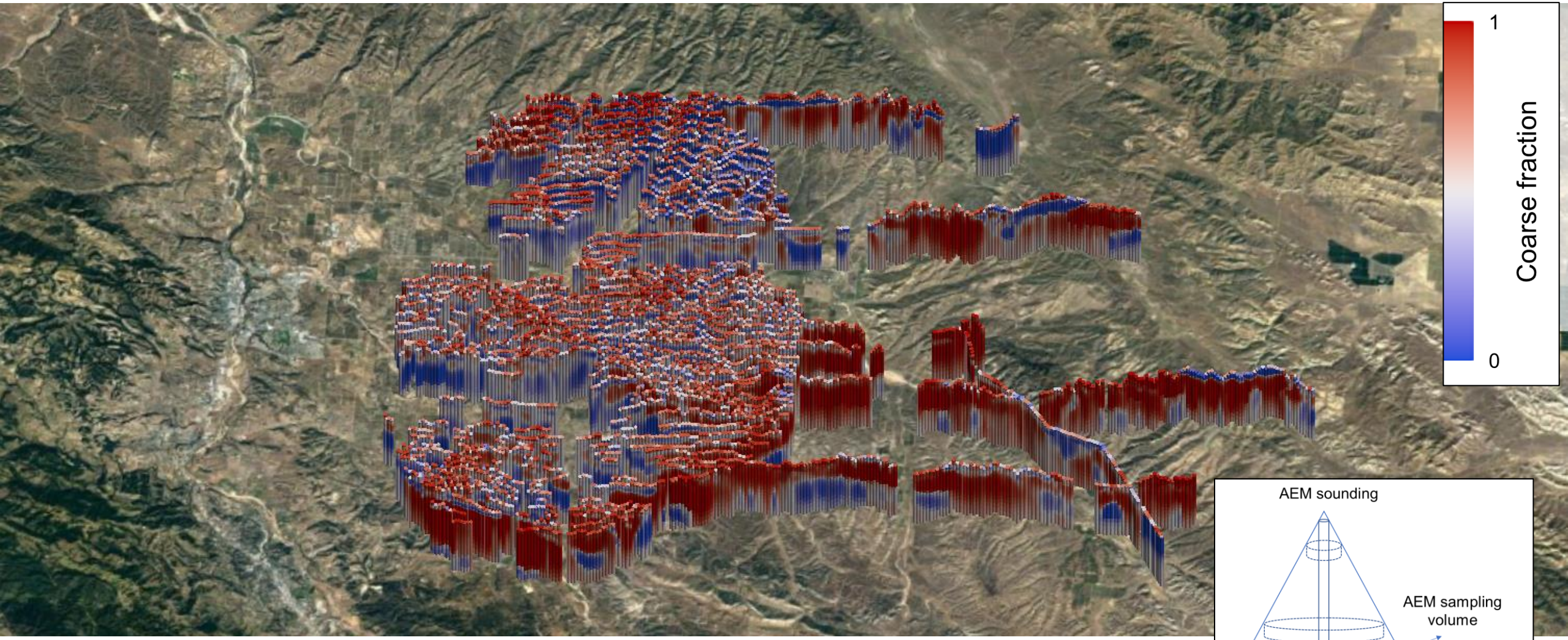

The AEM sampling volume is the volume of the subsurface that contributes to the sounding.

Standard deviation of 2002 CF models

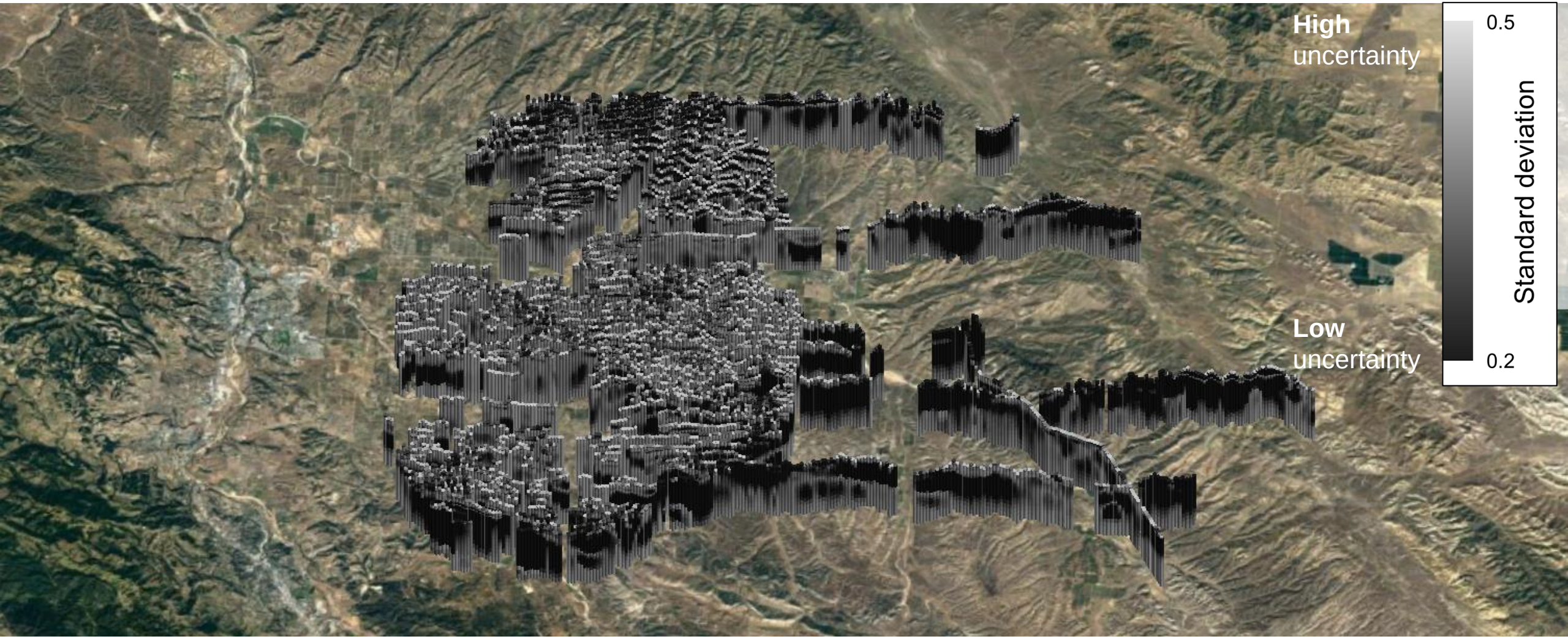

Obtain many 3D CF models from AEM

3D CF models

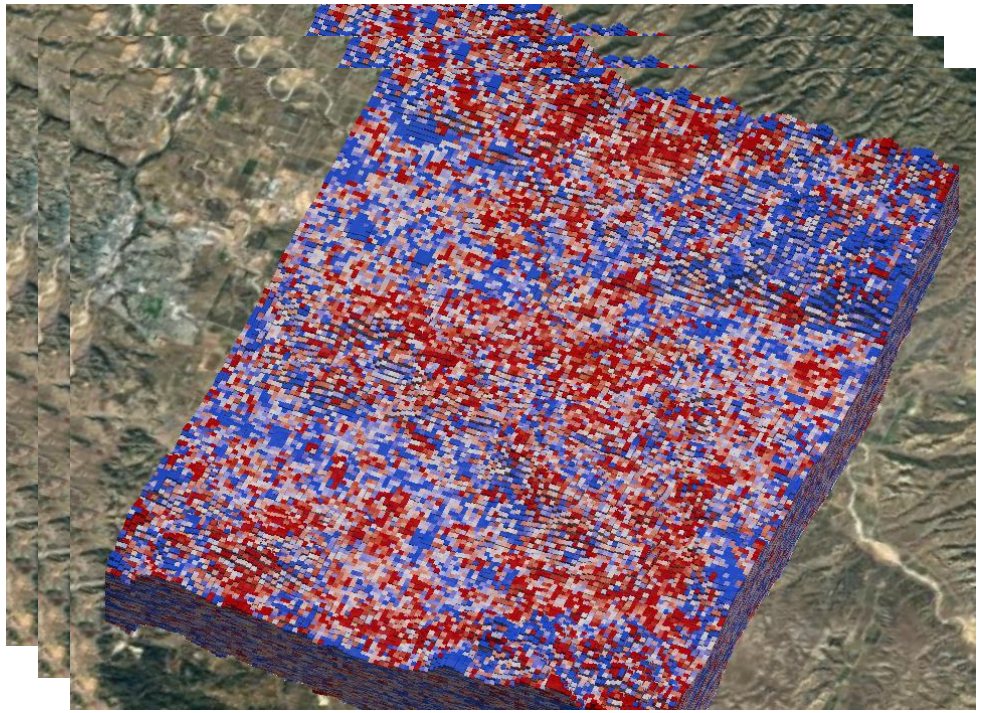

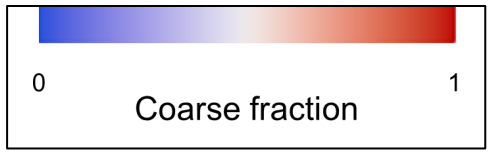

Mean of 3D CF models

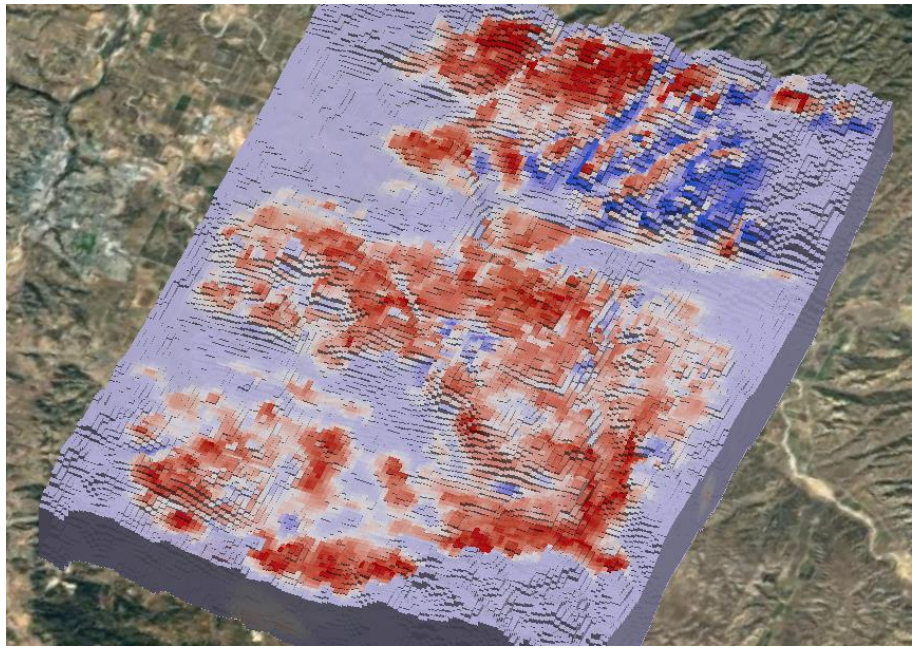

Step4: Construct a starting sediment-type probability model

3D CF models

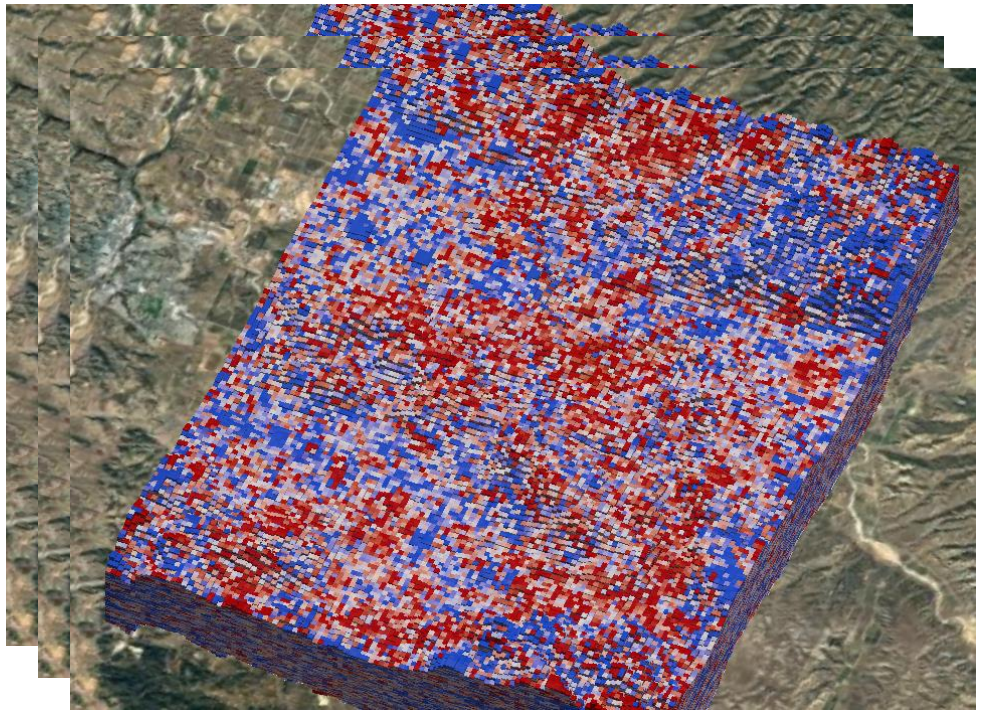

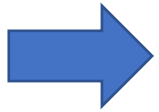

3D sediment-type models

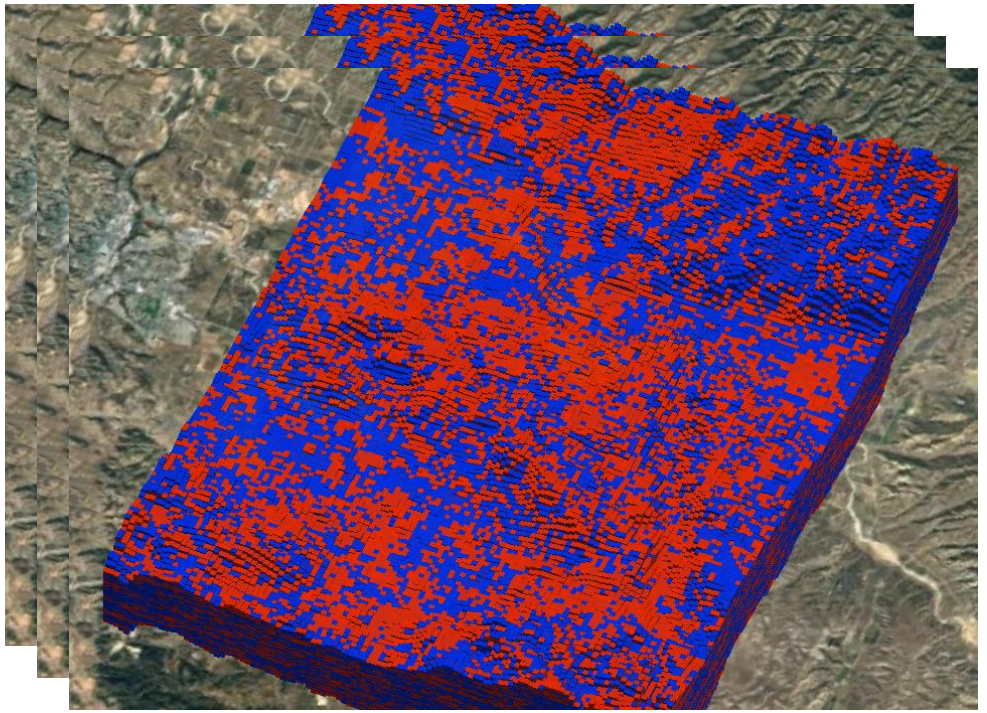

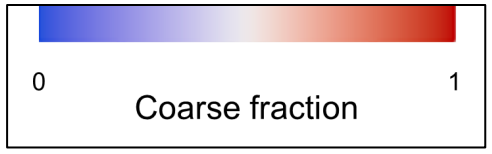

CF >= 0.5 is coarse-dominated
CF < 0.5 is fine-dominated
(above is Equation 1 in accompanying report)

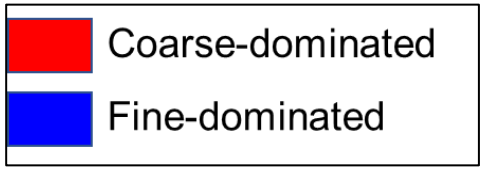

Step4: Construct a starting sediment-type probability model

3D sediment-type models

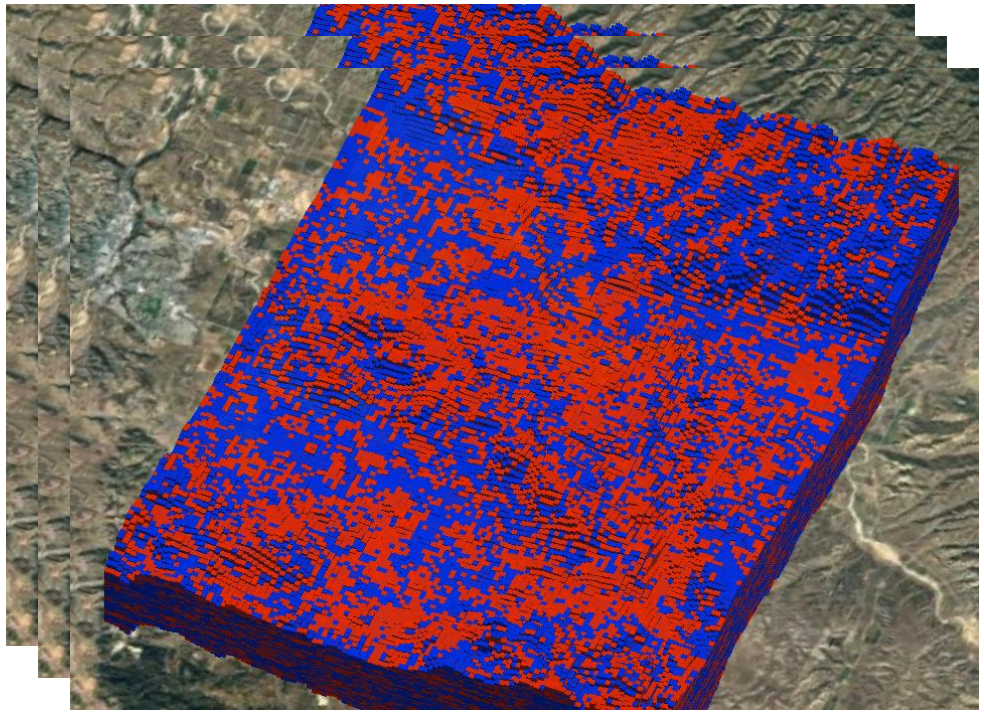

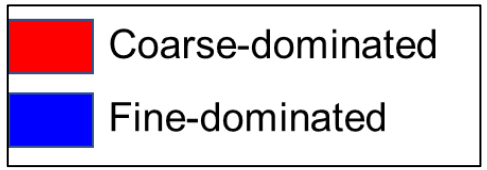

Probability model of coarse-dominated

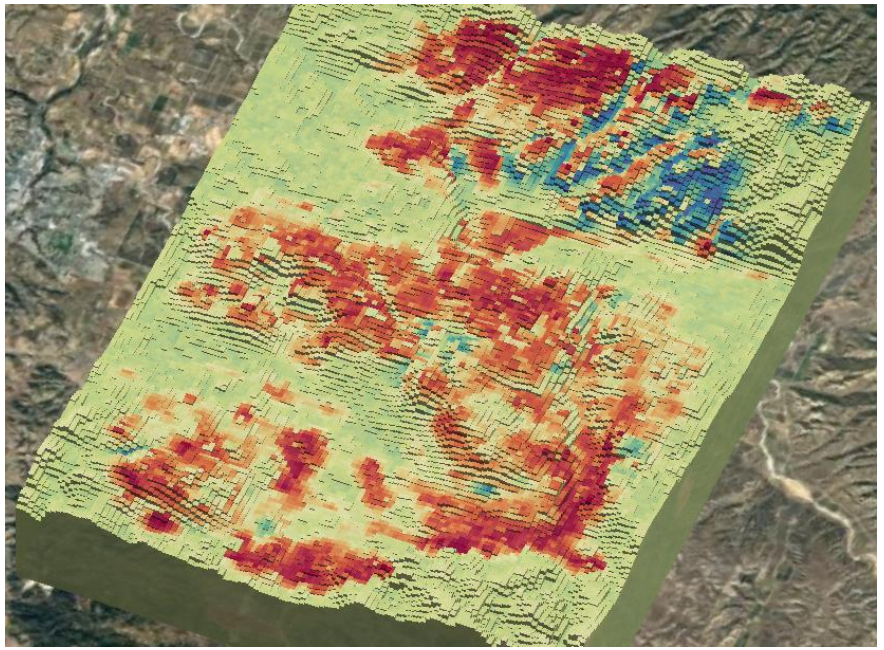

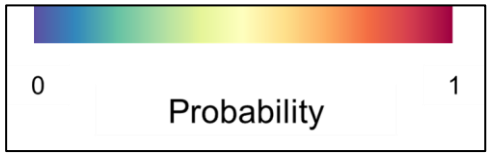

Workflow

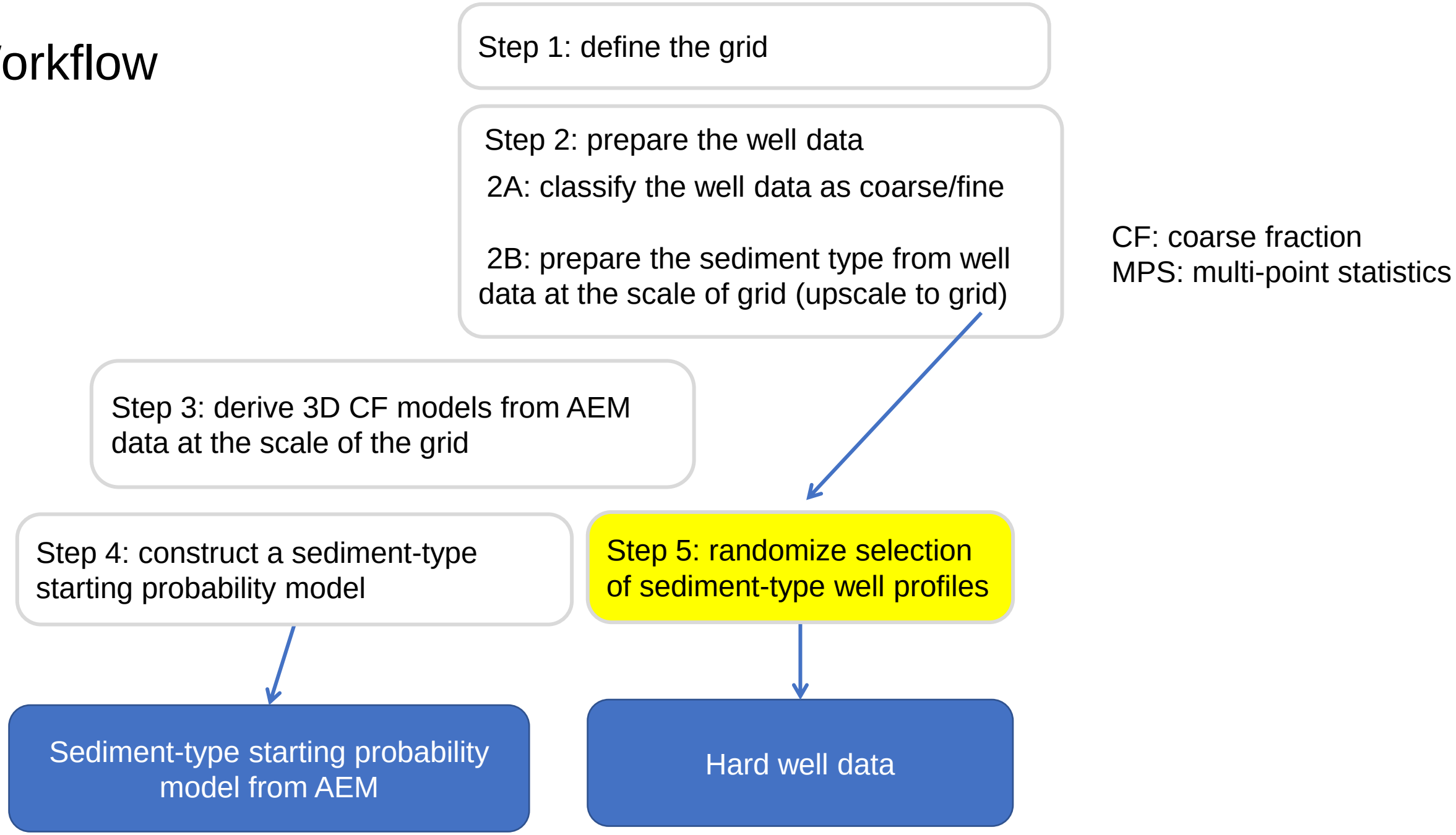

CF: coarse fraction
MPS: multi-point statistics

Step5: Randomize selection sediment-type well profiles

- Quality of drillers' logs varies due to many reasons
  - Drilling method
  - Care taken in preparing drillers' logs
  - Human errors in the digitization process

- There has been no classification of the quality of the drillers' logs, other than to rank in terms of location accuracy.
- We therefore randomized this selection process and generated many sets of sediment-type wells.
- For each MPS simulation we used a different set of sediment-type well profiles.
- As a result, we used all sediment-type well profiles, but in a randomized fashion.

Workflow

Step 1: define the grid

Step 2: prepare the well data

2A: classify the well data as coarse/fine

2B: prepare the sediment type from well data at the scale of grid (upscale to grid)

CF: coarse fraction
MPS: multi-point statistics

Step 3: derive 3D CF models from AEM data at the scale of the grid

Step 4: construct a sediment-type starting probability model

Step 5: randomize selection of sediment-type well profiles

Step 6: create a training image

Sediment-type starting probability model from AEM

Hard well data

Training image

Mean of 3D CF models from AEM with Paso Robles Fm.

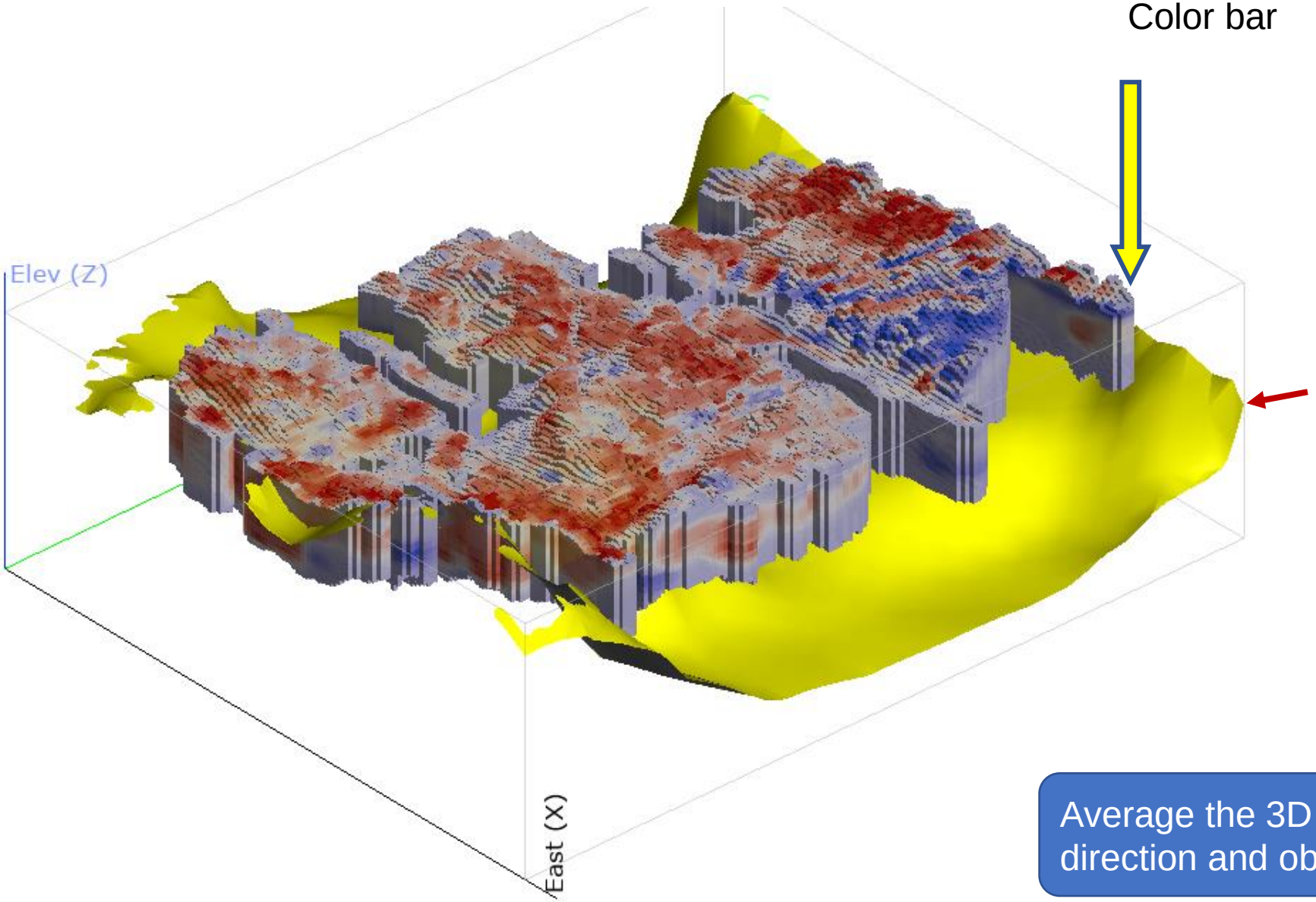

Color bar

Base of the Paso Robles Formation (from Ramboll)

Average the 3D coarse fraction in vertical direction and obtain a 2D map

Vertically integrated CF map from the AEM data
(within Paso Robles Fm.)

Estrella River

Depth slices:

- Top to 20 m
- 20 m to 50 m
- 50 m to base of Paso Robles Fm.
- Top to base of Paso Robles Fm.

Mostly coarse Alluvium

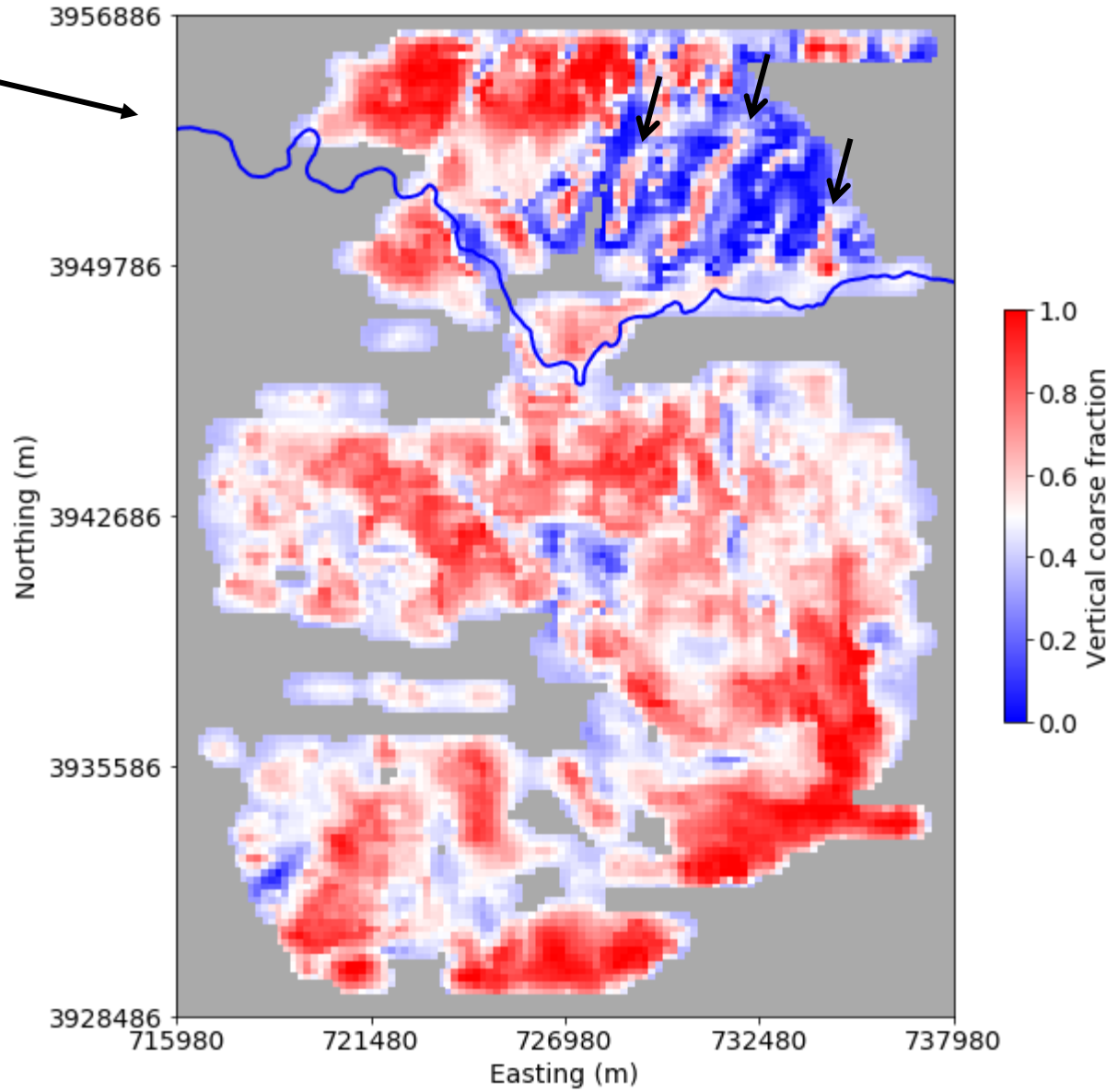

Vertically integrated CF map from the AEM data
(within Paso Robles Fm.)

Estrella River

Depth slices:

- Top to 20 m
- 20 m to 50 m
- 50 m to base of Paso Robles Fm.
- Top to base of Paso Robles Fm.

Much finer Paso Robles Fm.

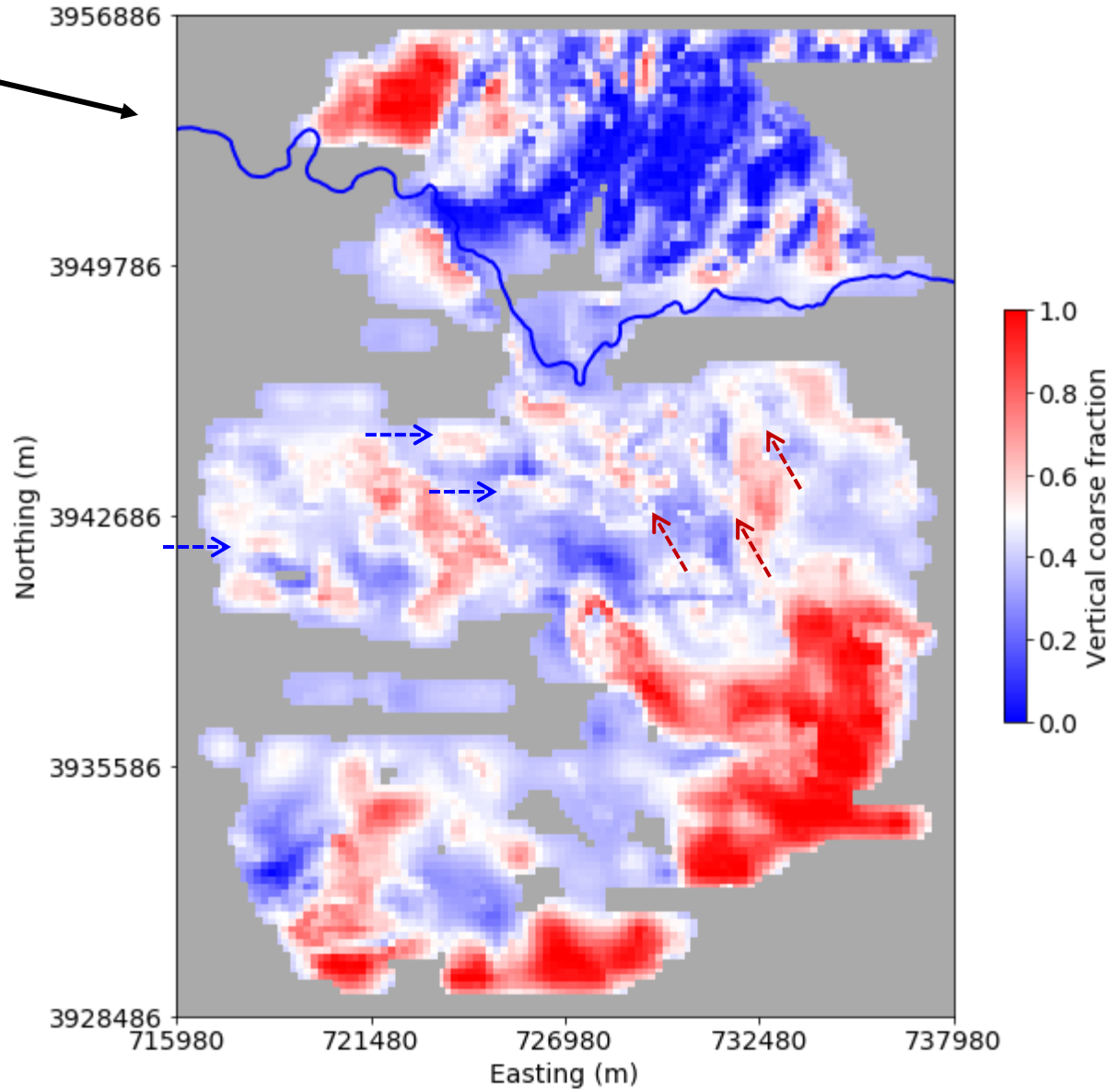

Vertically integrated CF map from the AEM data
(within Paso Robles Fm.)

Estrella River

Depth slices:

- Top to 20 m
- 20 m to 50 m
- 50 m to base of Paso Robles Fm.
- Top to base of Paso Robles Fm.

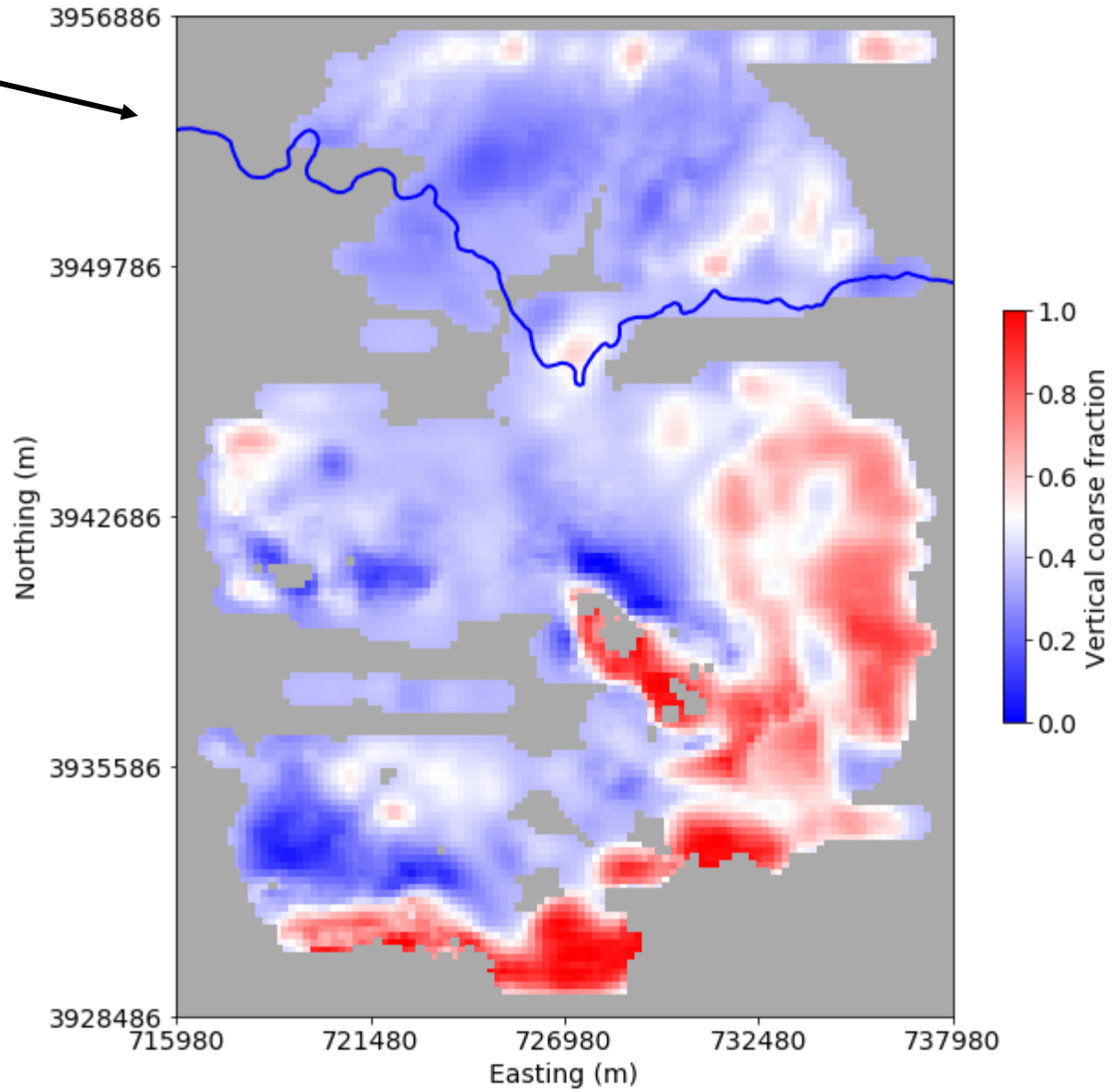

Vertically integrated CF map from the AEM data
(within Paso Robles Fm.)

Estrella River

Depth slices:

- Top to 20 m
- 20 m to 50 m
- 50 m to base of Paso Robles Fm.
- Top to base of Paso Robles Fm.

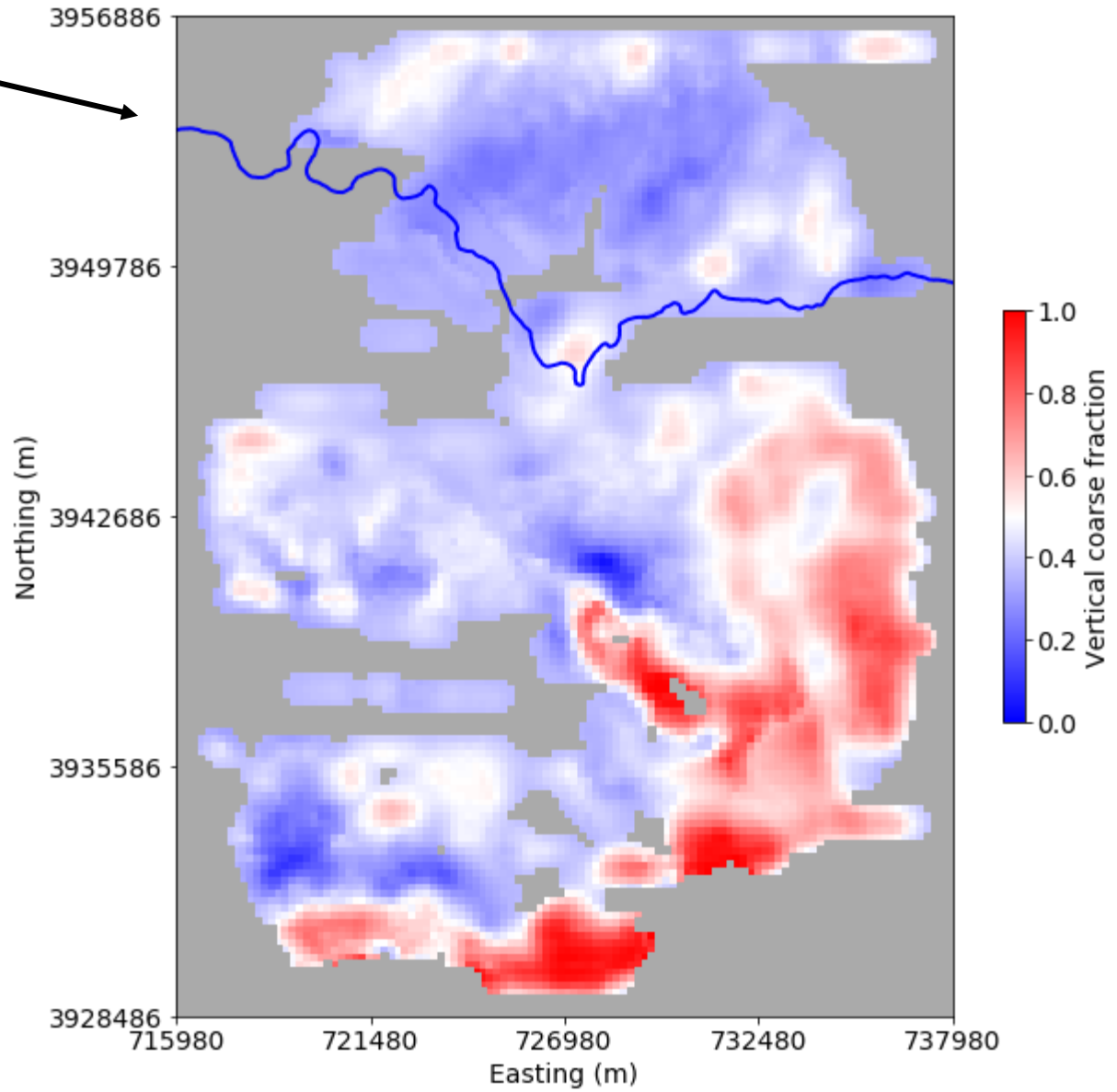

Paleo drainage forming Paso Robles Fm.

Santa Lucia Range
- Cenozoic uplift
- Deposition in early Pliocene
- Erosion & deposition of marine sediments
- Eastward channel direction

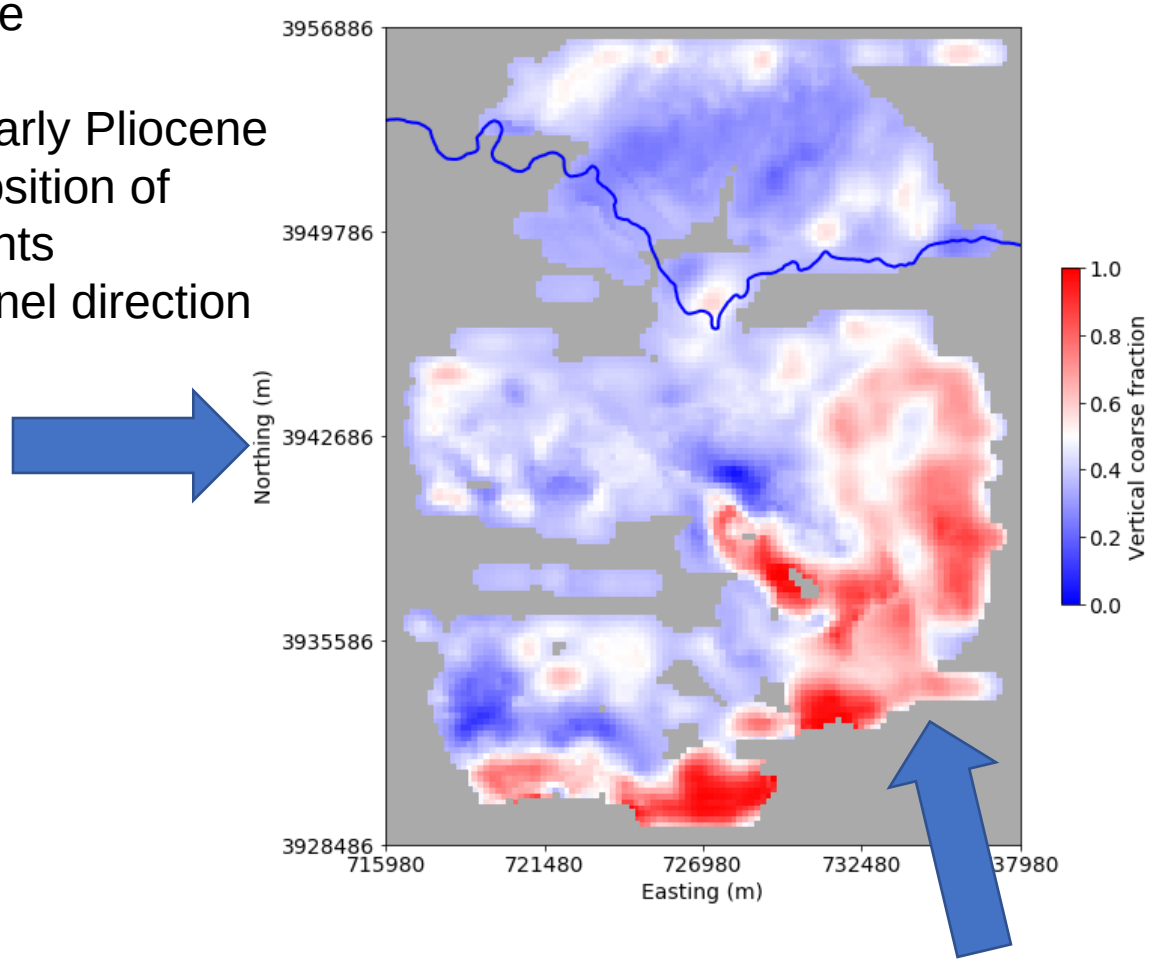

La Panza Range
- Cenozoic uplift
- Deposition in early Pliocene
- Erosion & deposition of sandstone and granitic materials
- North-northwestward channel direction

Paleo drainage forming Paso Robles Fm.

Santa Lucia Range
- Cenozoic uplift
- Deposition in early Pliocene
- Erosion & deposition of marine sediments
- Eastward channel direction

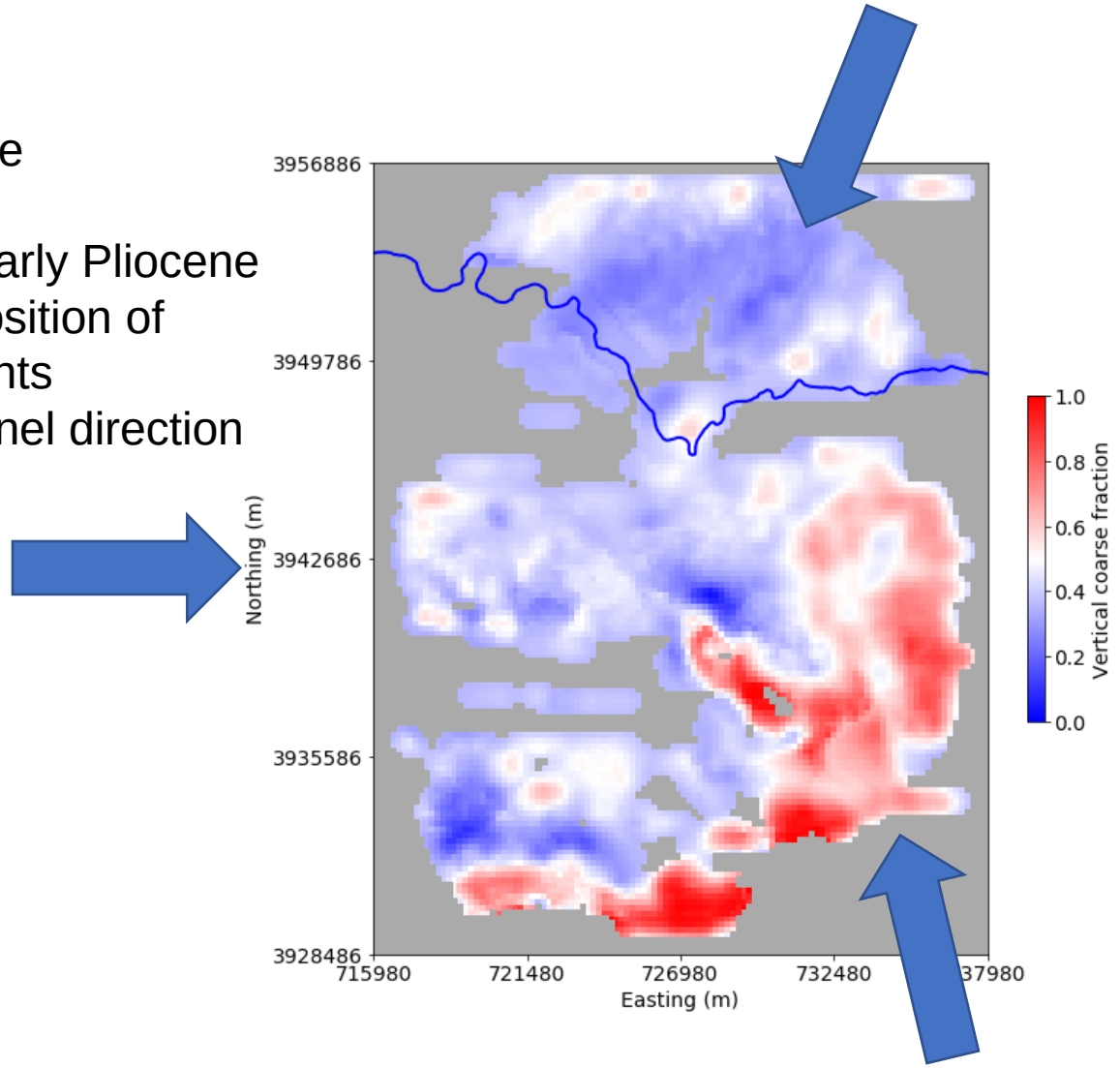

Temblor Range
- Pliocene (near the end) uplift
- South-southwestward channel direction

La Panza Range
- Cenozoic uplift
- Deposition in early Pliocene
- Erosion & deposition of sandstone and granitic materials
- North-northwestward channel direction

Paleo drainage forming Paso Robles Fm.

Santa Lucia Range
- Cenozoic uplift
- Deposition in early Pliocene
- Erosion & deposition of marine sediments
- Eastward channel direction

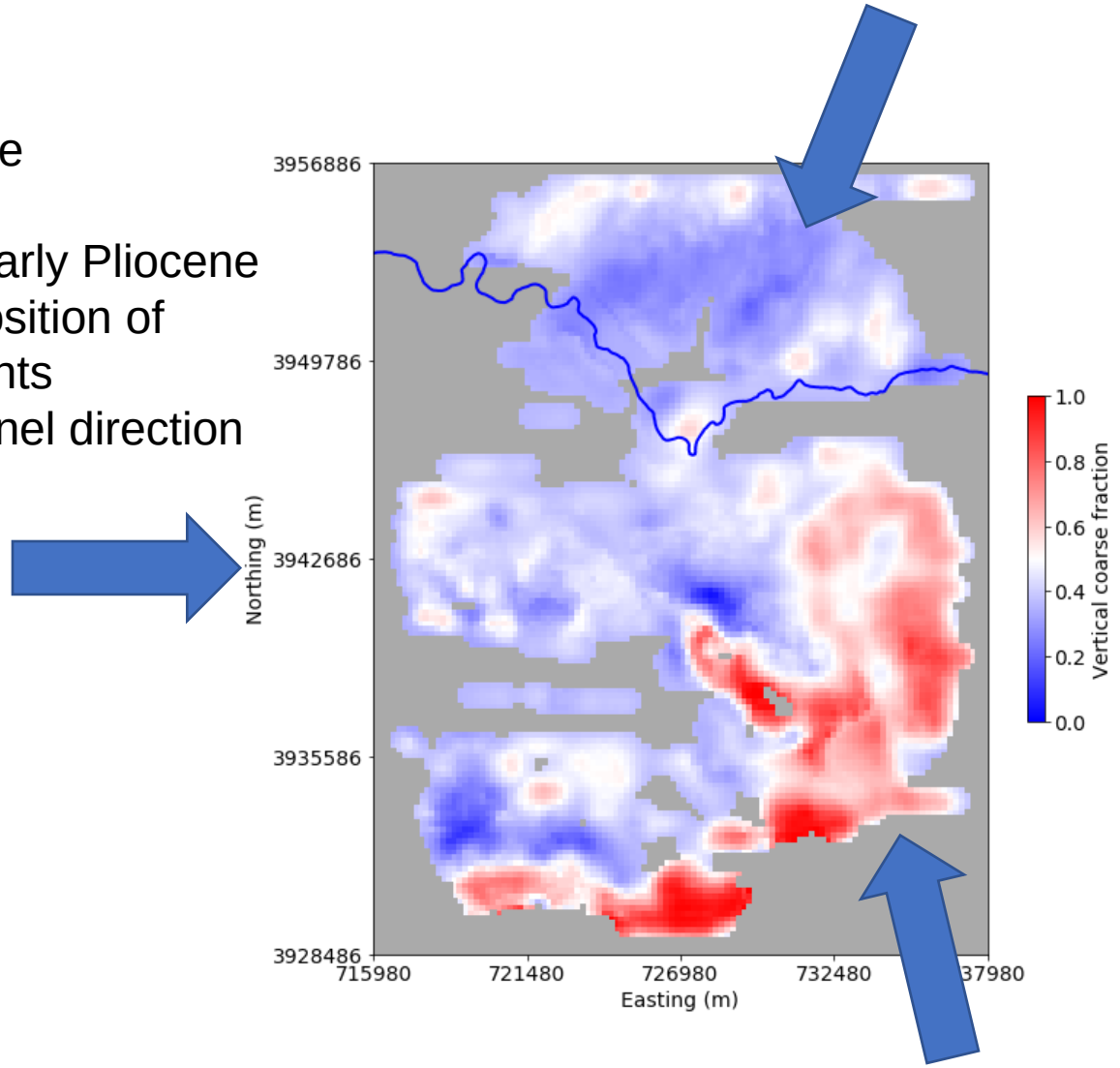

Temblor Range
- Pliocene (near the end) uplift
- South-southwestward channel direction

Originally channel deposits but significant deformation, so channel shape not preserved. Represented as sand lenses in a clay background.

La Panza Range
- Cenozoic uplift
- Deposition in early Pliocene
- Erosion & deposition of sandstone and granitic materials
- North-northwestward channel direction

Step6B: Create the Training Image

- Conceptual model
  - Sand lenses embedded in a clay background
  - Percentage of coarse-dominated is 36%
    (from the sediment-type well profiles)

- We use half-ellipsoids to emulate lenses

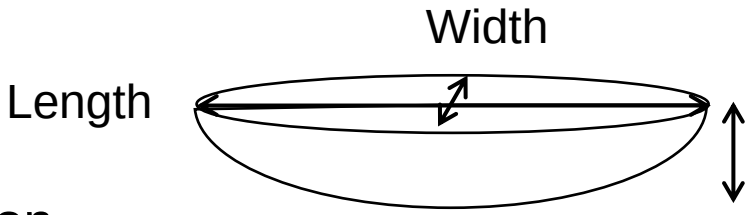

Training Image

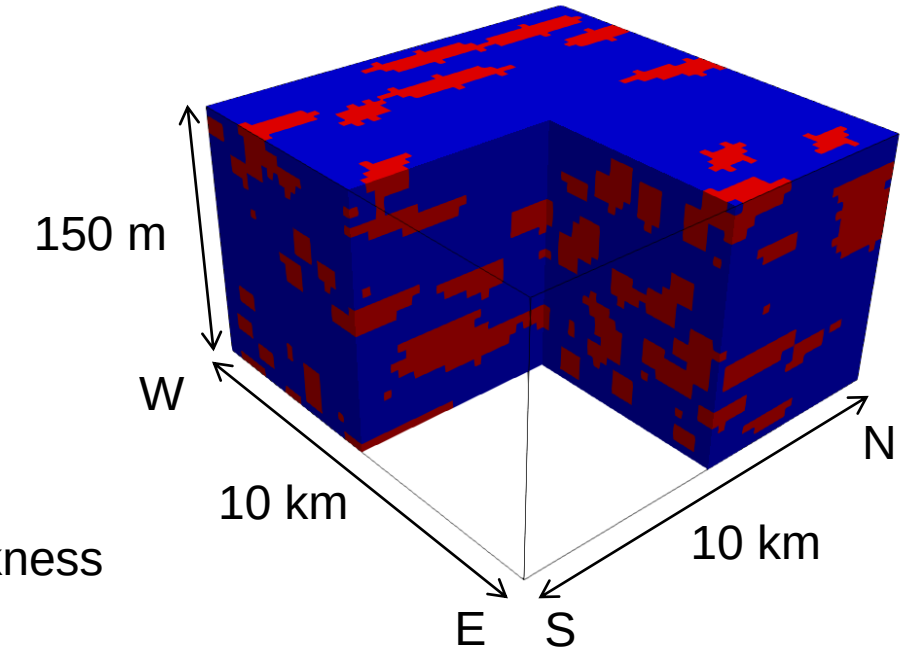

- Sand lens information

	Range	Distribution type	Source
Thickness	10-20 m	Uniform	Wells (variogram)
Width	0.4-0.6 km	Uniform	1) The 2D CF maps 2) Observation from channels in the Salinas River
Length	1.2-4 km	Uniform	
Direction (azimuth)	-20-20°	Triangular	

Step6B: Create the Training Image

- Conceptual model
  - sand/gravel lenses embedded in the clay/silt background

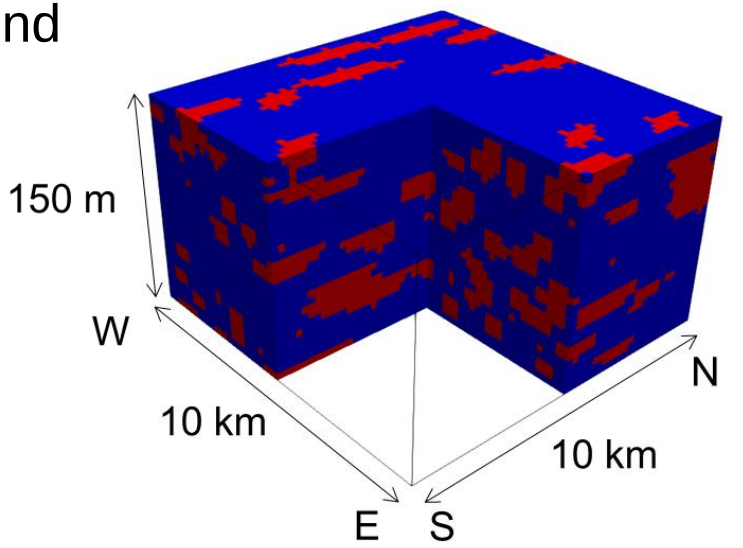

- Direction of the lenses:
  - Western region: Eastward (90 degree)
  - Southeast region: North-northwestward (-20 degree)
  - Northeast region: South-southeastward (20 degree)

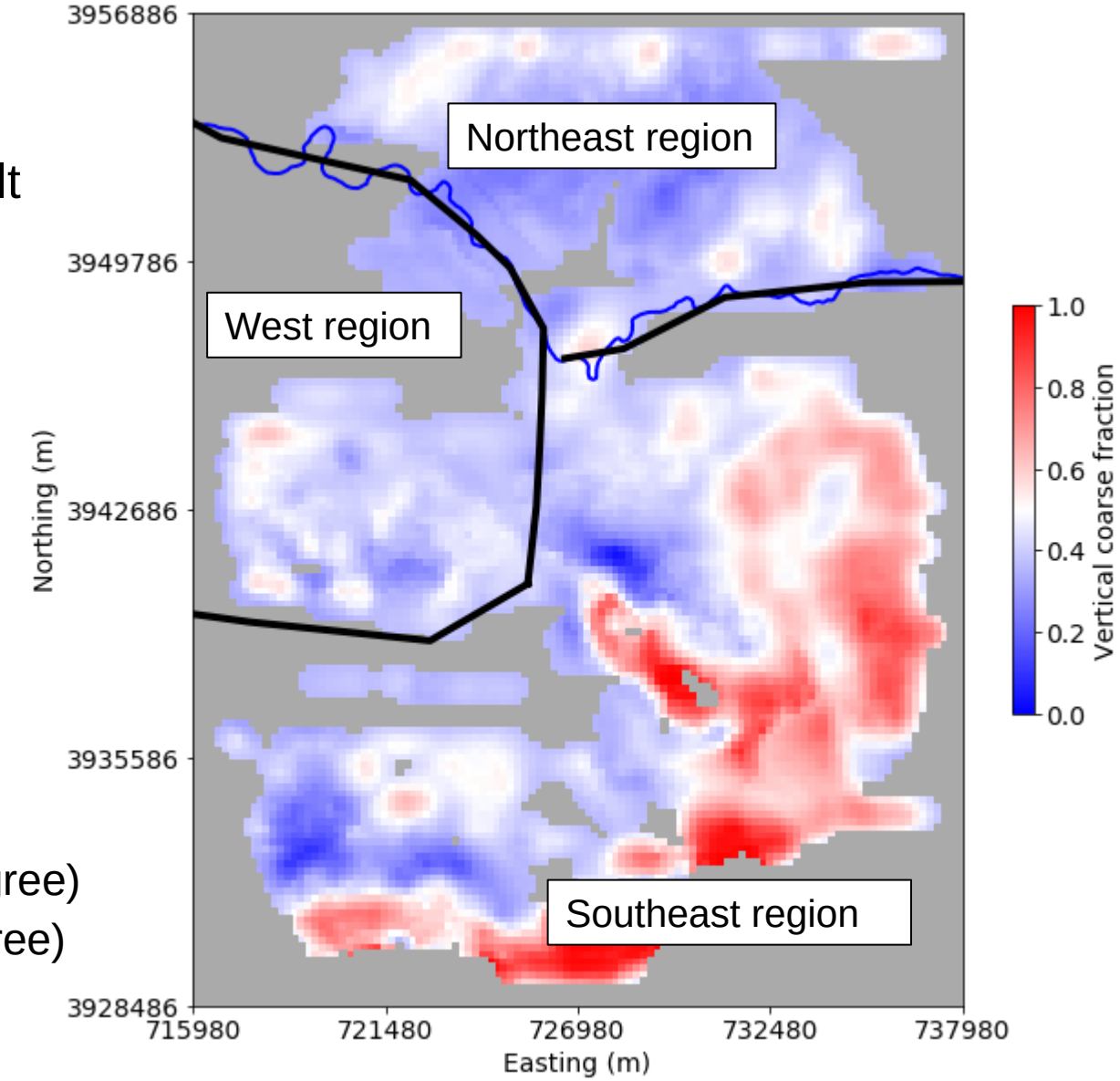

Applying Multi-point statistics (MPS) method to the SLO data

Starting sediment-type probability model from AEM

Resistivity models from AEM

↓

CF models from AEM

↓

3D CF models from AEM

↓

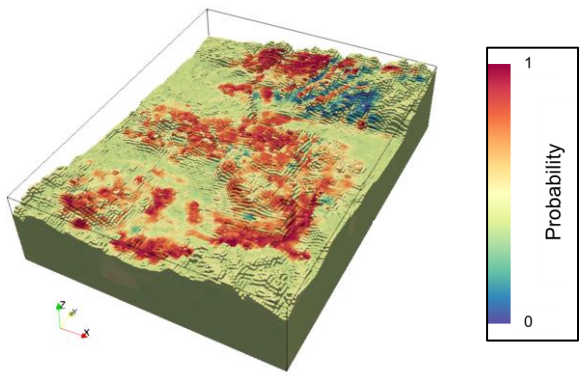

Hard well data

Classified well data (coarse/fine)

↓

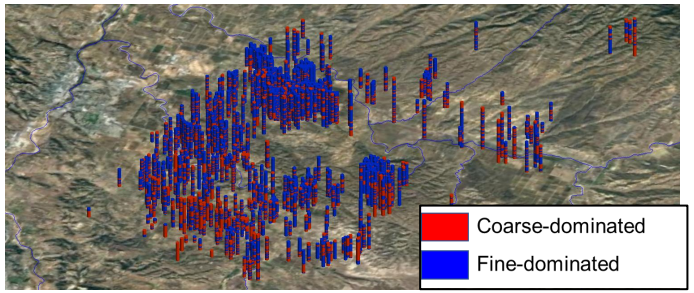

↓

Randomized selection of z_{wells}

Training images (geologic patterns)

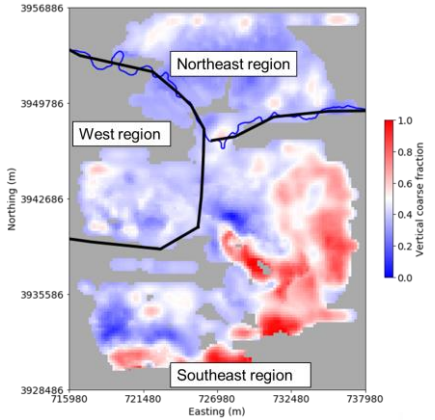

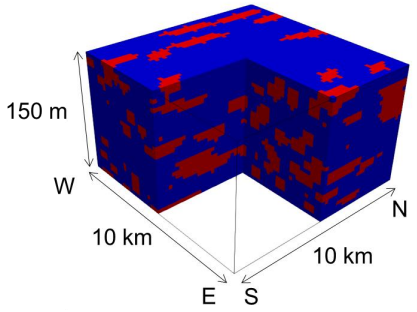

Output MPS sediment-type model

MPS sediment-type model 1

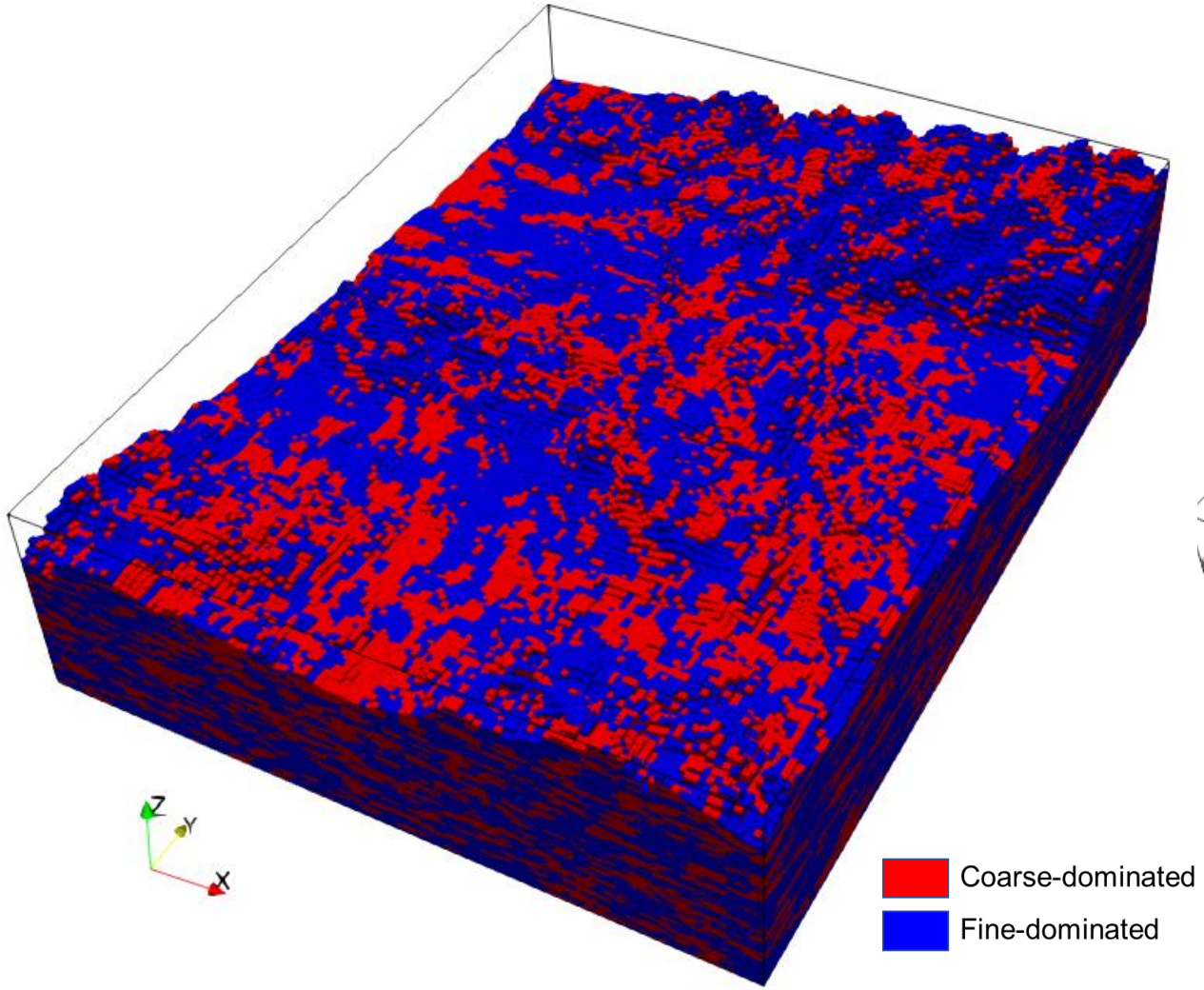

Region code

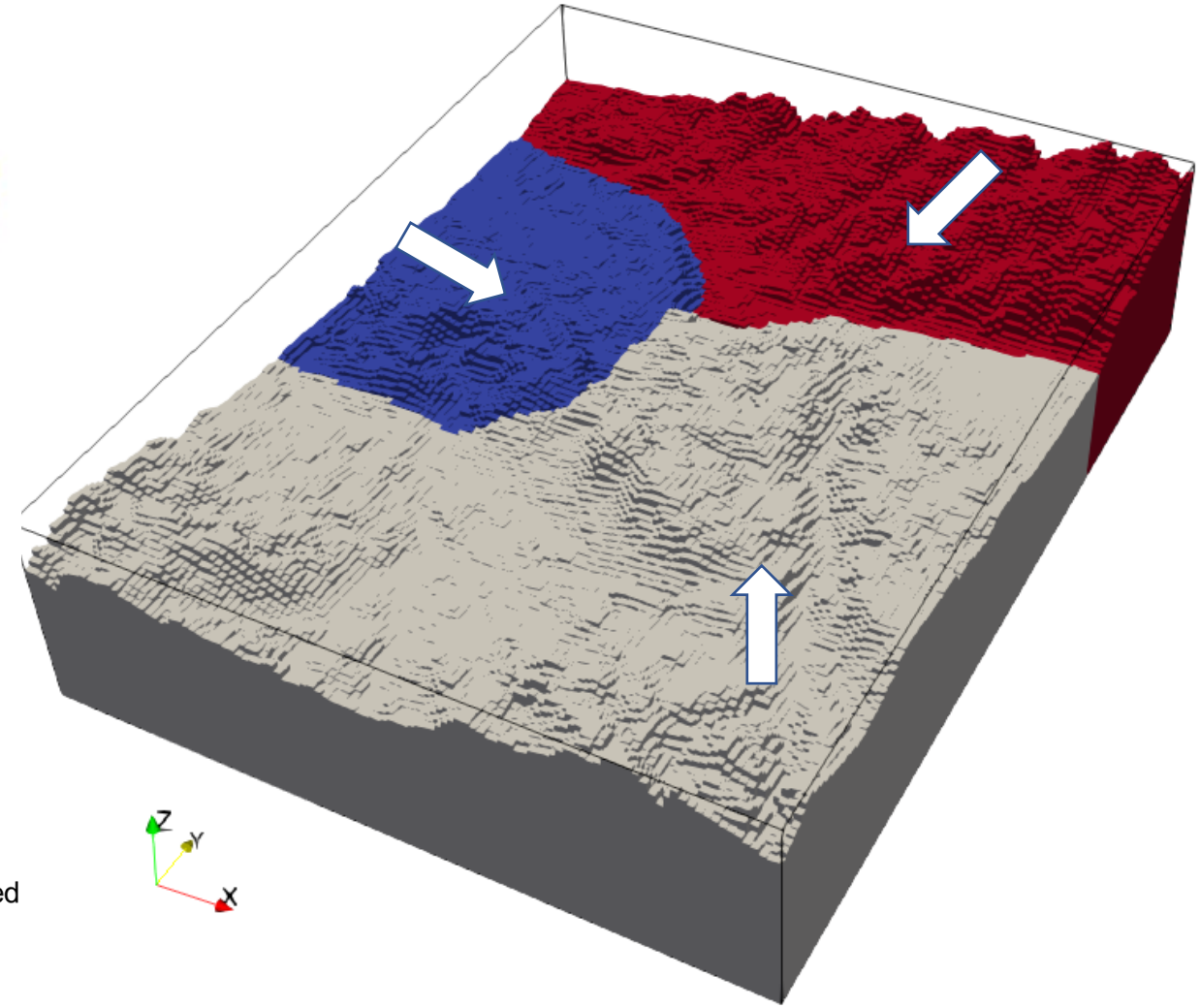

Output MPS sediment-type model

MPS sediment-type model 1

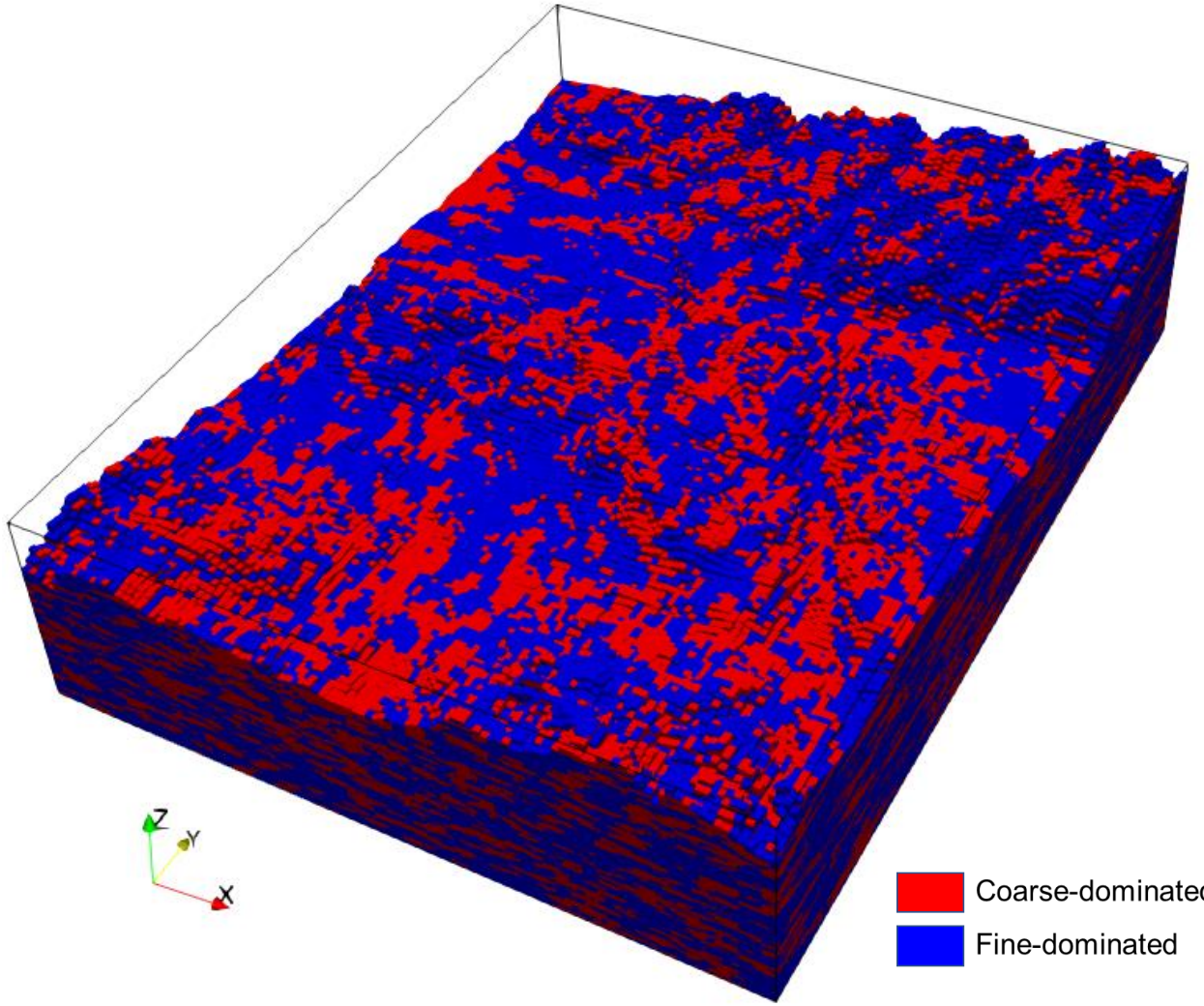

Probability model of coarse-dominated from AEM

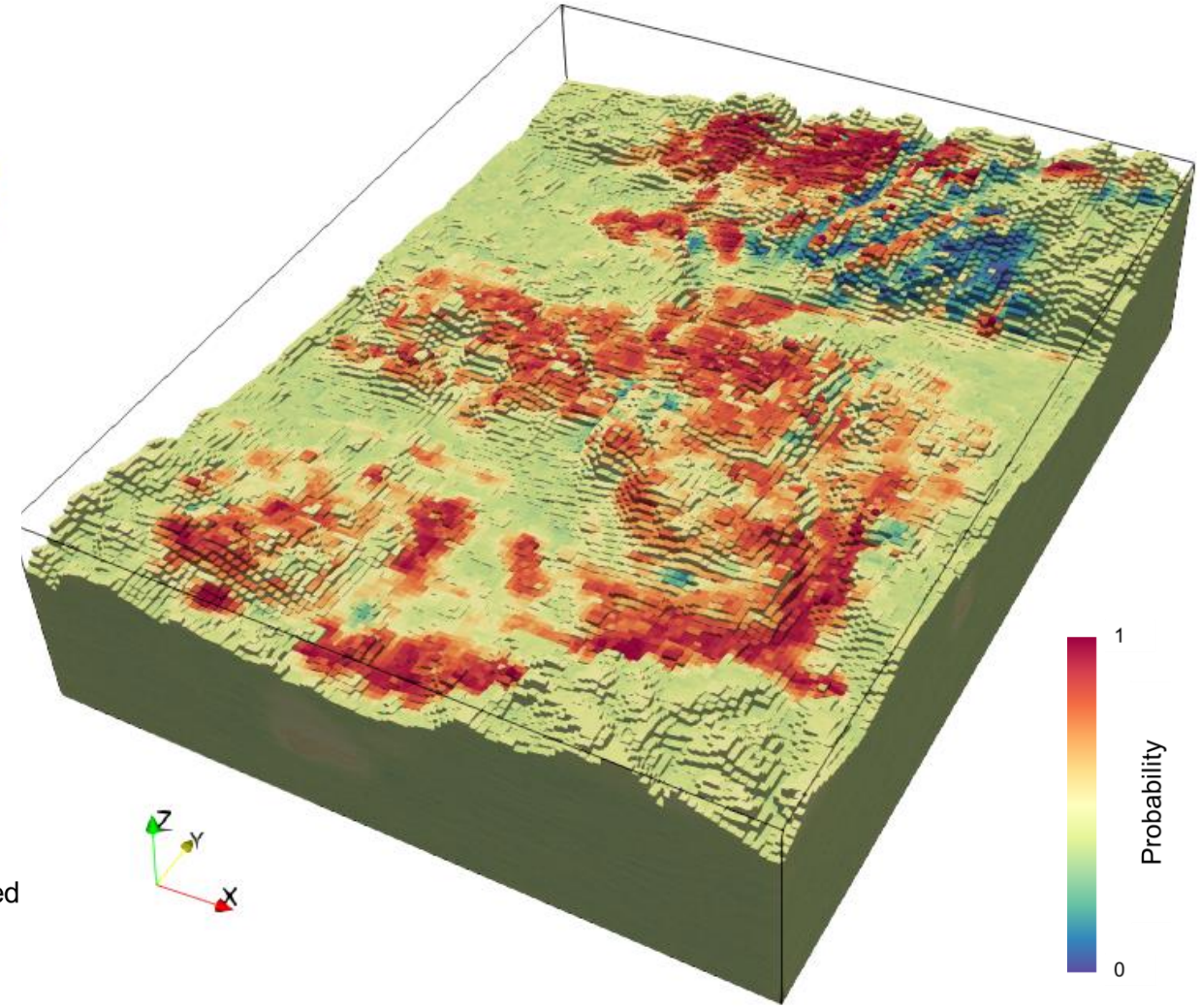

Two MPS sediment-type models

MPS sediment-type model 2

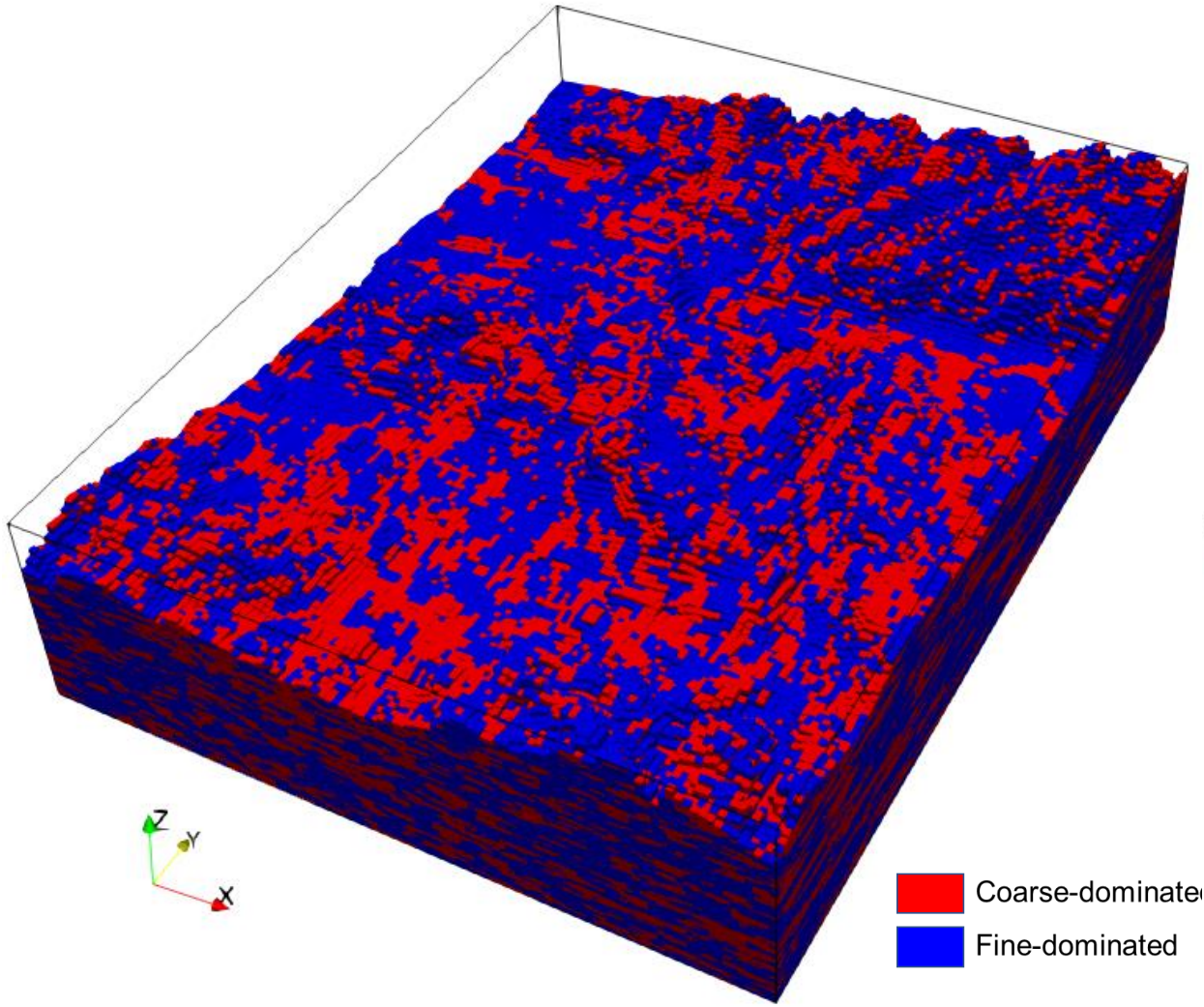

MPS sediment-type model 1

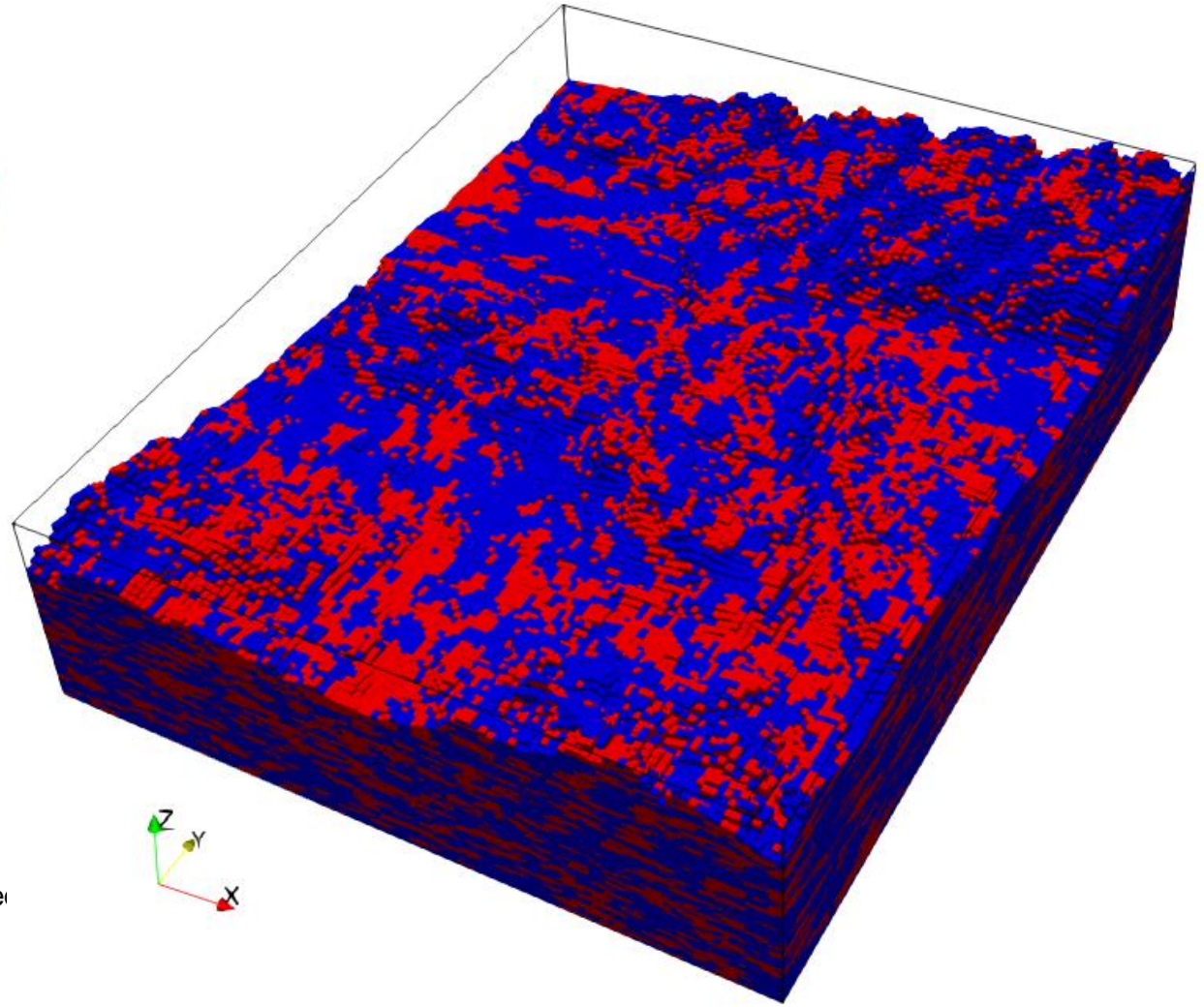

Obtain multiple realizations capturing uncertainty

Sediment-type starting probability model from AEM

Hard well data

Training image (geologic patterns)

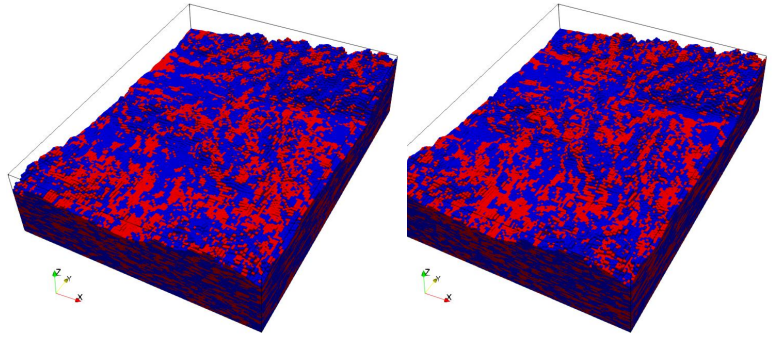

....

100 MPS sediment-type models

Comparison with geologic sections

A-A’

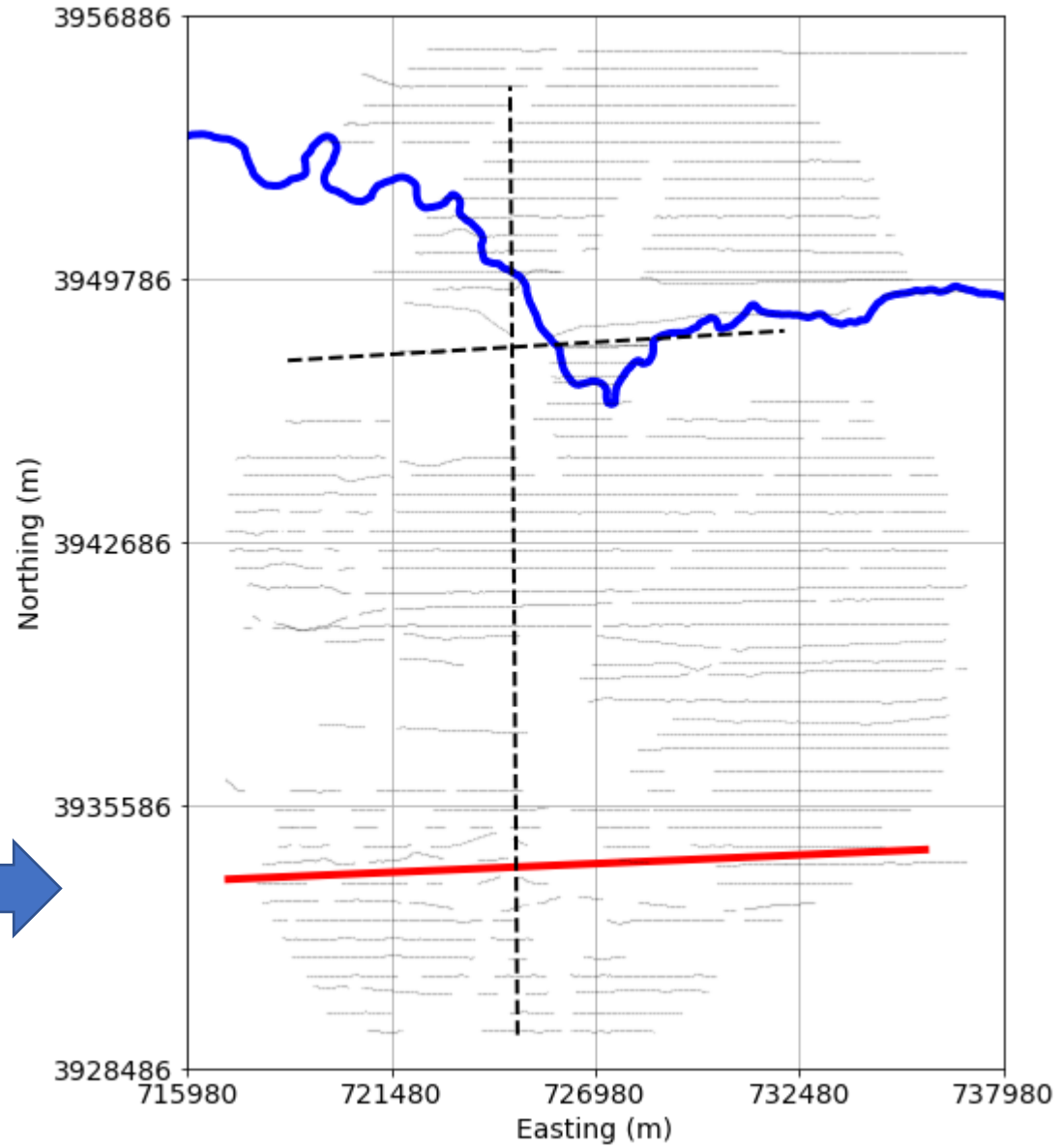

A-A’

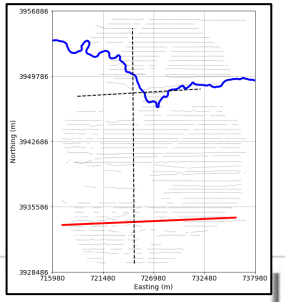

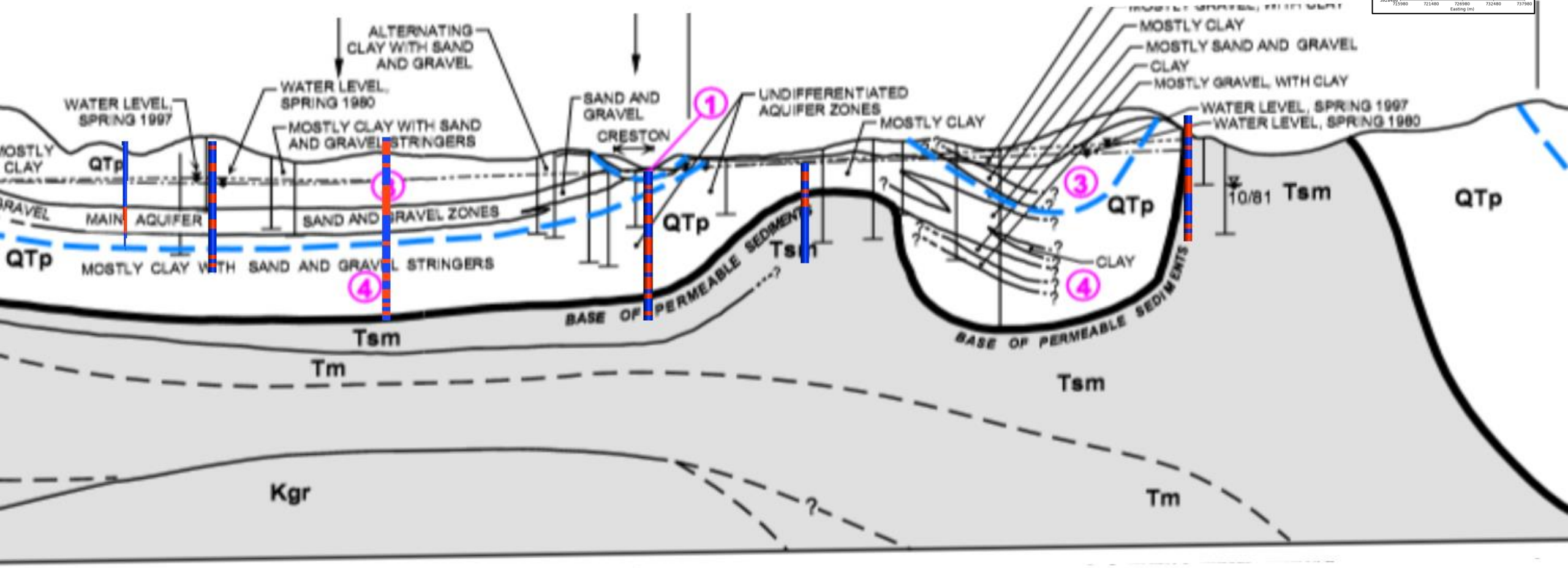
ALTERNATING CLAY WITH SAND AND GRAVEL
WATER LEVEL, SPRING 1997
WATER LEVEL, SPRING 1980
MOSTLY CLAY WITH SAND AND GRAVEL STRINGERS
SAND AND GRAVEL
CRESTON
UNDIFFERENTIATED AQUIFER ZONES
MOSTLY CLAY
MOSTLY CLAY
MOSTLY SAND AND GRAVEL
CLAY
MOSTLY GRAVEL, WITH CLAY
WATER LEVEL, SPRING 1997
WATER LEVEL, SPRING 1980
MOSTLY CLAY
QTp
MAIN AQUIFER
SAND AND GRAVEL ZONES
MOSTLY CLAY WITH SAND AND GRAVEL STRINGERS
QTp
QTp
Tsm
BASE OF PERMEABLE SEDIMENTS
QTp
10/81
Tsm
QTp
CLAY
BASE OF PERMEABLE SEDIMENTS
Tsm
Tm
Kgr
Tm
1
2
3
4

~20 km

A-A’

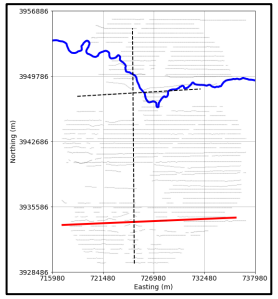

Sand/gravel zone

Alluvium

Paso Robles Fm.

Others

300m

~20 km

Probability model of coarse-dominated from AEM at A-A’

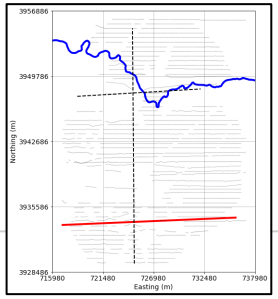

Sand/gravel zone

Alluvium

Paso Robles Fm.

Others

0

1

Probability

300m

~20 km

MPS sediment-type model 1 at A-A’

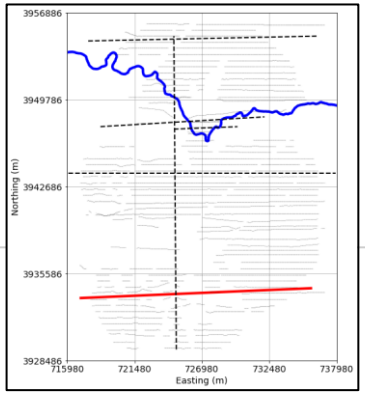

Sand/gravel zone

Alluvium

Paso Robles Fm.

Others

300m

Coarse-dominated

Fine-dominated

~20 km

MPS sediment-type model 2 at A-A’

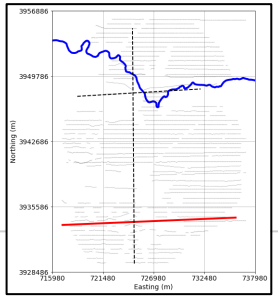

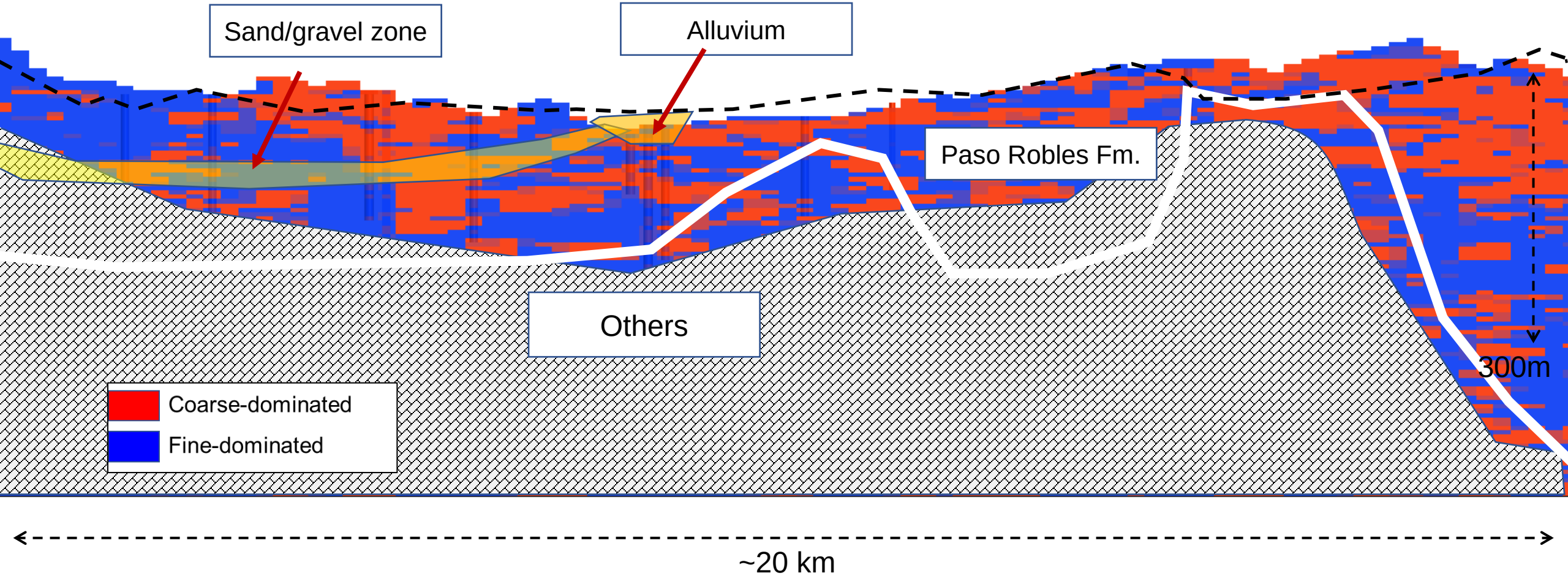

Plan map for geologic sections

B-B’

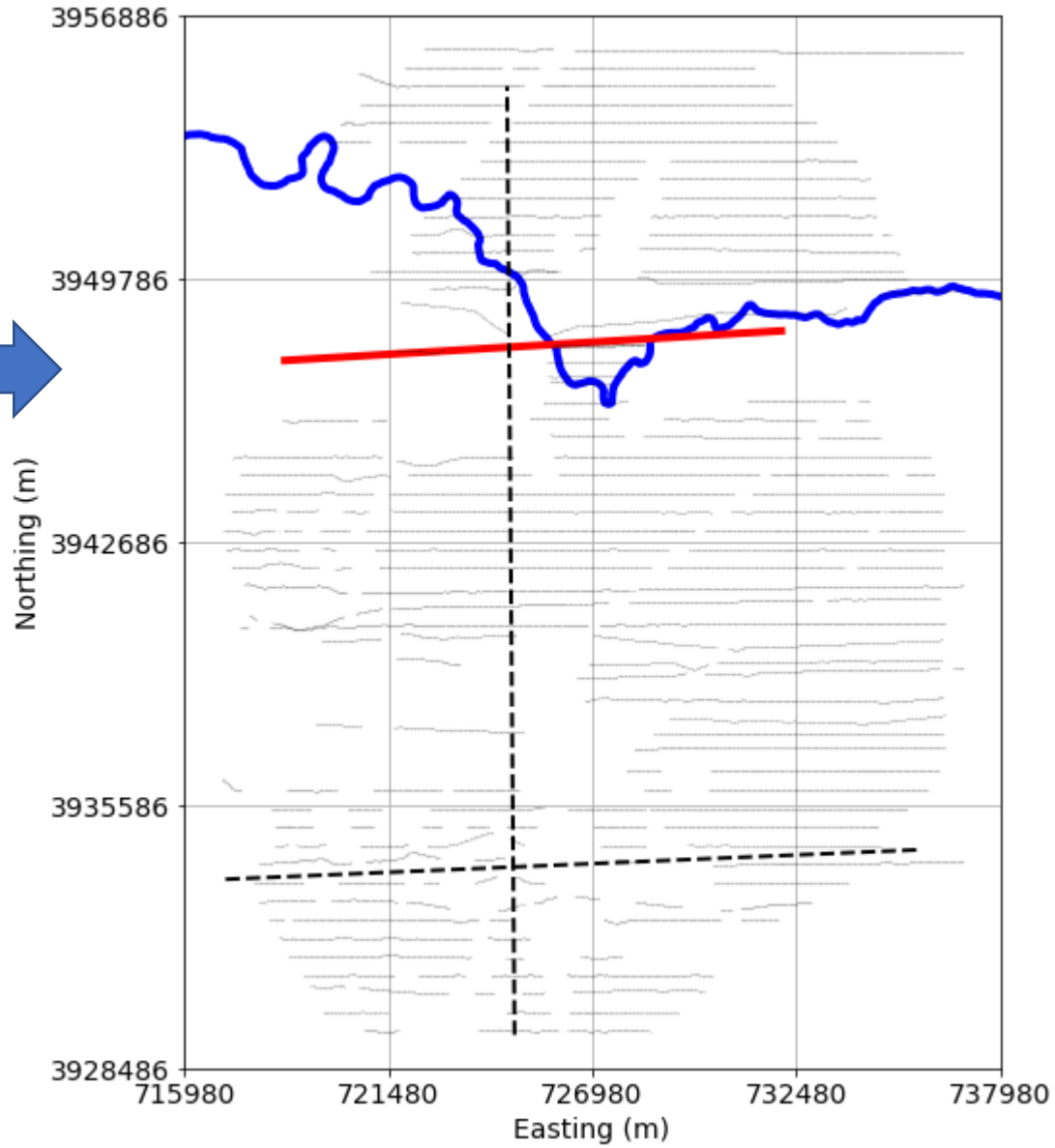

B-B’

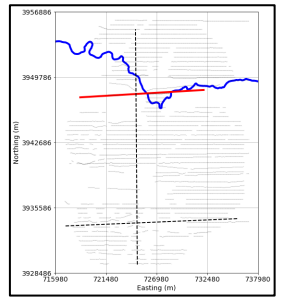

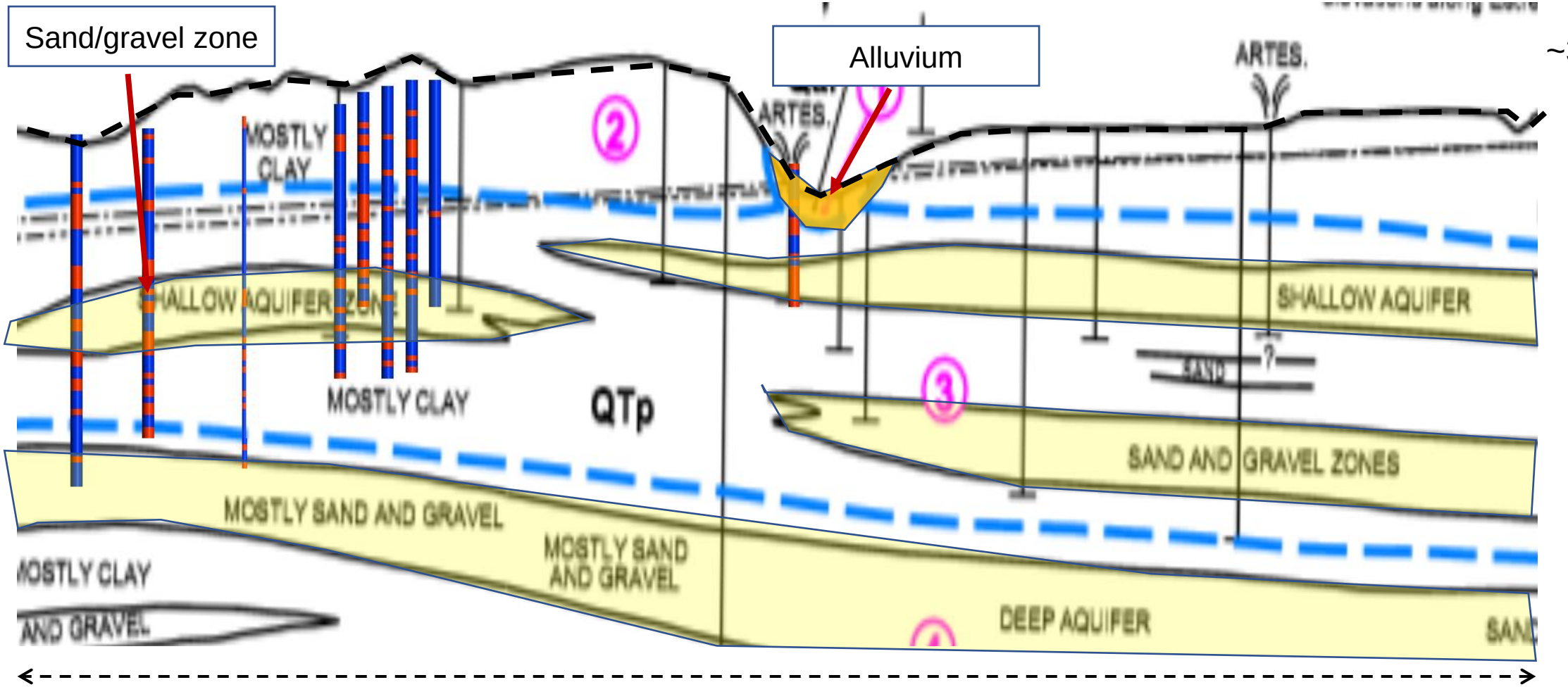
Sand/gravel zone
Alluvium
~300 m
MOSTLY CLAY
ARTES.
SHALLOW AQUIFER
MOSTLY CLAY
QTp
SAND AND GRAVEL ZONES
MOSTLY SAND AND GRAVEL
MOSTLY SAND AND GRAVEL
DEEP AQUIFER
~13 km

B-B’

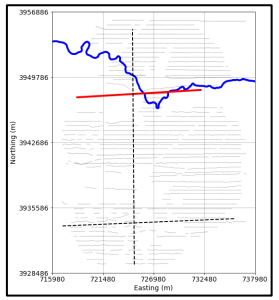

Sand/gravel zone

Alluvium

~300 m

~13 km

Probability model of coarse-dominated from AEM at B-B’

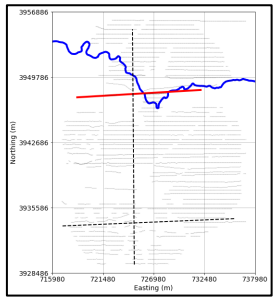

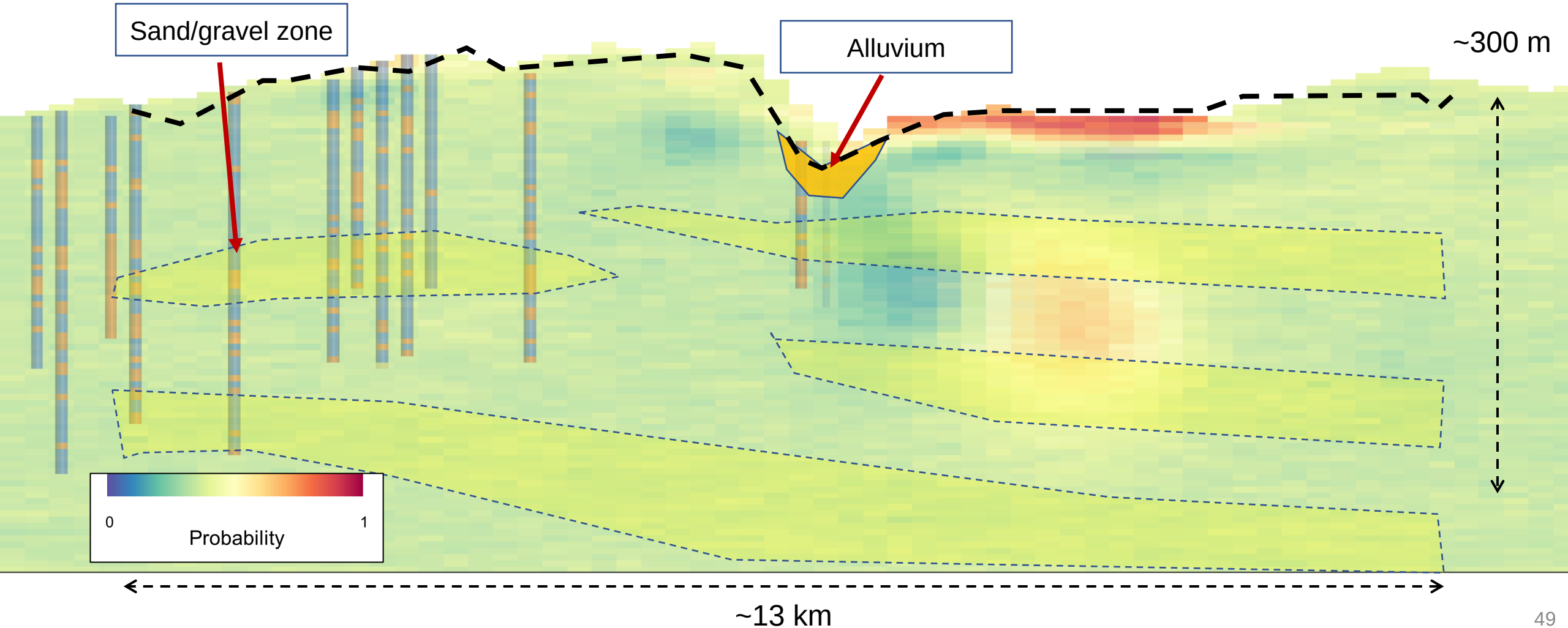

MPS sediment-type model 1 at B-B’

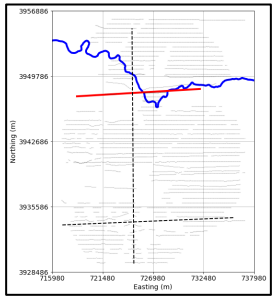

Sand/gravel zone

Alluvium

~300 m

Coarse-dominated

Fine-dominated

~13 km

MPS sediment-type model 2 at B-B’

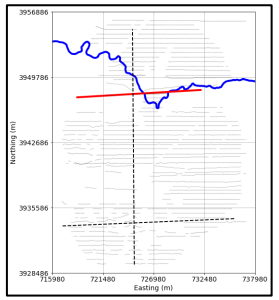

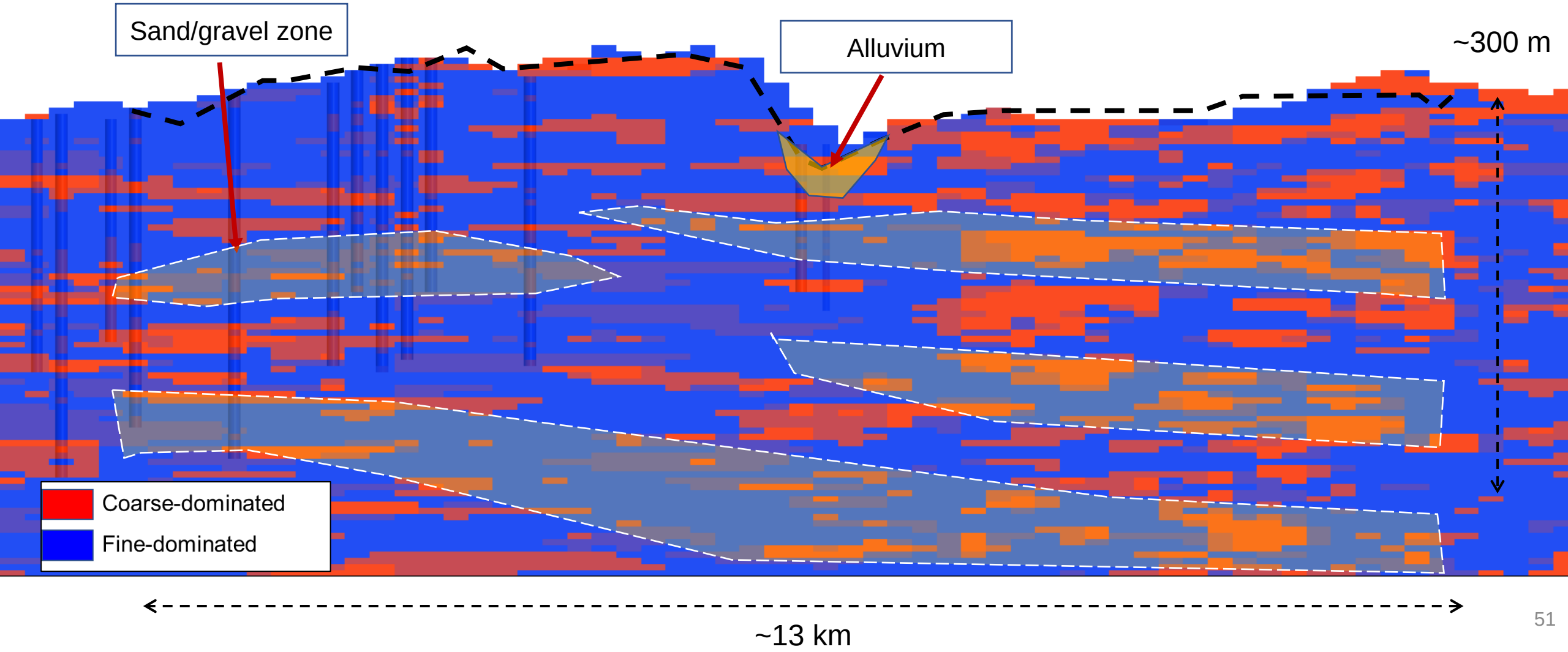

Plan map for geologic sections

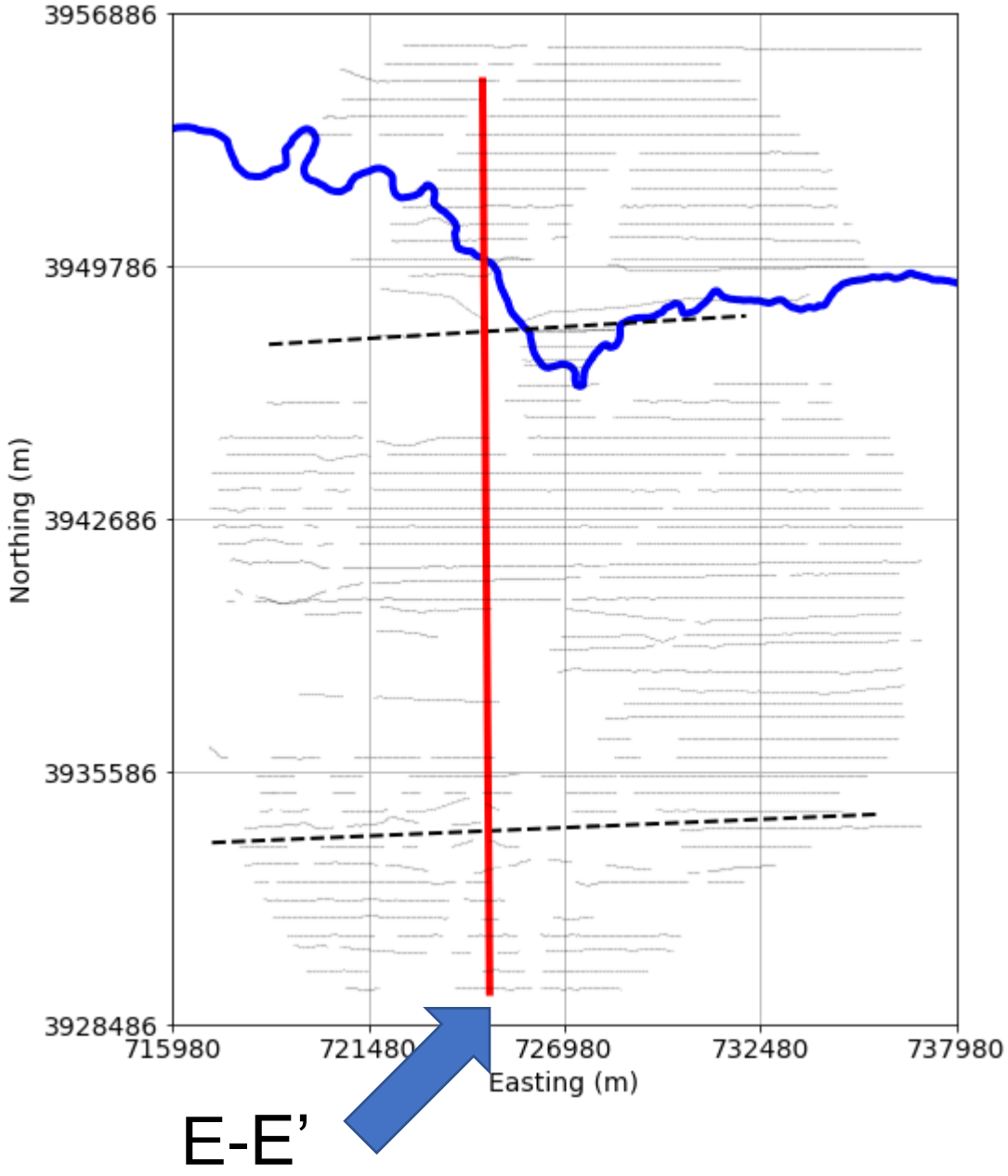

E-E’

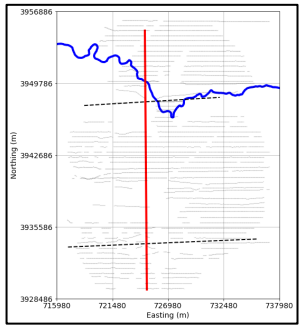
3956886
3949786
3942686
3935586
3928486
Northing (m)
715980
721480
726980
732480
737980
Easting (m)

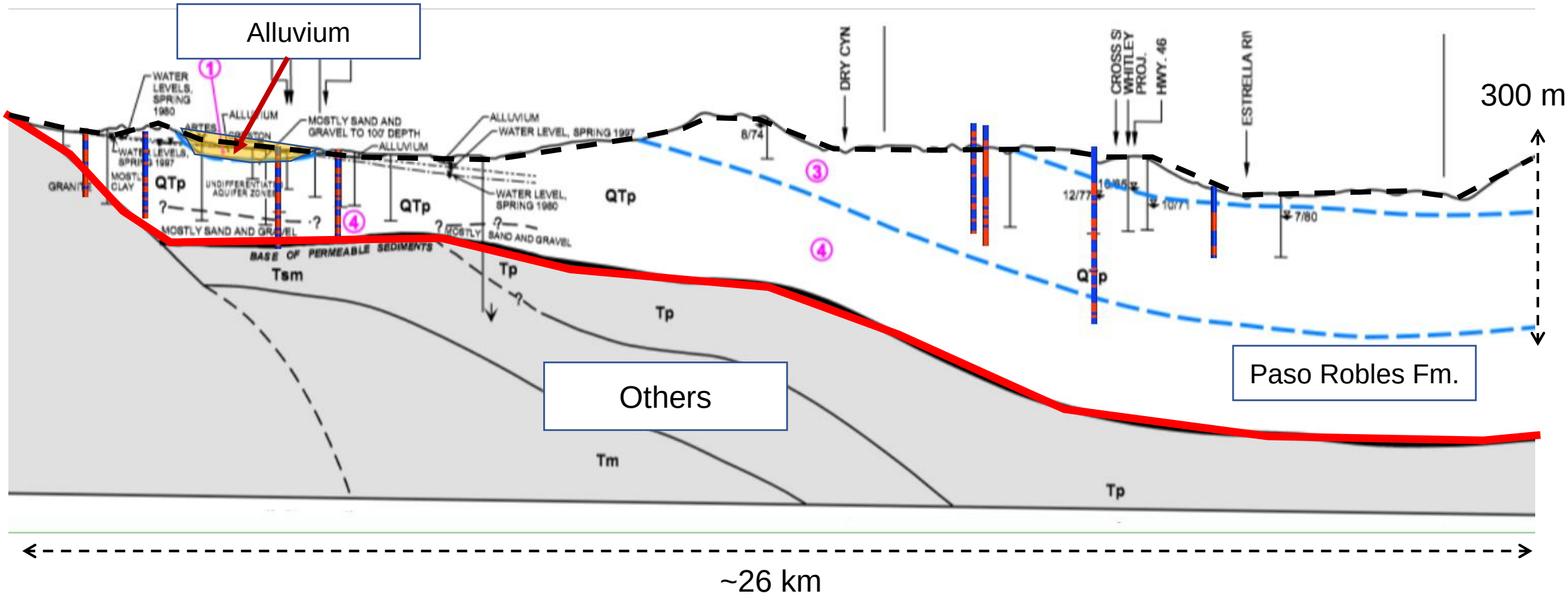
Alluvium
300 m
Paso Robles Fm.
Others
~26 km
WATER LEVELS, SPRING 1980
MOSTLY SAND AND GRAVEL TO 100' DEPTH
ALLUVIUM
WATER LEVEL, SPRING 1997
WATER LEVEL, SPRING 1980
DRY CYN
CROSS ST
WHITLEY PROJ.
HWY. 46
ESTRELLA RD
GRANITE
MOST. CLAY
QTp
MOSTLY SAND AND GRAVEL
BASE OF PERMEABLE SEDIMENTS
Tsm
Tp
Tm
8/74
12/77
10/71
7/80

E-E’

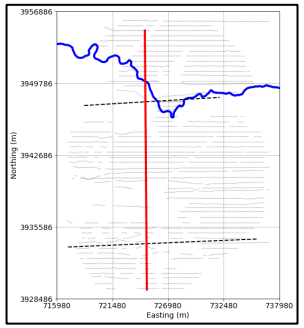

Alluvium

300 m

Others

Paso Robles Fm.

~26 km

Probability model of coarse-dominated from AEM at E-E’

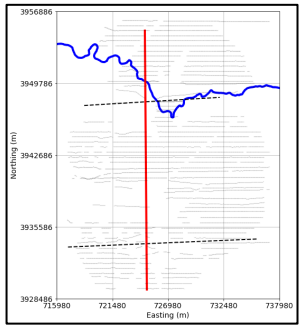

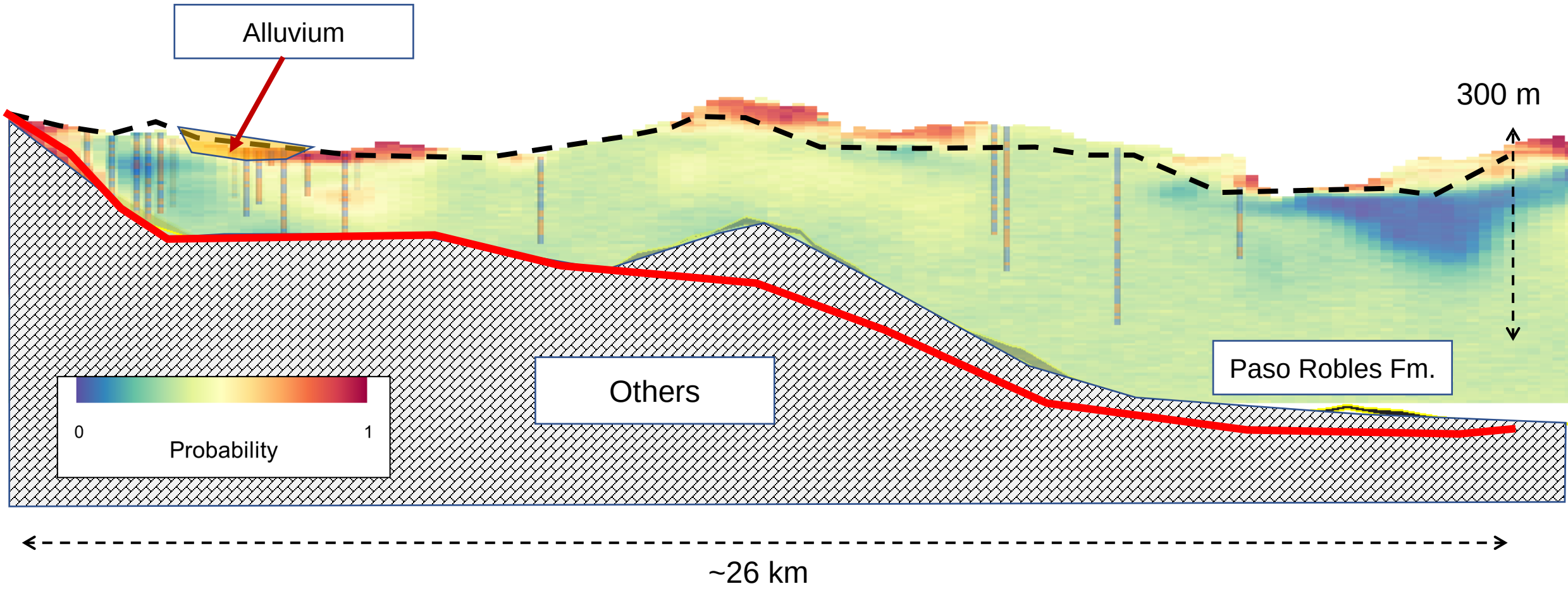

MPS sediment-type model 1 at B-B’

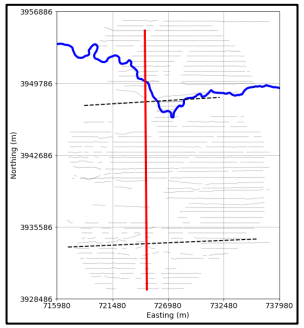

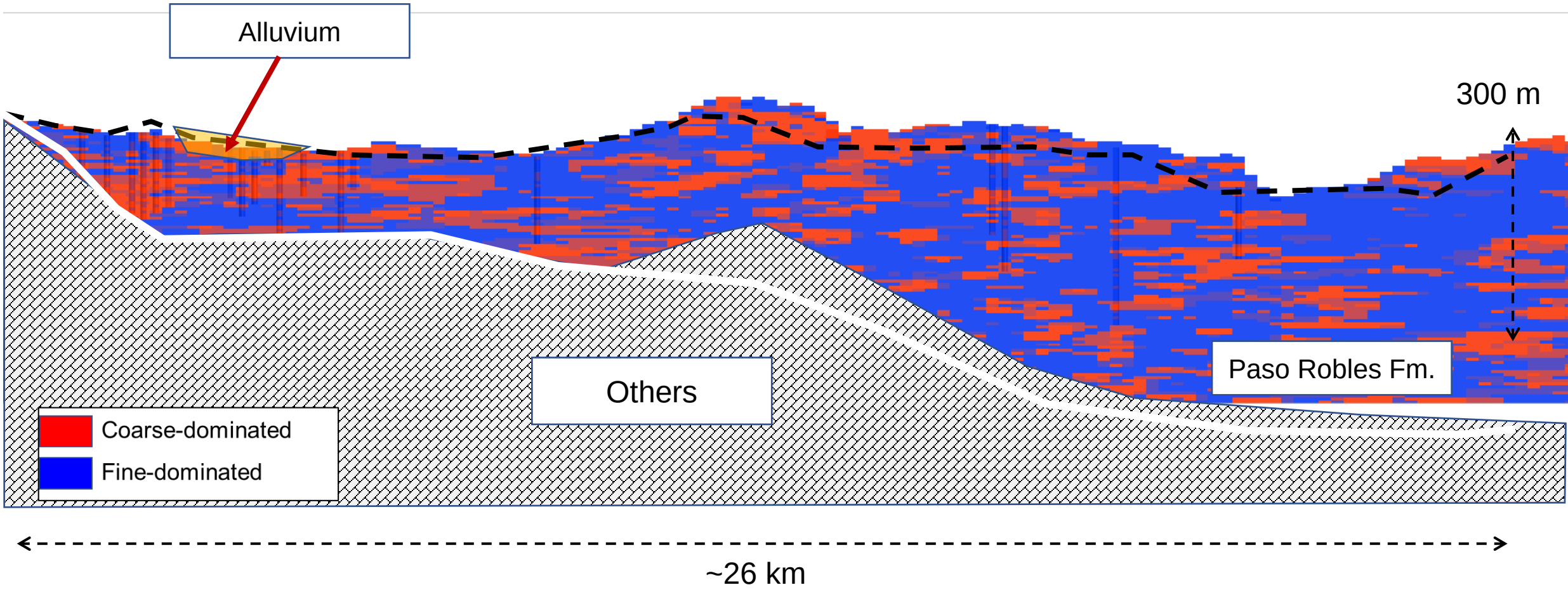

MPS sediment-type model 2 at B-B’

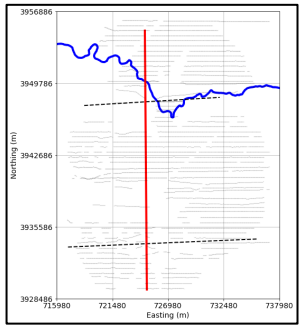

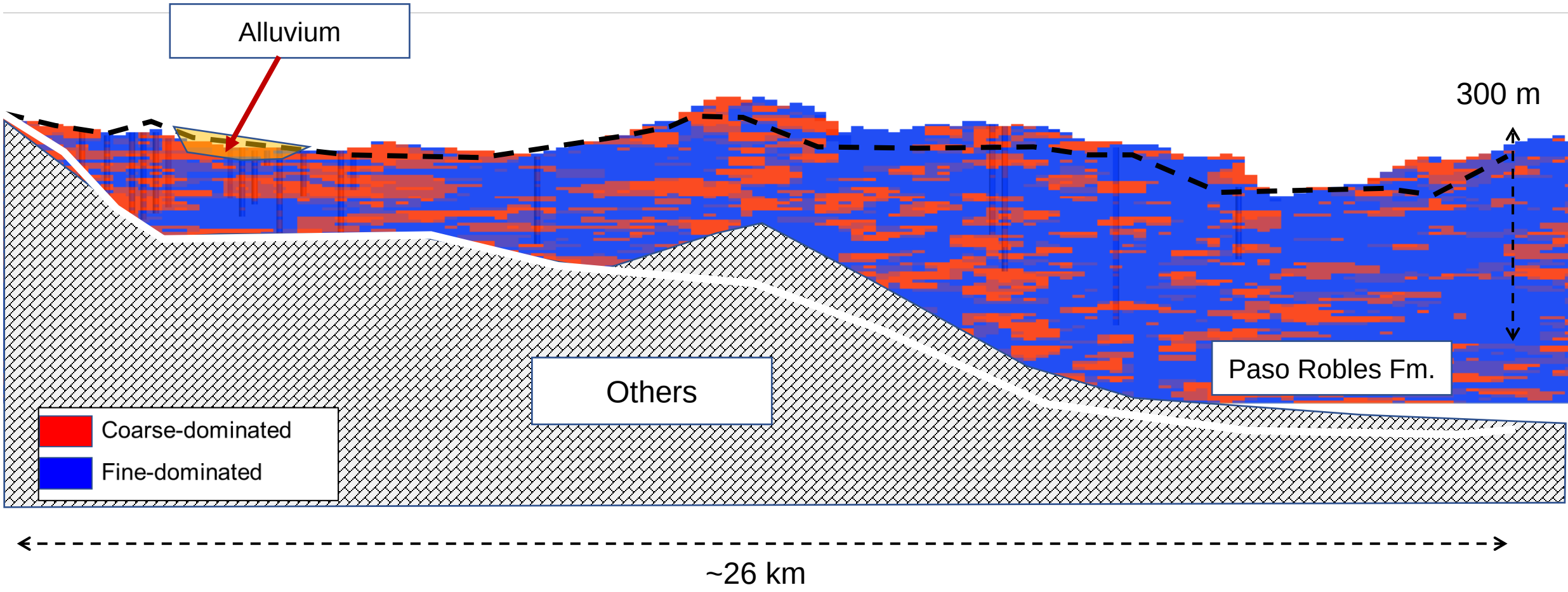

Answering question

#1 What is the extent of the clay layer at the Estrella River?

"The nature of the near-surface sediments along the Estrella River and if/how they transition to coarser materials away from the river to the northeast. This issue has two potentially significant benefits: 1) better understanding of how surface water in Estrella River recharges the underlying Paso Robles Formation for evaluation of potential recharge-related areas, and 2) potentially focusing on active surface infiltration projects (recharge projects) on the northeast flank of the river and basin, rather than focusing on the river itself, which appears to me to be a poor location for recharge projects." (from Paul)

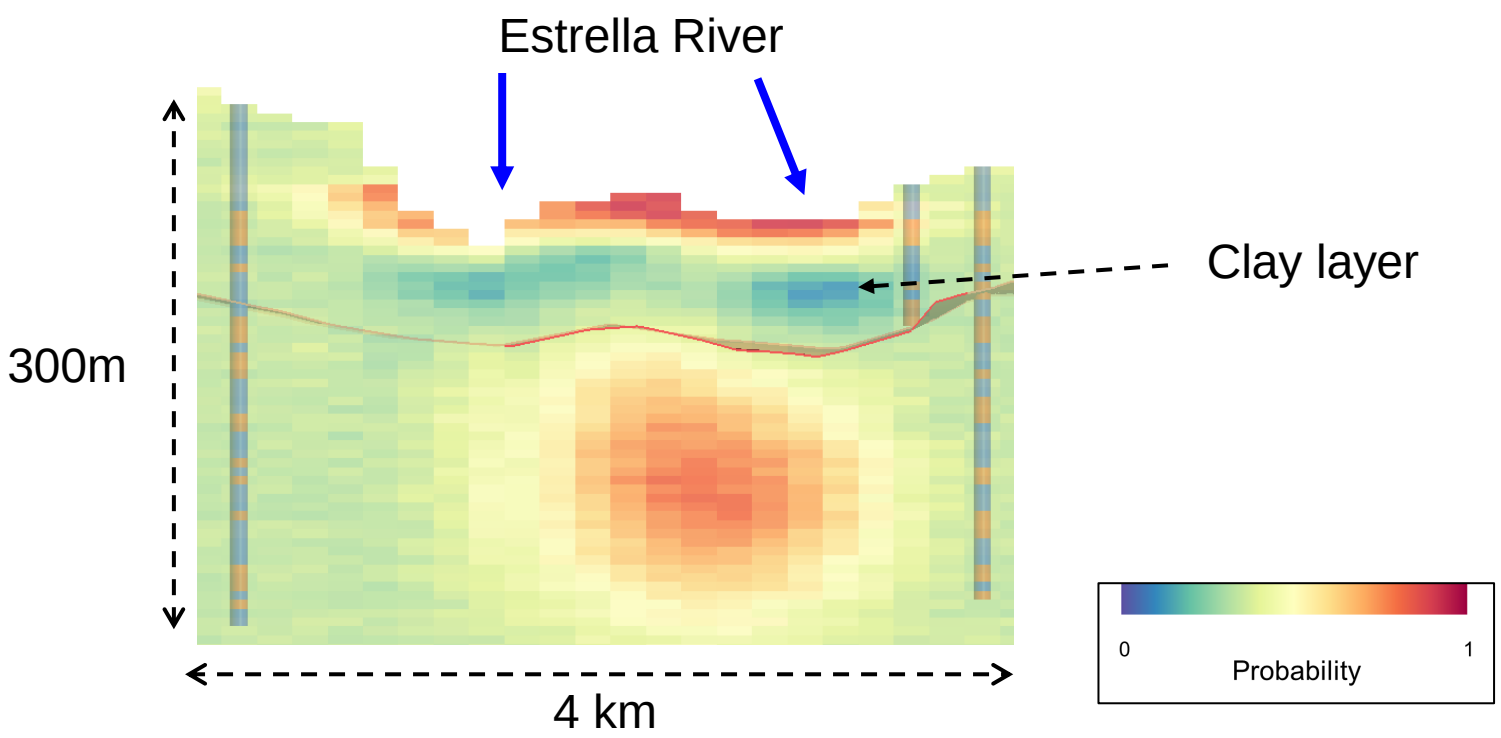

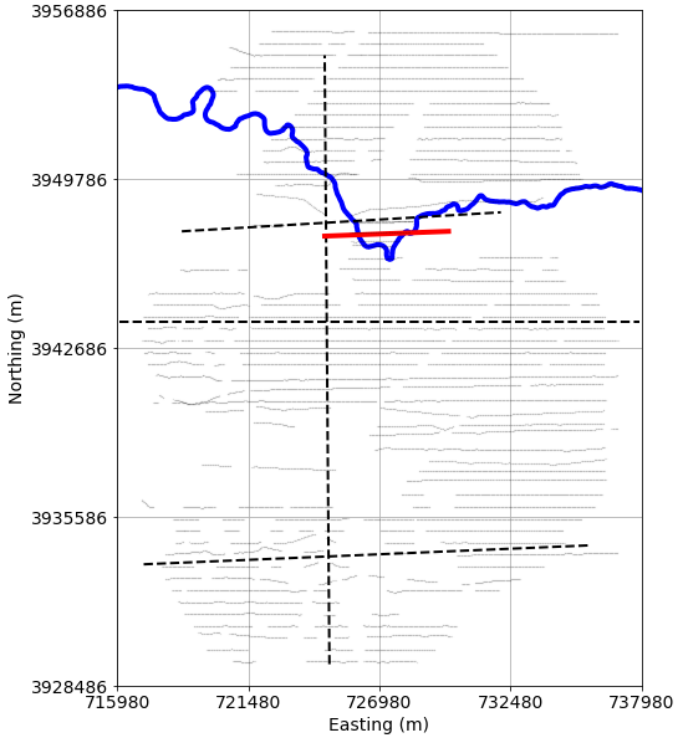

Define the base of the clay layer
(using the probability of coarse-dominated from AEM)

Base of the clay layer

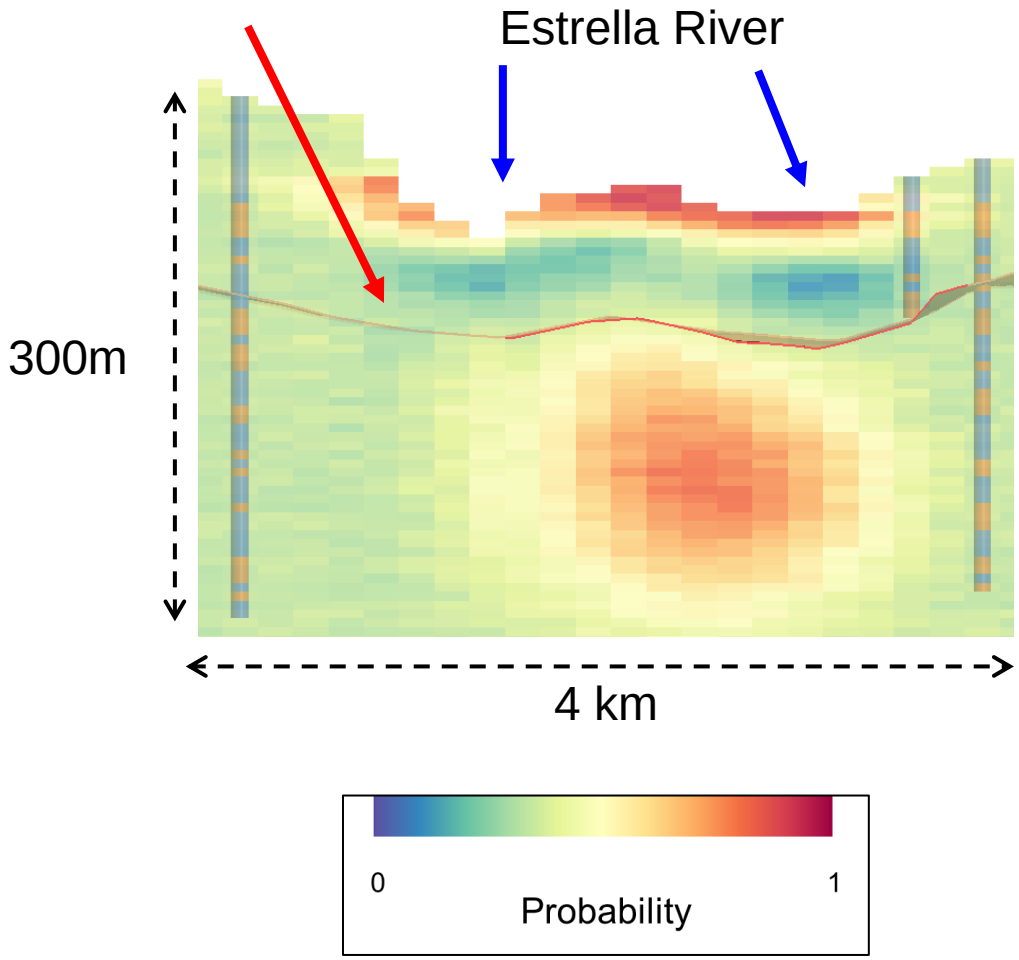

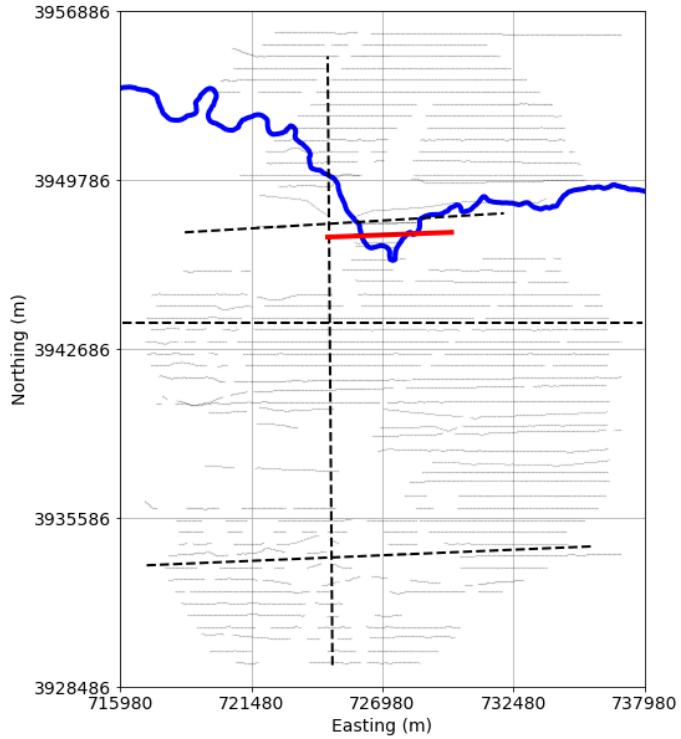

Compute the vertical percentage of coarse-dominated (above the base of the clay layer)

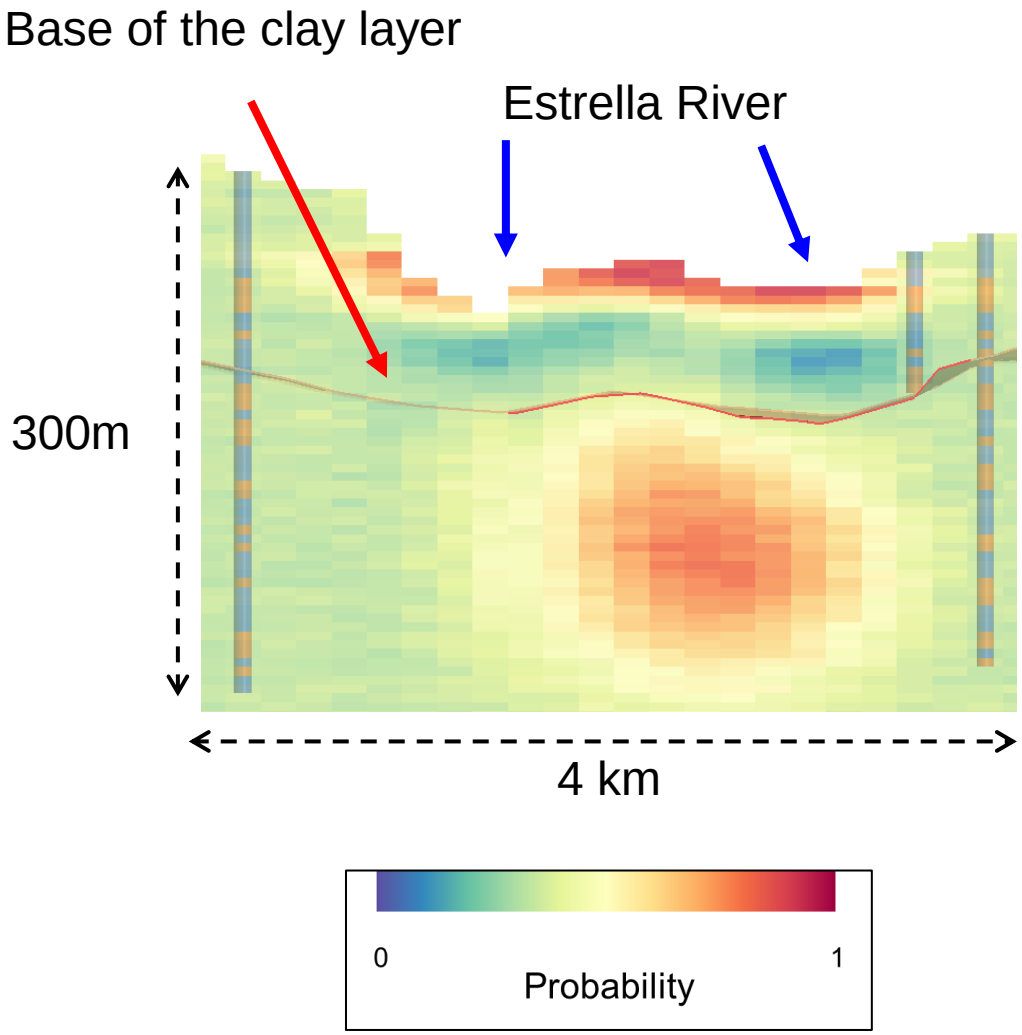

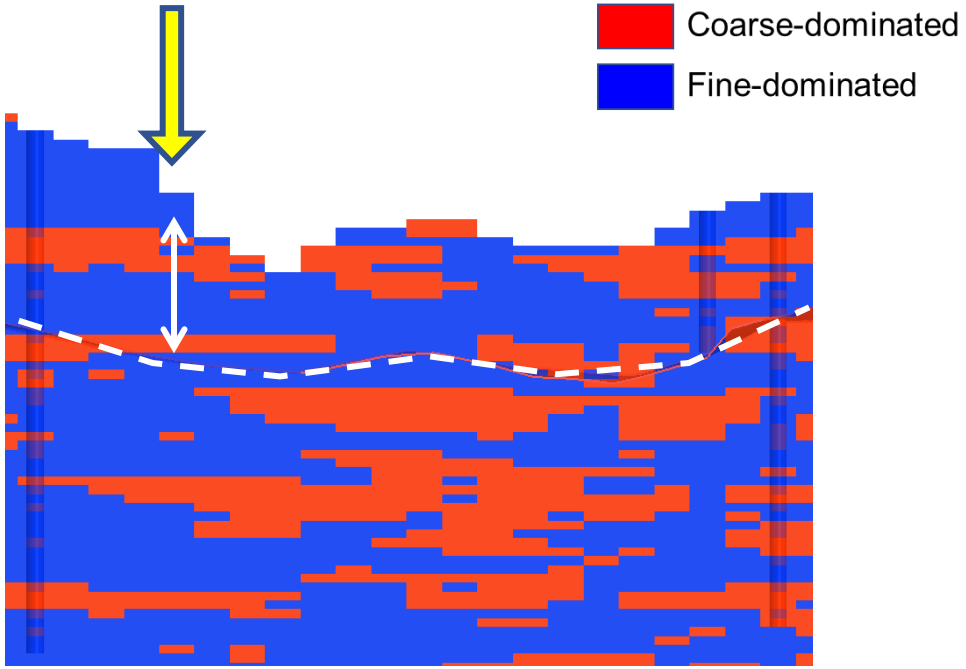

In order to investigate vertical connectivity

Compute the vertical percentage of coarse-dominated (above the base of the clay layer)

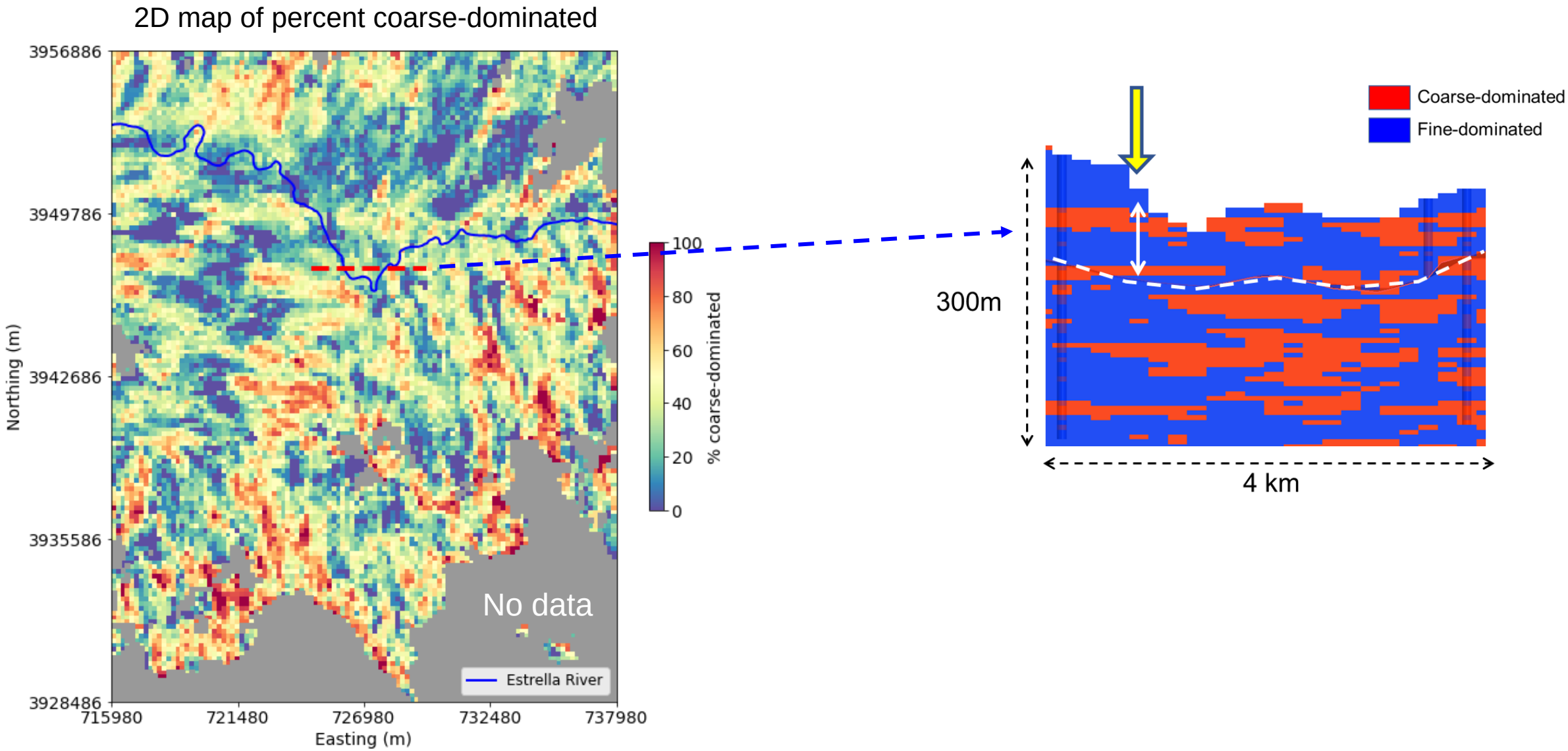

Compute the vertical percentage of coarse-dominated (above the base of the clay layer)

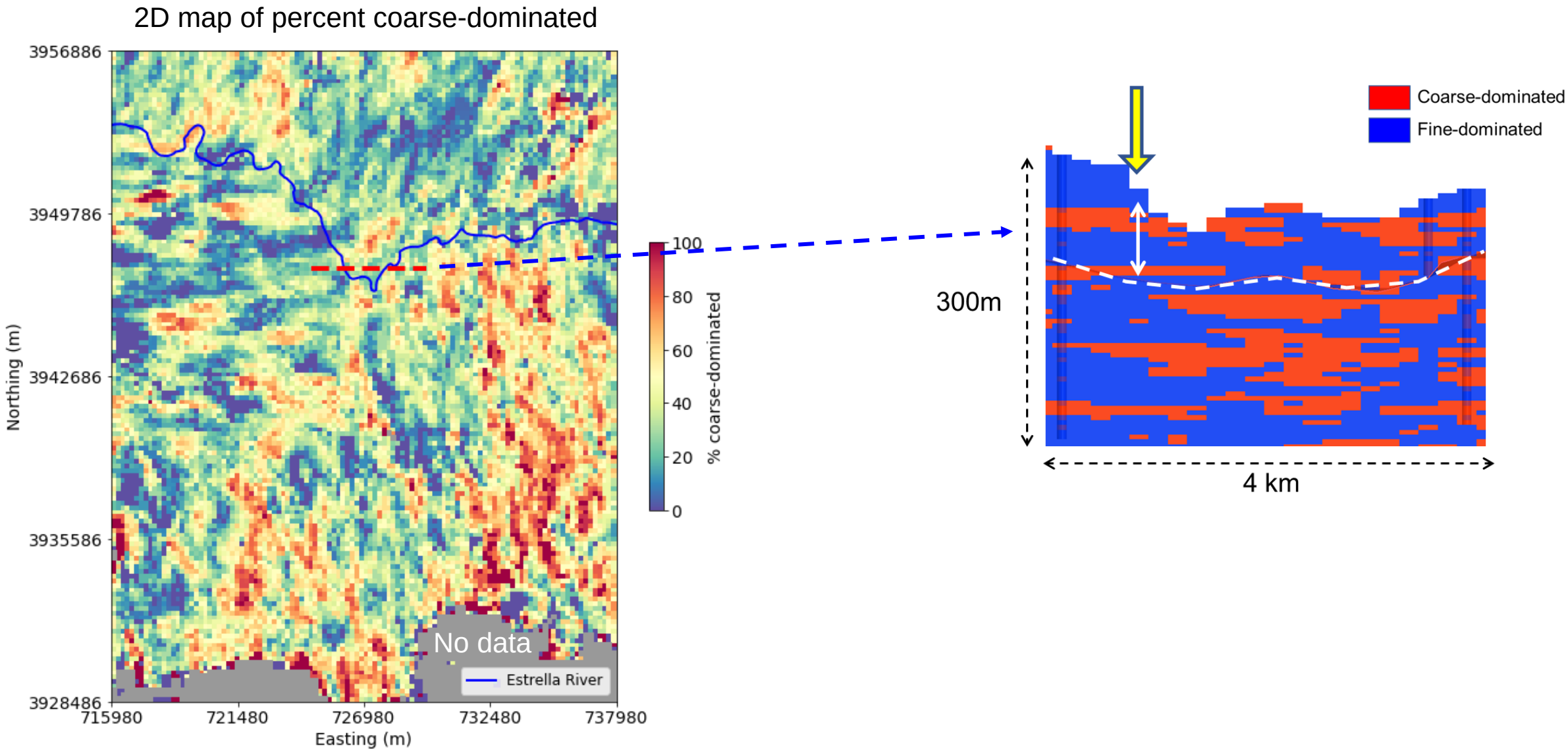

Compute the vertical percentage of coarse-dominated (above the base of the clay layer)

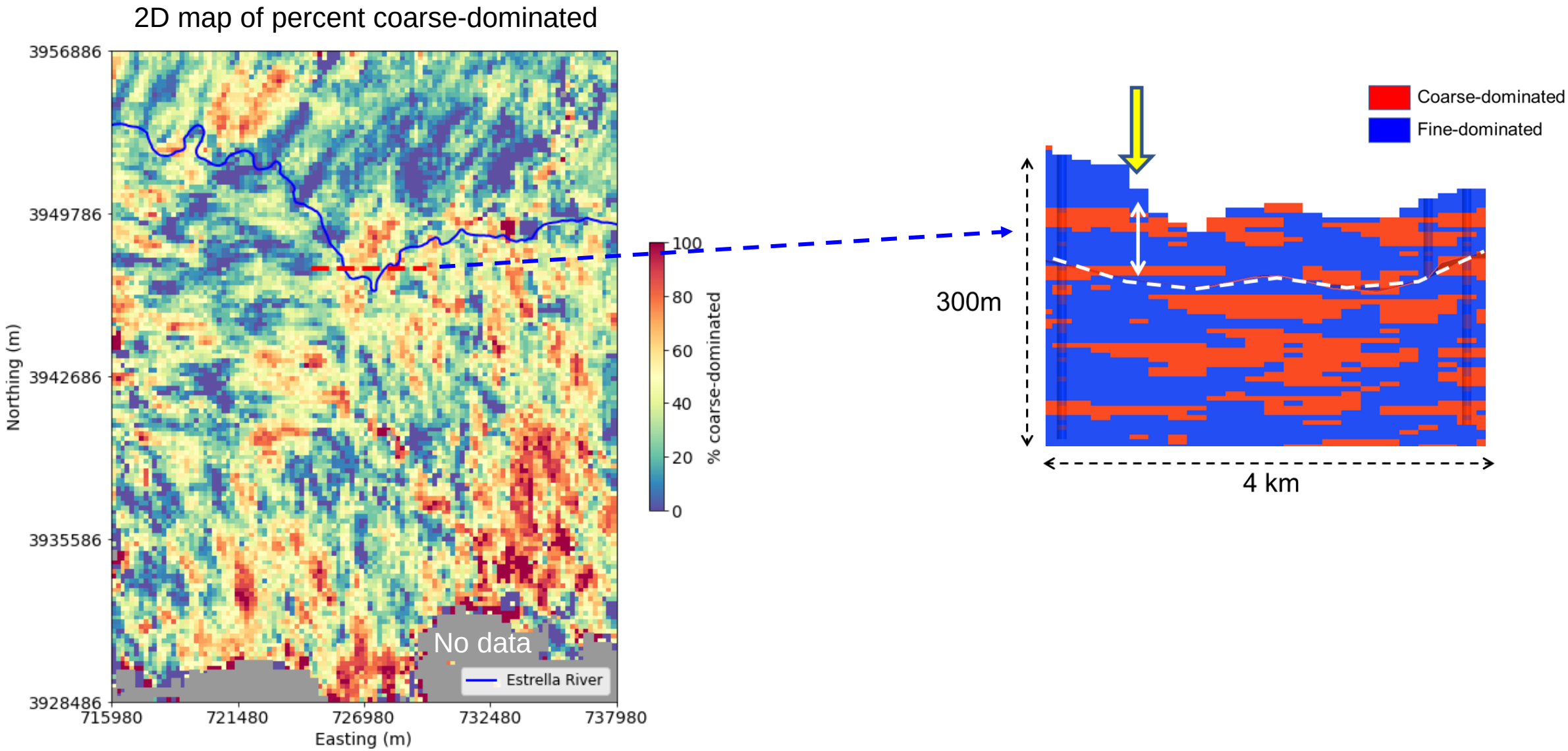

From 100 2D maps of percent coarse-dominated

Mean of percent coarse-dominated

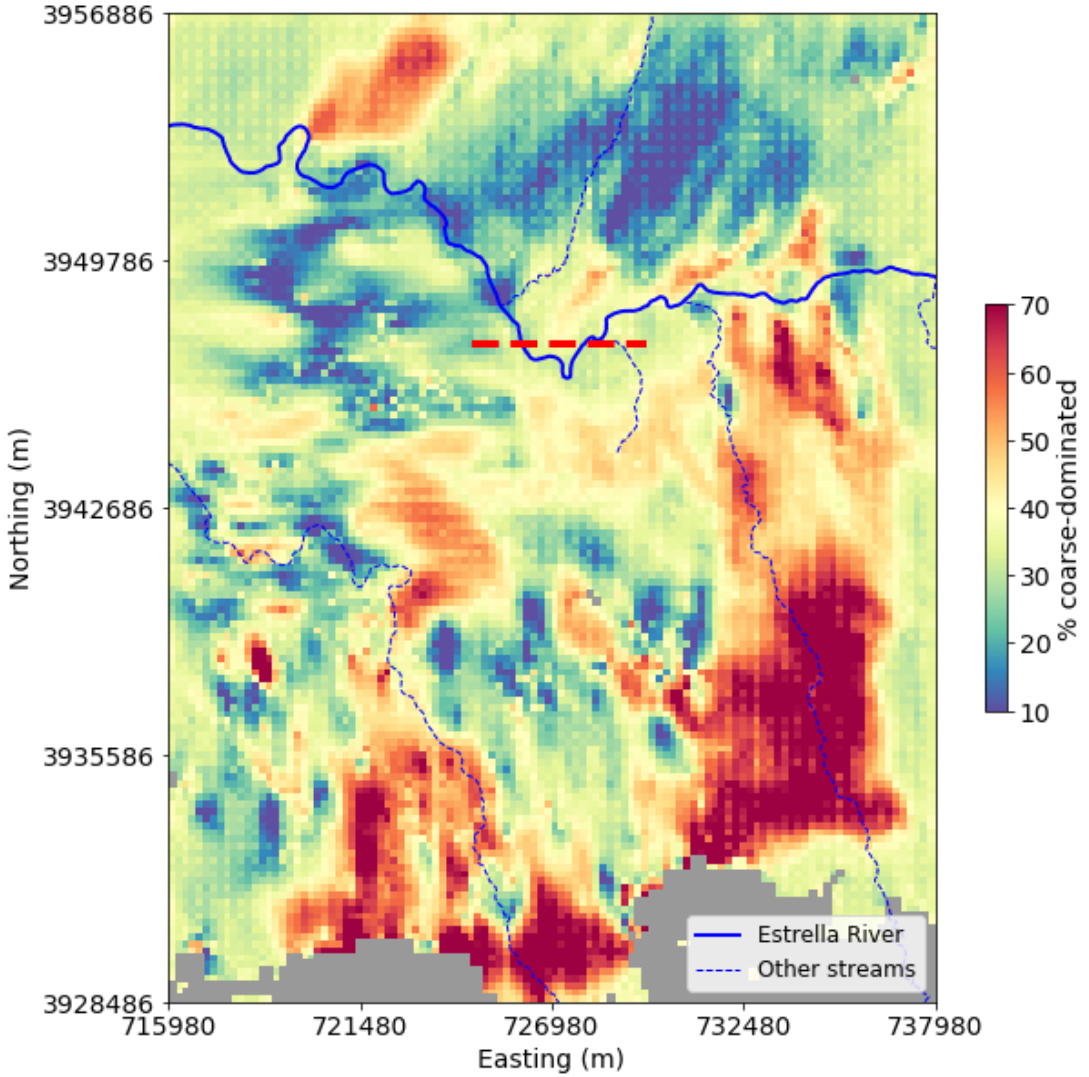

Standard deviation of percent coarse-dominated maps

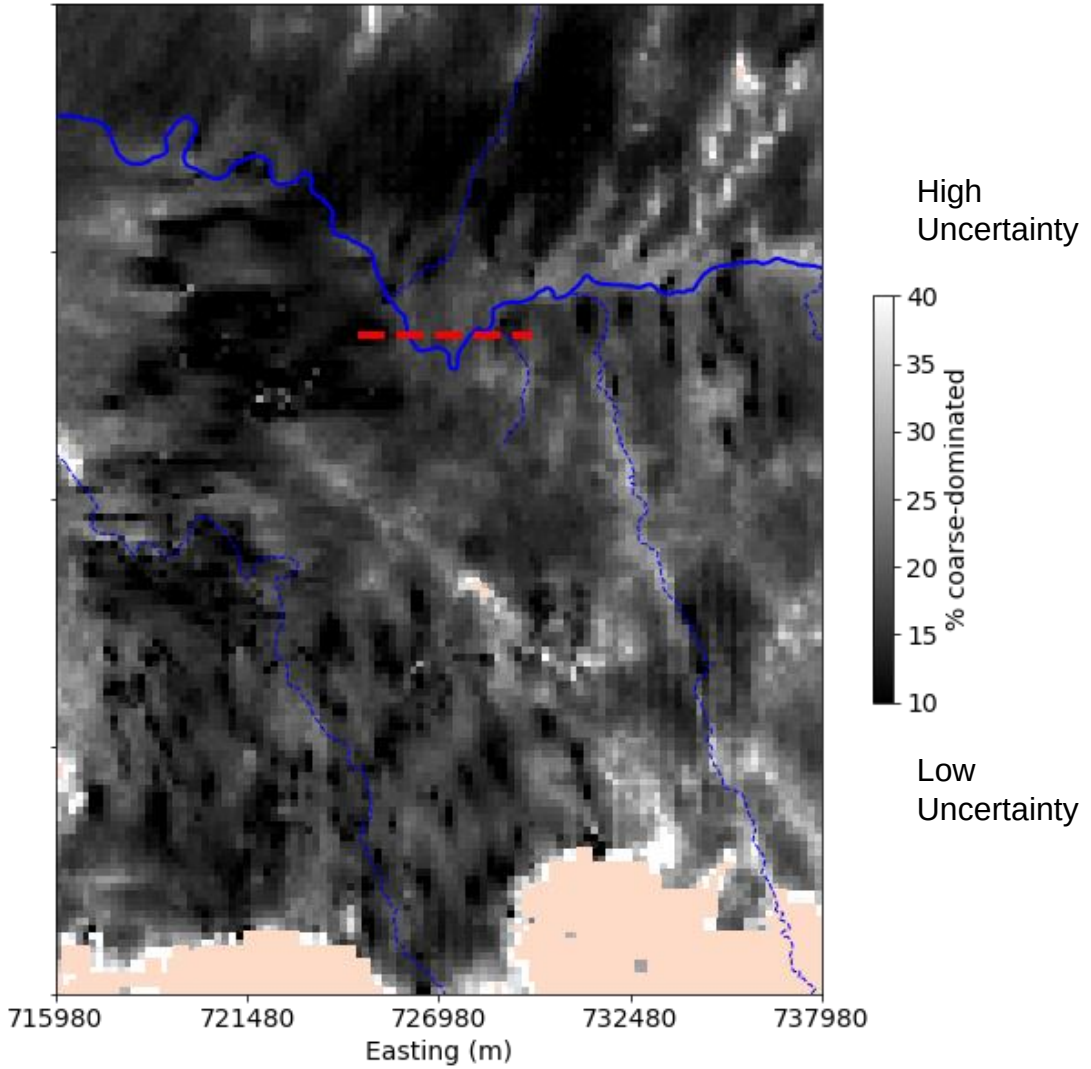

So, what can we tell?

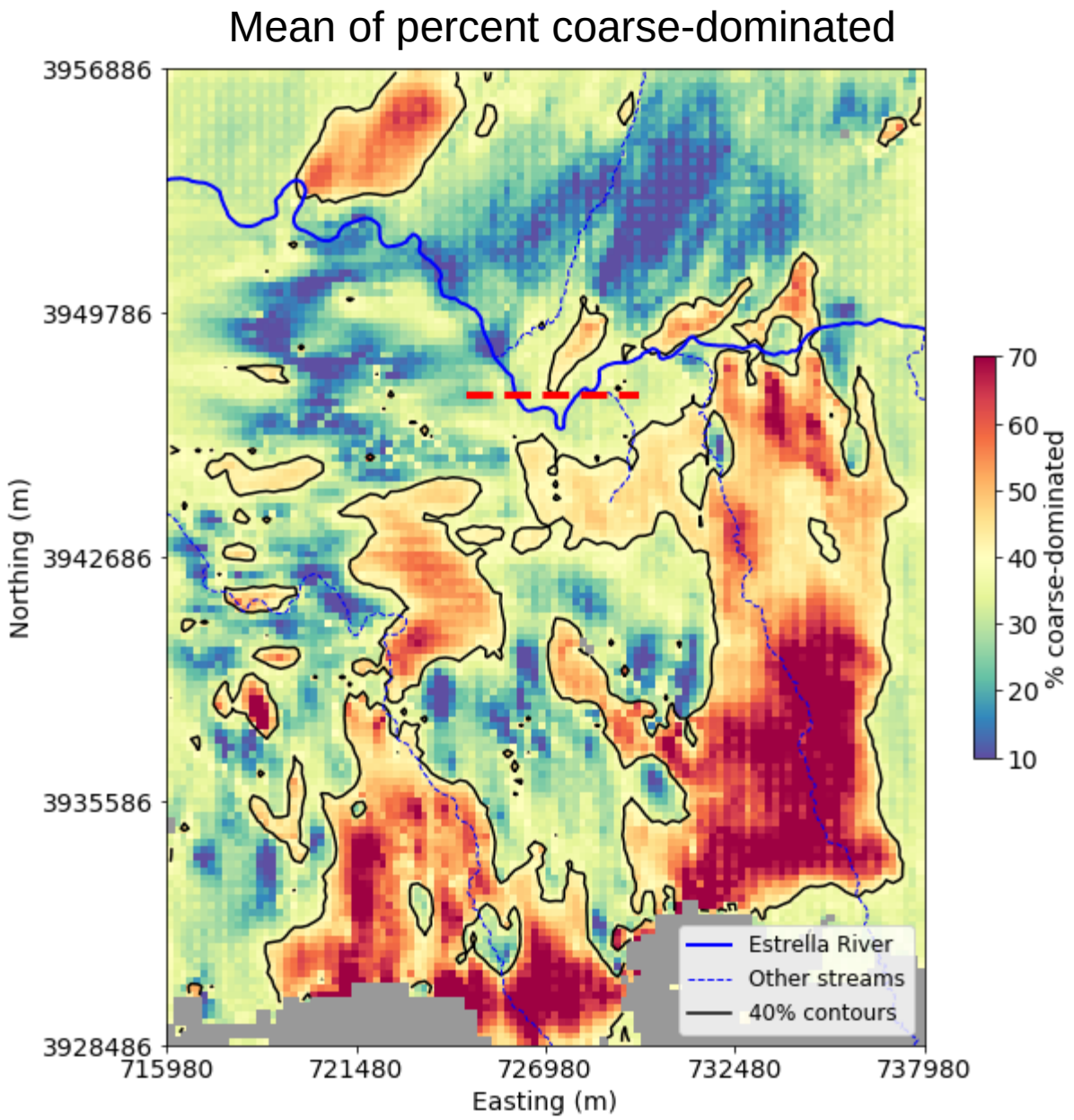

Along the Estrella River, there are relatively low values of percent coarse-dominated (<40%) except for small zones on the east side of the river.

We interpret there being low recharge potential along the river in the western half of the figure on the left and higher potential in the eastern half.

So, what can we tell?

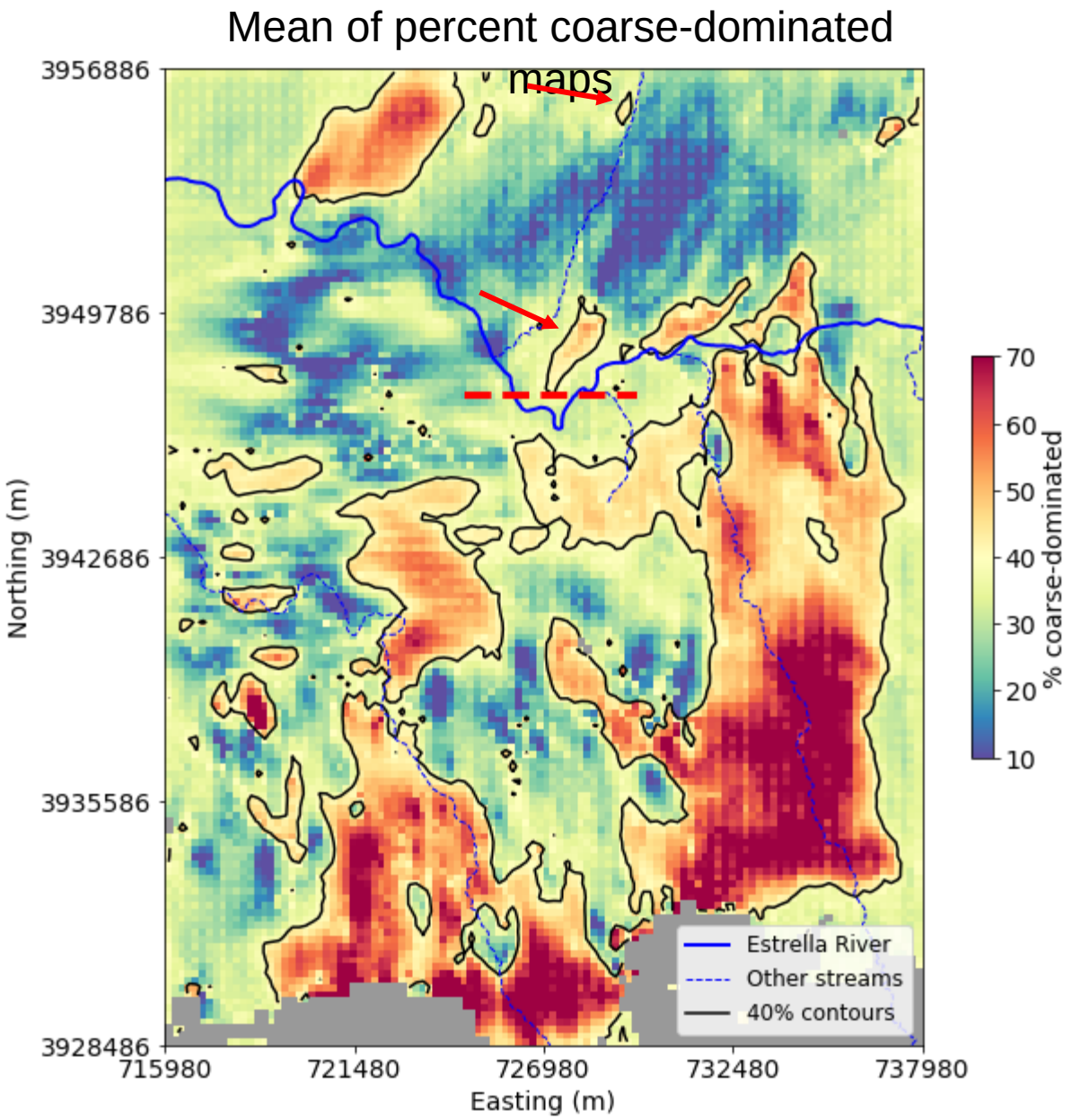

In the northeast side of the river and basin in general, we see low values of percent coarse-dominated (~10%) except for a few small zones.

So, what can we tell?

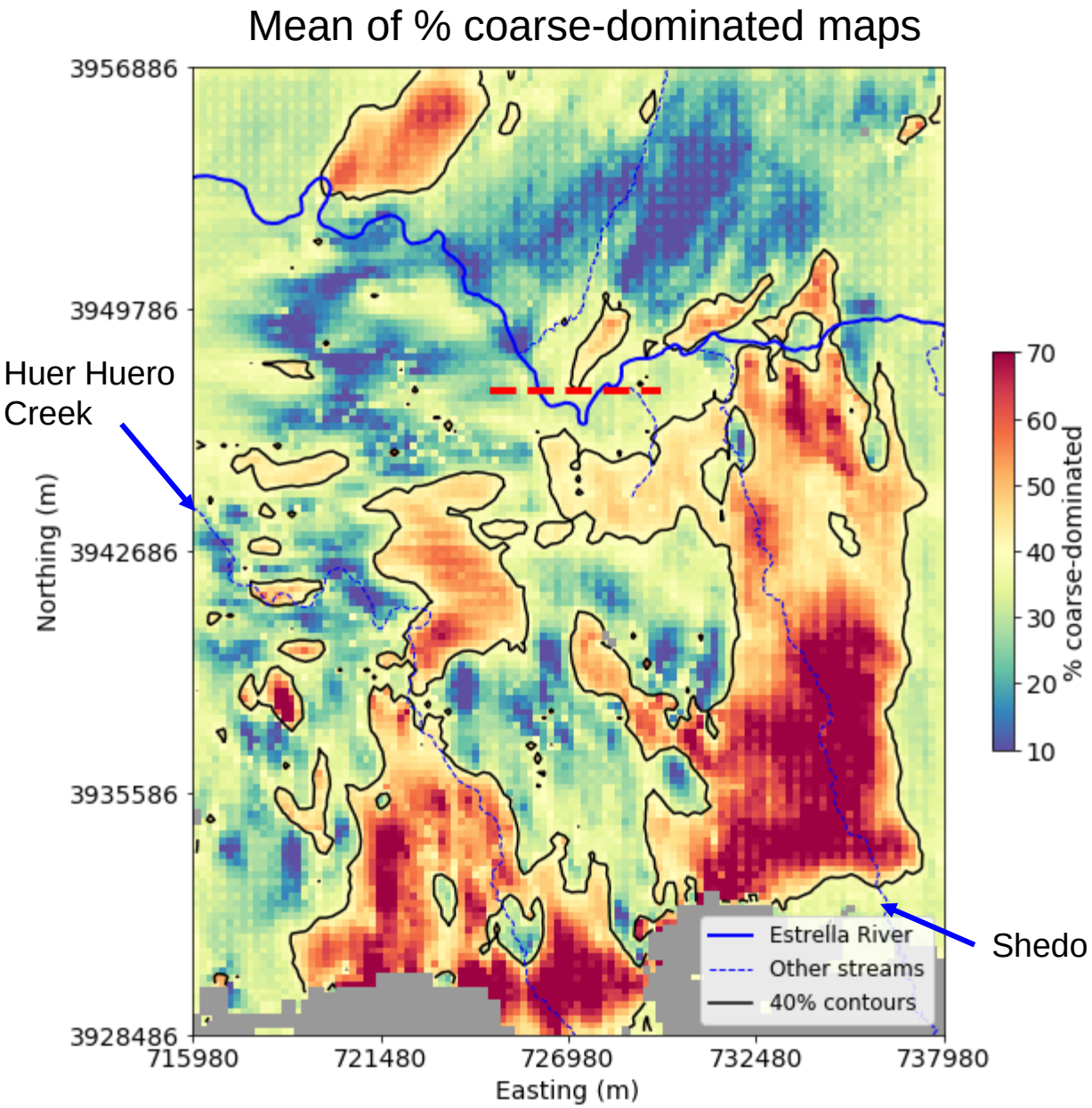

In contrast, along the Huer Huero Creek and Shedo Canyon, we see relatively high values of percent coarse-dominated (>40%).

We interpret there being high recharge potential along the Huer Huero Creek and Shedo Canyon.

Finally, the 2D map of percent coarse-dominated that we provided is not likely to be capturing spatial variation in the soil in top 30 cm, so we recommend integrating other soil maps with our percent coarse-dominated map when assessing potential recharge locations in the study area.